(Geo)Technical Booklet No1

On the compaction of filtered tailings

Ahead of collapsibility and dilatancy

A. Pérez Gallardo

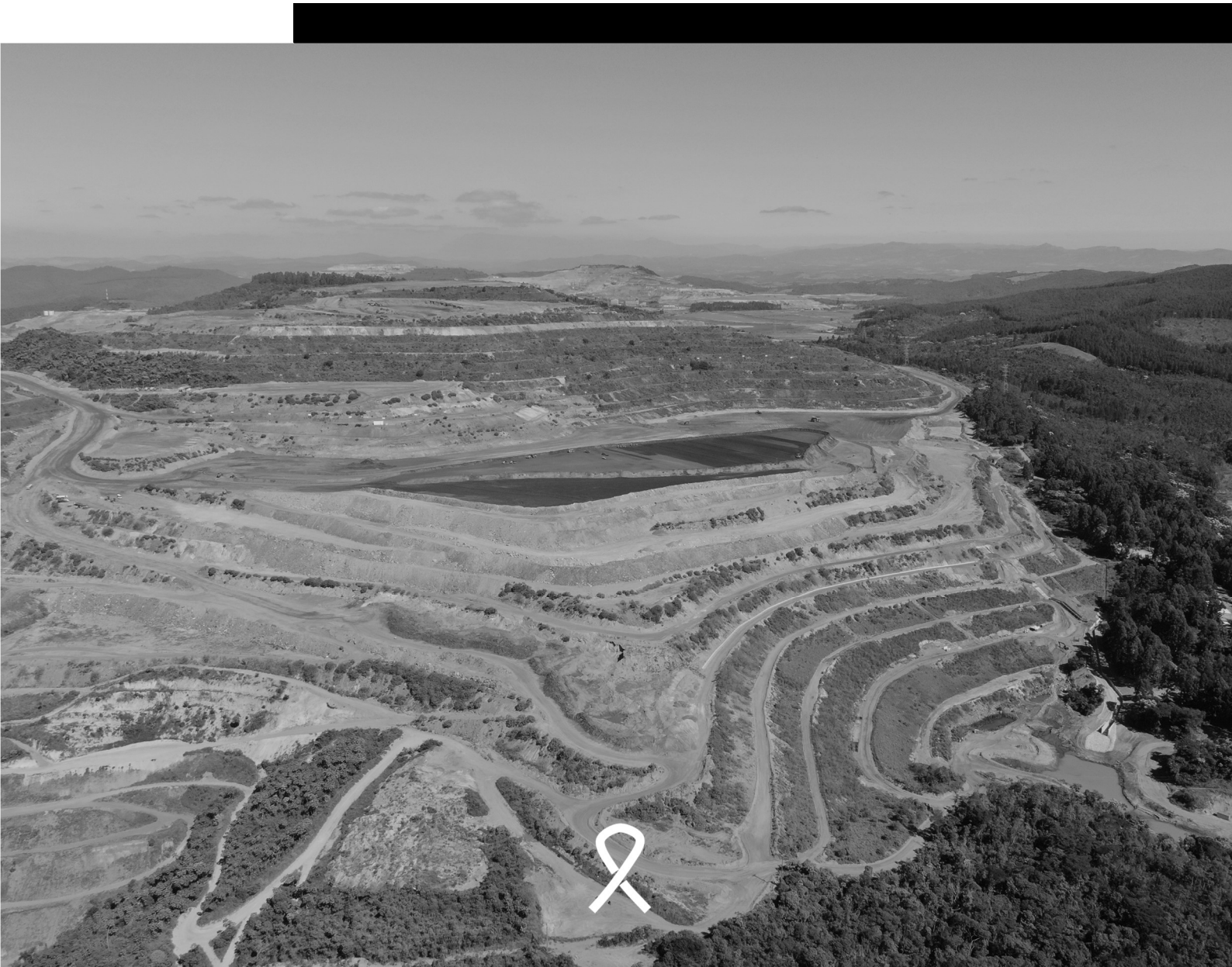

FOREWORD

According to the author himself, with so many interesting things for a civil engineer on the onset of older age to do, writing about dry stacking of mine waste was the last one he dreamt he would be doing one day. But, being forced by professional duty to go up and down man-made mountains of powder abandoned somewhere on the wilderness, he thought that leaving some written impressions could be a good way to make up for his useless sporting effort. Some, alternatively, would simply prefer to issue a landscapes photo album with the sunset on the horizon and possibly the effect would be more appealing. Man is building mountains of powder and expecting them to be eternal. The joy of having high scientific expectations is the theme of this booklet and the author promised us surprising revelations about the science behind the mountain builders' expectations. Be aware of where you hike, he says. You may be swallowed up…

The universe of technical publishing is full of illuminating sureness and there seems to be little room for not knowing or not understanding. But, not knowing and not understanding may be a positive driving force and deserves, we think, a space like the present collection of (Geo)Technical Booklets, dedicated to a branch of civil engineering that sometimes seems to lack civil interest and engineering reasoning. This is the English free translation of the first booklet of the collection, issued for the first time in September 2023 on the author's mother tongue. While doubts persist on matters of technical nature and as long as there is goodwill to deconstruct them openly, booklets like this one could continue endlessly. Others will follow.

The collection of (Geo)Technical Booklets is not peer reviewed, is free of editorial guidance and is completely gratuitous. No rights are reserved and respect for the author's moral rights should be a matter of concern for the contents' users, as are the consequences of its misuse. Black ribbon free publications, Lisbon.

1. PREAMBLE

Let V denote a volume of soil and W its respective weight and let the indexes a, w and s refer to each of the three phases coexisting on the same volume, respectively air, water and solids. Index v refers to voids, that is the volume of soil occupied by air and water. We call the ratio between weight and volume the unit weight:

$$\gamma = W/V \quad [1]$$

Some essential phase relationships can be defined, namely the void ratio, e:

$$e = \frac{V_a + V_w}{V_s} = \frac{V_v}{V_s} \quad [2]$$

The saturation degree, S:

$$S = V_w/V_v \times 100\% \quad [3]$$

The water content, ω:

$$\omega = W_w/W_s \times 100\% \quad [4]$$

And finally, the dimensionless quantity called specific gravity of solids, G_s:

$$G_s = \gamma_s/\gamma_w \quad [5]$$

Based on these definitions, an important relationship between them can be established starting from equation 2:

$$e = \frac{V_v}{V_s} = \left(\frac{V_v}{V_w}\right) \cdot \left(\frac{V_w}{V_s}\right) = \left(\frac{1}{S}\right) \cdot \left(\frac{W_w/\gamma_w}{W_s/\gamma_s}\right) = \left(\frac{1}{S}\right) \cdot \left(\frac{W_w}{W_s} \cdot \frac{\gamma_s}{\gamma_w}\right) = \frac{\omega \cdot G_s}{S} \Longrightarrow \frac{e}{G_s} = \frac{\omega}{S} \quad [6]$$

Now, let us define the dry unit weight, γ_d, and relate it to the previously introduced quantities:

$$\gamma_d = \frac{W_s}{V} = \frac{W_s}{V_s + (V_a + V_w)} = \frac{W_s}{V_s + V_v} = \frac{\gamma_s \cdot V_s}{(1 + V_v/V_s) \cdot V_s} = \frac{G_s \cdot \gamma_w}{1 + e} \quad [7]$$

Using equations 6 and 7, the dry unit weight becomes:

$$\gamma_d = \frac{\gamma_w}{1/G_s + \omega/S} \quad [8]$$

An expression that we will recurrently use later. Equation 07 states that for a certain soil, made of particles with a certain specific gravity, the lower the volume of voids is, the greater is the weight of soil particles contained on it or, in other words, the denser the solid mass is. Maintaining the mass of water, compaction is called the action of reducing the volume occupied by air at cost of an external mechanical energy application, replacing it with solids. Compaction may be a detrimental man-action, as is the case of trafficking on agricultural lands, or a beneficial action, as is, possibly, the "engineered" construction of mountains of powder. The relationship between the void ratio and the dry unit weight is univocal. Less air, a denser mass of solids within the same volume. Ridiculously obvious even for the most ingenious person.

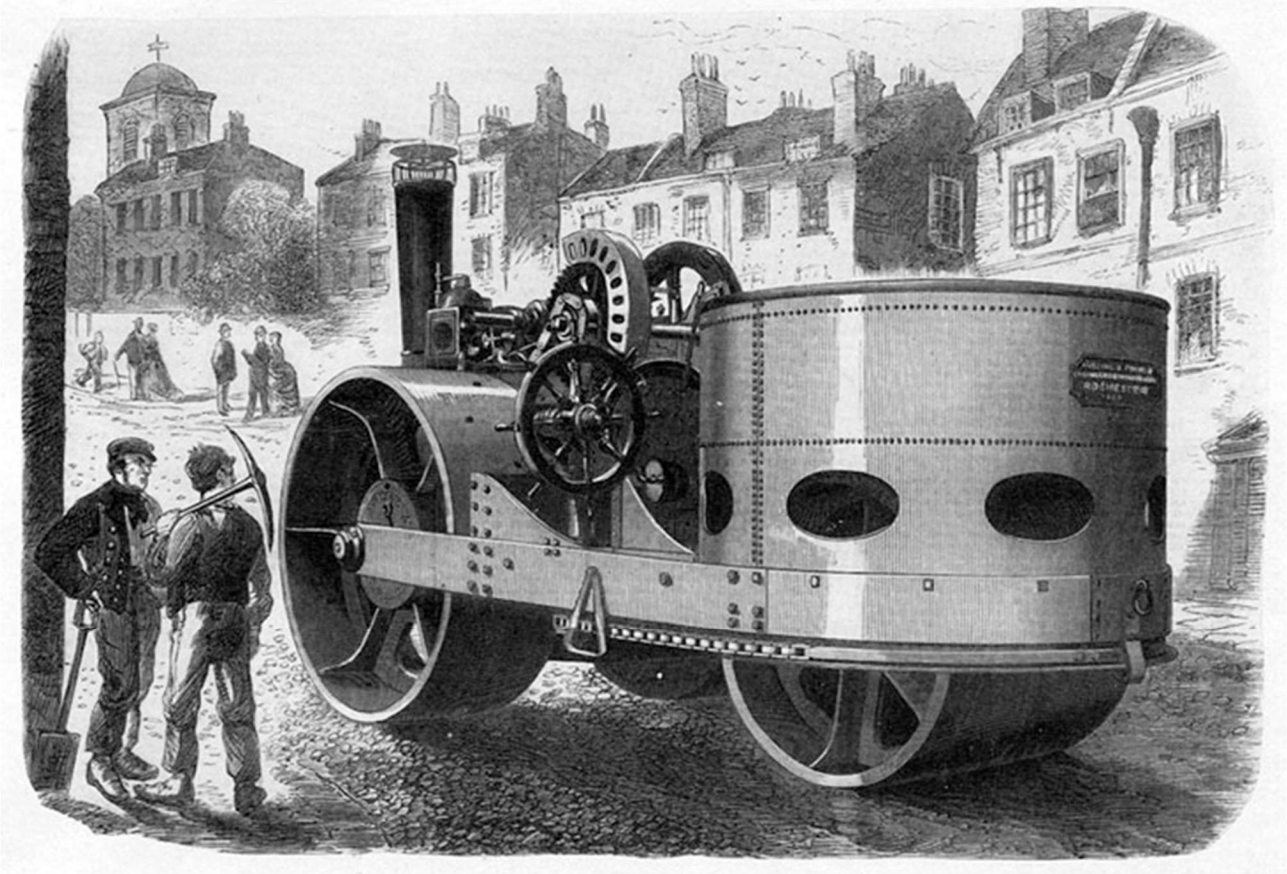

STEAM ROLLER FOR THE STREETS OF LIVERPOOL

Figure 1

Soil compaction as an intentional engineering action is said to go back thousands of years. To demonstrate how old the subject is, Figure 1 shows an illustration of one of the first steam road rollers, a 30 ton one produced by Aveling & Porter in the UK in 1867. For more than one and a half century, man has been "industrially" compacting soils and building embankments with successive layers of compacted soil.

Equation 8 reveals that, for the same soil and the same external effort, the soil dry unit weight depends on the amount of water used on the compaction process. The Proctor compaction test, named in honor of Ralph Proctor who developed it in the thirties of past century, allows to determine the optimum content of water, ω_{opt}, for which the dry unit weight is maximum, $\gamma_{d,max}$, and is still the reference standard laboratory test used for compaction control procedures. Proctor's theory of lubrification or subsequently Hogentogler's theory of moisture films are among the earlier attempts to explain the role of water in the ability of forcing solid particles

into the voids filled with air and that was almost ninety years ago. It will be around the dry-weight curve, as Proctor called it, that a part of this writing is dedicated to. The curve obtained experimentally relates γ_d with ω and is the material form of Equation 8, which on itself remains indeterminate unless the ratio ω/S can be expound.

Commonly, specifications for earthworks are made in terms of the degree of compaction, R, representing the percentage of dry unit weigth obtained on field, in relation to the maximum obtained on laboratory:

$$R = \gamma_d/\gamma_{d,max} \times 100\% \quad [9]$$

If we denote e_{min} as the minimum void ratio corresponding to the maximum dry unit weight obtained with a certain energy, then:

$$R = \frac{\gamma_d}{\gamma_{d,max}} = \frac{1 + e_{min}}{1 + e} \quad [10]$$

Which emphasises that controlling the dry unit weight is the same as controlling the void ratio, although experimentally being more reliable to obtain the former. So far, the prolegomenon of this booklet may seem odd, since it is no more than an unattractive collection of formulas that could be taken from any introductory soil mechanics textbook. Perhaps they were just taken. However, we needed to reach Equation 10 detachedly to make the following chapter, where our true motivation gains visibility, more interesting or perhaps so. Before moving on, a few additional definitions must be remembered.

For soils with a small content of fine grains, compaction control can be based on the relative density, D_r:

$$D_r = \frac{e_{max} - e}{e_{max} - e_{min}} \times 100\% \quad [11]$$

Or, having Equation 7 in mind, alternatively:

$$D_r = \frac{1/\gamma_{d,min} - 1/\gamma_d}{1/\gamma_{d,min} - 1/\gamma_{d,max}} = \frac{(\gamma_d - \gamma_{d,min}) \cdot \gamma_{d,max}}{(\gamma_{d,max} - \gamma_{d,min}) \cdot \gamma_d} \times 100\% \quad [12]$$

Formally, relative density and degree of compaction are related:

$$R = \frac{\gamma_{d,min}/\gamma_{d,max}}{1 - D_r \cdot (1 - \gamma_{d,min}/\gamma_{d,max})} = \frac{1 + e_{min}}{(1 + e_{max}) - D_r \cdot (e_{max} - e_{min})} \quad [13]$$

To give an idea of numbers, for a fine-grained soil (50% material passing the ASTM sieve Nº200) typically $\gamma_{d,min}/\gamma_{d,max} \approx 0{,}68 \pm 0{,}08$. Finaly, once we have associated compaction with the reduction of the air voids, the percentage of air voids, N_a, is defined as:

$$N_a = \frac{V_a}{V} \times 100\% \quad [14]$$

Some earthwork specifications require achieving a minimum state of compaction corresponding to a fixed maximum percentage of air voids for water contents at the dry limit for acceptability. Using the quantities previously defined, an alternative form to the compaction curve can be obtained as follows:

$$V_a + V_w + V_s = V \Longrightarrow \frac{V_a}{V} = 1 - \frac{V_w}{V} - \frac{V_s}{V} \Leftrightarrow N_a = 1 - \frac{W_w}{\gamma_w \cdot V} - \frac{W_s}{\gamma_s \cdot V} \Leftrightarrow N_a = 1 - \frac{\omega \cdot W_s}{\gamma_w \cdot V} - \frac{\gamma_d}{\gamma_s} \Leftrightarrow$$
$$\Leftrightarrow N_a = 1 - \frac{\omega \cdot \gamma_d}{\gamma_w} - \frac{\gamma_d}{G_s \cdot \gamma_w} \Longrightarrow \gamma_d = \frac{(1 - N_a) \cdot \gamma_w}{1/G_s + \omega} \quad [15]$$

Using either Equation 8 or Equation 15, curves with equal degree of saturation or equal percent of air voids, respectively, become determinate on the space ω-γ_d for any soil with a known specific gravity of solids. These curves coincide with each other whenever the following equality is satisfied:

$$N_a = \frac{(1 - S) \cdot G_s \cdot \omega}{S + G_s \cdot \omega} \quad [16]$$

Now, being sure that everyone can walk through the above basic definitions with their eyes shut, we are in a good position to make a proper introduction to this booklet.

2. MOTIVATION

2.1. What, when and why

The author was, not too long ago, asked to comment on Figure 2, presented on next page, and, as well, a bombastic statement that accompanied it on a technical summit about the compaction of filtered tailings. The dry stacking of this mining by-product is currently an adored activity in the industry, after having been concluded that the infamous tailings dams are unsafe by definition and nature. We would add that tailings dams are unsafe, if unproperly designed, constructed, explored and closed. In many cases that we have studied, they were. The same should happen with any other structure, including a mountain of powder. By the time this booklet is being written, discussing the compaction of unsaturated filtered tailings is almost as fancy inside the industry as is, for the scholars serving the industry from outside, the writing of articles about the static liquefaction of loose saturated tailings and the critical states behind which the explanation of the phenomenon hides.

According to the statement, the specification of the end-product and the control of this special soil compaction is nothing else but impossible whilst the degree of compaction is used as the controlling variable. Instead, paraphrasing the statement, the controlling variable must be the void ratio. You may be so kind to concede that, the day he saw the figure and heard the accompanying statement, the author already knew, eventually with his eyes shut, the basics presented in the previous chapter. So, all this might be so surprising for the reader as it was for the author to know that soil mass density or unit weight and voids are allegedly unrelated, at least on the avant-garde of the mountain builders' community.

One may be thinking that the author has been in "bad companies" and should be looking elsewhere for literary inspiration. Let´s see, the declarant and the enthusiastic assembly that welcomed his innovative thinking are among the industry leaders, people empowered with the construction of artificial mountains of powder, not one but ranges of them. Gigantic. Endless. We are talking about real works in the real world. Places where one can hike without knowing what rests below the exuberating greenery.

Figure 2, on next page, shows the results of compaction control tests that were being done on the initial stage of construction of a gigantic tailings pile and intends to illustrate the alleged lack of relationship between the degree of compaction and the void ratio of the end-product. Curiously, the in-situ void ratio on the first construction stage was always greater than 0,6. Compaction control had been done up until then using Hilf's method, having the degree of compaction as controlling variable. After the referred technical summit, with the base of the pile construction already approved and accepted by the owner, a new compaction control procedure would be followed onwards and upwards, under the strict and unique requirement of an end-product containing a maximum void ratio value of 0,6. The initial requirement of a minimum deviation of −3% on the placement of water content was also relaxed, if not over-relaxed. As a first thought from the author, new heavier rollers (smooth drum vibratory compaction rollers) should be already on site. In fact, they were, not just heavier rollers, but the heaviest available on the land.

The author, in those days, was serving as consultant, or a kind of, for a mining corporation. A big one, one disputing a place in the top ten of multibillionaire revenues. His opinion was sought in the context of an internal audit regarding the quality control procedures followed on site and, as the inspectors were not engineers or even alike, some advice was required for them to accomplish their "highly confidential" mission.

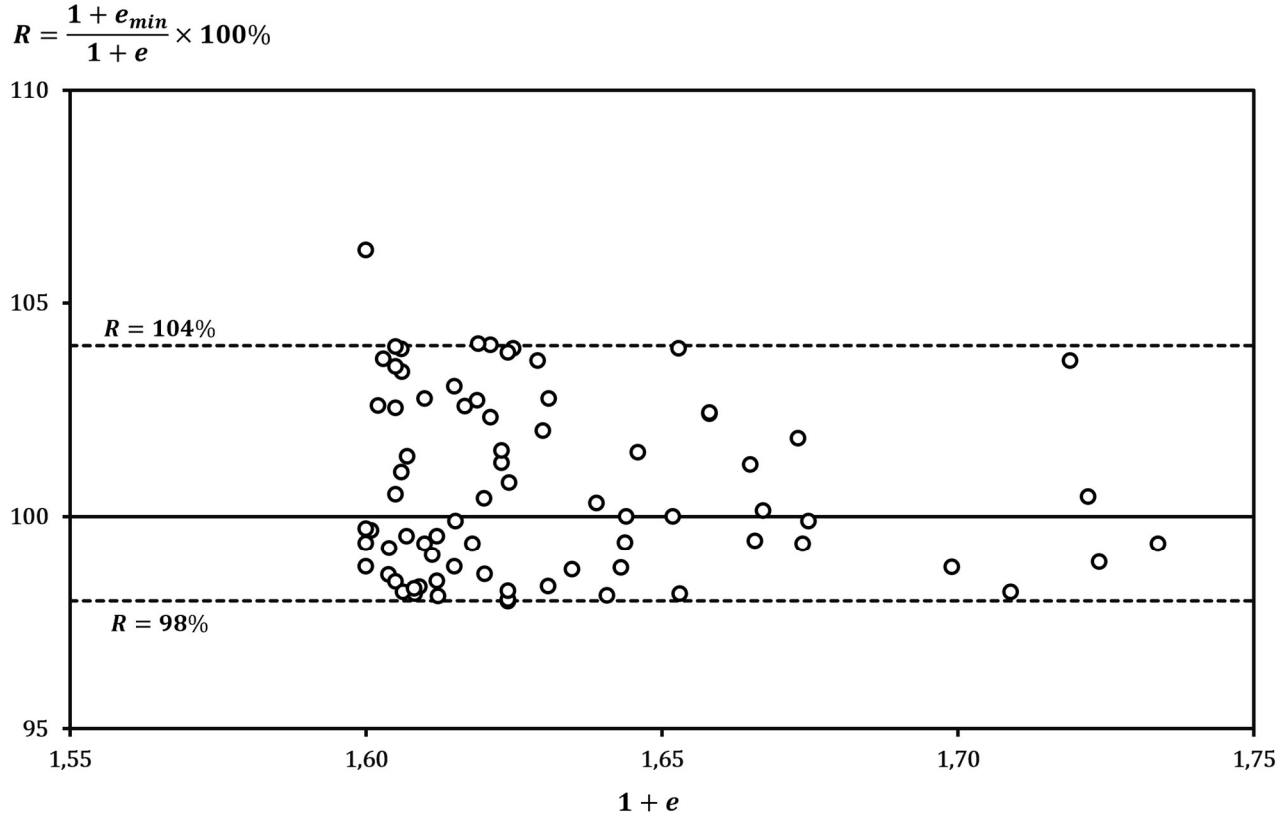

Figure 2

Although having detected that a change in the compaction criteria had taken place recently, the chief inspector ended up concluding that, nevertheless, the best construction practices were being followed by the big corporation. They always are. The reasoning behind the audit verdict shows the same as an orchestra playing with several maestros. It is true, he reasoned, that the newly adopted criteria imply the base of the pile to be highly under-compacted, but it is also true that both the initial and the following earthworks were constructed in strict conformance with the design specifications ruling at their respective times. So, construction adhered to the standards and that was good practice enough. Meanwhile, not too far away, the same mining company was building another gigantic pile of filtered tailings. For this other pile, the “0,6 maximum void ratio” criterium had not yet won sympathy, and things went as they have been going from the beginning. Poorly compacted, allegedly. Susceptible to liquefaction, presumedly.

As we were not asked to comment if the change of criteria was justified, nor were we asked to be concerned about the alleged lack of density of the pile base, our answer was given in the form of Figure 3, on the next page. That is what good consultancy is. And good auditing too. Instead of representing a relative quantity against an absolute quantity, as in Figure 2, on this next figure two absolute quantities are represented one against each other, and the unequivocal veracity of soil mechanics basics becomes true again. As the inspectors concluded, this sample of compaction testing demonstrates that a minimum degree of compaction of 98% was achieved during the initial stage of construction, exactly as required on the specification ruling at the time.

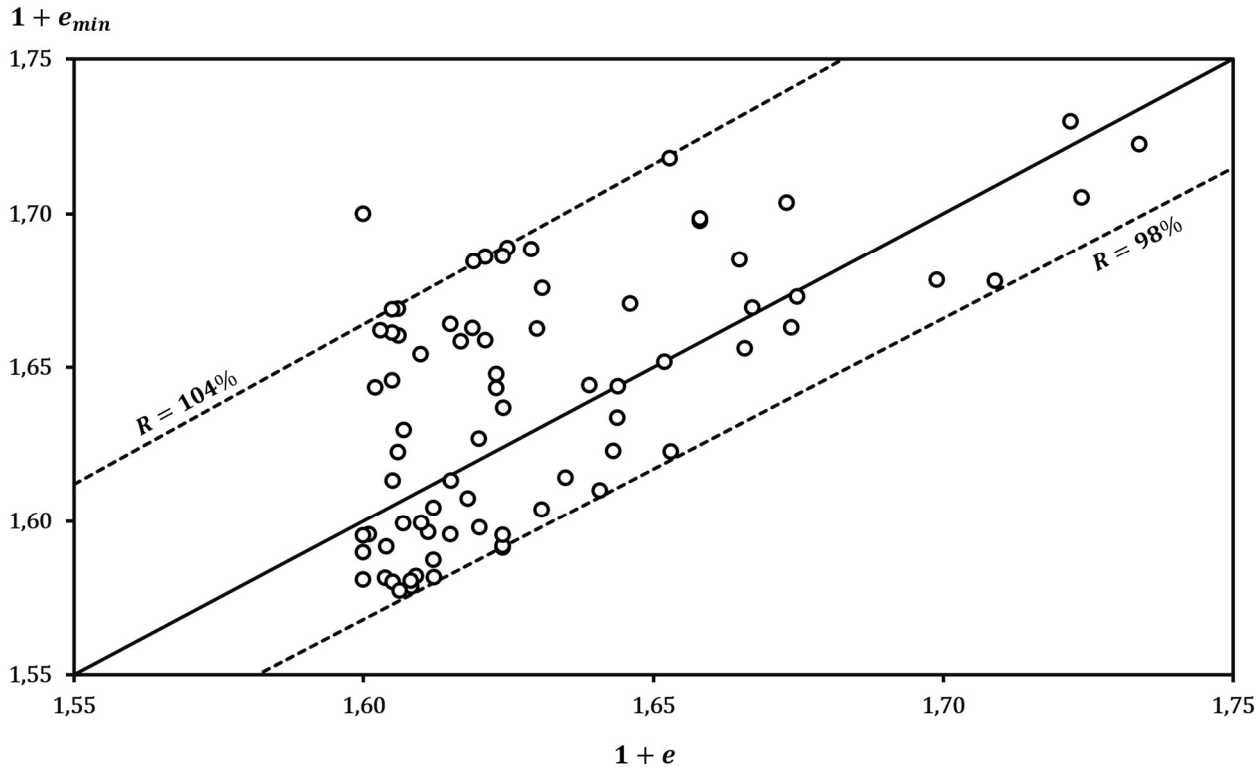

Figure 3

Figure 3 also shows that the 0,6 void ratio was the minimum achieved, not the maximum. Reasons for the criteria change and more specifically the physical relevance of the new condition has been parked on the author´s mind until now, corroding his curiosity.

2.2. What for

The last sentence of the previous subchapter says it all. The author wanted to know why and had no flesh and blood engineer to ask for a response, so here is his truth-seeking booklet about the compaction of filtered tailings. As far as it seems, filtered mining tailings are not faced as common silty sands or sandy silts and, therefore, the current rules of practice do not allegedly apply to them. There is something at a micro-level that makes tailings different and inaccessible to common engineers. If the reader does not agree with this “theory”, he may face the remaining as a personal study on the compaction of non-plastic silts. Another one. Although having deserved attention from the media and being the object of several crowded lectures, the “0,6 maximum void ratio” mark is still bewildering. Perhaps it is related to the static liquefaction susceptibility of saturated loose tailings being avidly studied by the most eminent scholars... Compacted is loose, dry is saturated and static is spontaneous?

What we know are some of the practical consequences of this game-changing approach to soil compaction. We have already seen how easy it is to condemn the highly stressed base of a pile and continue from there as if it was nothing. No one was really expecting some million tons of powder to be dug and recompacted, albeit not a single gram of it being compliant with the requirements lately considered the proper ones, to ensure the eternal safety of the powder mountain. Eyes closed; mouth shut.

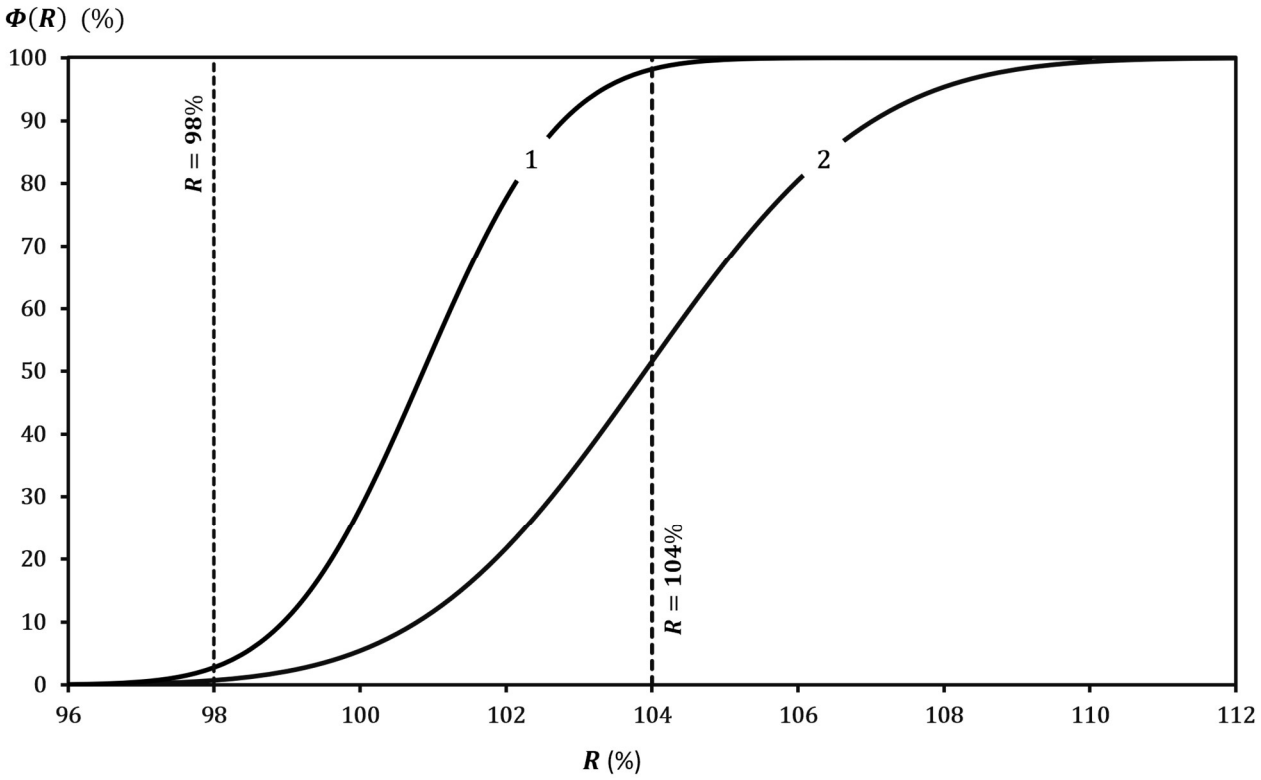

Figure 4

In practical terms, the consequences of changing the specification translated into Figure 4, where the cumulative distributions of the degree of compaction evaluated by the Hilf's method are shown for each stage. The curve numbered with one corresponds to the compaction works done according to the initial criteria (just approved layers), being that a degree of compaction comprised between 98% and 104% with a water content deviation from optimal between -3% and $+1\%$. The curve numbered with two corresponds to the latter stage works, when any compaction control strip with a void ratio greater than 0,6 was rejected. The curve presented for the first stage is based on 2932 checkable determinations for 7,3 million tons of placed material and the curve for the second stage is based on 23 checkable determinations for 6,3 million tons of placed material until the audit date, noting that on the latter period compaction control was no longer being done with Hilf's method. The reference test is the normal Proctor.

Due to the lack of determination of the specific gravity of solids during the initial stage, comparison could not be made independently in terms of void ratio. However, based on the sub-sampling presented in Figure 2, the probability of finding material on the base of the pile with a void ratio lower than 0,6 is surely very low. If the material placed on the pile base was spread in a layer of 1m, over 50 football pitches would be required to accommodate it.

3. (ONE POSSIBLE) COMPACTION CURVE MATHEMATICS

3.1. Fundamentals

Picking on Equation 8, from Chapter 1, for a soil with a certain specific gravity of solids compacted under a certain energy, the compaction curve is given by:

$$\gamma_d(\omega) = \frac{\gamma_w}{1/G_s + \omega/S(\omega)} \quad [17]$$

And this equation will become fully determined if we are able to express the saturation degree as a function of the water content. Whichever is the framework, for instance the mechanics of unsaturated soils, such relationship, $S = S(\omega)$, will end up having to emerge empirically from experimental data. Therefore, the most straightforward approach is to define that function directly from the standard compaction tests. If the specific weight is known, compaction tests provide at least five points (ω, S) from which a function able to describe with good approximation the experimental data can be eventually built. This function needs to be generalisable, and its parameters should be expressible as functions of some pertinent soil index properties.

Equation 6 requires a monotonically non-decreasing function ($dS(\omega)/d\omega \geq 0$) to be chosen, so that, for a certain specific gravity and for a certain void ratio, there is a growing one-to-one relationship between the water content and the saturation degree. Also, being a differentiable function, at least a point of maximum dry unit weight should be afterwards obtained, what will be possible as long as:

$$\frac{d\gamma_d(\omega)}{d\omega} = \frac{\gamma_w \cdot \left(\omega \cdot \frac{dS(\omega)}{d\omega} - S(\omega)\right)}{\left(\frac{S(\omega)}{G_s} + \omega\right)^2} = 0 \Longrightarrow \omega \cdot \frac{dS(\omega)}{d\omega} - S(\omega) = 0 \quad [18]$$

Which is a simple differential equation with separable variables whose solution will be the optimum water content, ω_{opt}:

$$\omega = \omega_{opt} = k \cdot S(\omega_{opt}) = k \cdot S_{opt} \quad [19]$$

Where k is some integration constant. Solving Equation 19 and placing its result in Equation 17, the maximum dry unit weight will be obtained, $\gamma_{d,max} = \gamma_d(\omega_{opt})$. Some further considerations will be discussed on the next subchapter.

There are a few explanations for us to follow a phenomenological path hereafter that is worth to clarify in advance. First, our goal is to understand how a void ratio limiting value can be established on the same conditions that it was presumedly established by others, that is, as there is nothing else, based on standard laboratory test results, namely compaction tests and few triaxial tests. No experimental support is at our reach and a finer theoretical path would lead us nowhere, that not intellectual growth. For this purpose, a quiet large database of laboratory tests was, not without great effort and much patience, compiled and treated so that a representative sampling of a “unique” material could be now used.

Secondly, it is exactly because of that sampling that we know beforehand that not just the inherent variability of our "unique" material properties is very high, as we know that the measurement errors are so significative that anything than a high-level conclusion would be withdrawn on the grounds of practicality. In fact, remitting to Figure 2, or to its alternative Figure 3, data variability is as high as to make someone doubt of basic soil mechanics concepts. We are not among the doubters.

3.2. Our $S(\omega)$ function

From all the infinite possibilities, our candidate function will be obeying several rules that we will now state. If, on the dry branch of the compaction curve, we want the dry unit weight to be non-null at a zero-water content and if, simultaneously, we want to have an increasing relationship between the water content and the dry unit weight up to the optimum point, then firstly:

$$\left.\frac{dS(\omega)}{d\omega}\right|_{\omega=0} > 0 \qquad [20]$$

This hypothesised condition, not necessarily required, will conduct to a single peak compaction curve, which we know fitting well to the available test data. Secondly, if, on the wet branch of the compaction curve, we want the degree of saturation to become constant beyond a certain maximum value of water content, ω_m, then:

$$\left.\frac{dS(\omega)}{d\omega}\right|_{\omega=\omega_m} = 0 \qquad [21]$$

Leading to a maximum degree of saturation, $S_m = S(\omega_m)$, beyond which compaction becomes eventually impossible. On the hypothesis of water incompressibility, this latter rule traduces the virtual impossibility of having an undrained compression of the soil skeleton. This way, the wet branch of the curve will smoothly converge to a saturation line, away from the complete saturation one, but close to it. From these two rules, a family of possible functions is:

$$S(\omega) = \left.\frac{dS_1(\omega)}{d\omega}\right|_{\omega=\omega_m} \cdot \omega + S_1(\omega) \qquad [22]$$

Being $S_1(\omega)$ any convenient auxiliary function, to which we will require that:

$$S_1(\omega = 0) = 0 \qquad [23]$$

And:

$$\left.\frac{dS_1(\omega)}{d\omega}\right|_{\omega=\omega_m} < 0 \qquad [24]$$

Before proposing an auxiliary function, we will, for convenience, transform the explanatory variable, ω, and our response variable, S, to non-dimensional forms, as follows:

$$\omega = \bar{\omega} \cdot \frac{\omega_m}{\bar{\omega}_m} \quad [25]$$

$$S = \bar{S} \cdot \frac{S_m}{\bar{S}_m} \quad [26]$$

Where ω_m e S_m, whose physical meaning was explained earlier, become the scale parameters, independent of each other, of our $S(\omega)$ model. There are multiple valid candidates for the auxiliary function, and we have chosen this one:

$$\bar{S}_1(\bar{\omega}) = \bar{\omega}^m \cdot (1 - \bar{\omega})^n \quad \text{para} \quad \bar{\omega} \leq \bar{\omega}_m < 1 \quad [27]$$

Which introduces two independent shape parameters on the model, m and n and a restraint, $\bar{\omega}_m$, which represents the point of maximum saturation on the transformed space and connects the non-dimensional space to the dimensional one. The first derivate of $\bar{S}_1(\bar{\omega})$ is:

$$\frac{d\bar{S}_1(\bar{\omega})}{d\bar{\omega}} = -\bar{\omega}^{m-1} \cdot (1 - \bar{\omega})^{n-1} \cdot (m \cdot (1 - \bar{\omega}) - n \cdot \bar{\omega}) \quad [28]$$

And the second one is:

$$\frac{d^2\bar{S}_1(\bar{\omega})}{d\bar{\omega}^2} = -\bar{\omega}^{m-2} \cdot (1 - \bar{\omega})^{n-2} \cdot \cdot \left(m^2 \cdot (1 - \bar{\omega})^2 - m \cdot (1 - \bar{\omega}) \cdot \left((2 \cdot n - 1) \cdot \bar{\omega} + 1\right) + (n - 1) \cdot n \cdot \bar{\omega}^2\right) \quad [29]$$

To satisfy the condition given by Equation 24, we will have to impose:

$$\bar{\omega}_A \leq \bar{\omega}_m \leq \bar{\omega}_B \quad [30]$$

Being the limiting values given by:

$$\left.\frac{dS_1(\bar{\omega})}{d\bar{\omega}}\right|_{\bar{\omega}=\bar{\omega}_A} = 0 \Rightarrow \bar{\omega}_A = \frac{m}{m+n} \quad [31]$$

And:

$$\left.\frac{d^2 S_1(\bar{\omega})}{d\bar{\omega}^2}\right|_{\bar{\omega}=\bar{\omega}_B} = 0 \Rightarrow \bar{\omega}_B = \frac{m^2 + m \cdot n - m + \sqrt{m \cdot n \cdot (m+n-1)}}{m^2 + 2 \cdot m \cdot n - m + n^2 - n} \quad [32]$$

Finally, we arrive to our tentative explanatory model containing five independent parameters:

$$\bar{S}(\bar{\omega}) = \bar{\omega}^m \cdot (1-\bar{\omega})^n - \left({\bar{\omega}_m}^{m-1} \cdot (1-\bar{\omega}_m)^{n-1} \cdot (m \cdot (1-\bar{\omega}_m) - n \cdot \bar{\omega}_m)\right) \cdot \bar{\omega} \quad [33]$$

Where:

$$\bar{\omega} = \omega \cdot \frac{\bar{\omega}_m}{\omega_m} \quad [34]$$

$$\bar{S} = S \cdot \frac{\bar{S}_m}{S_m} \quad [35]$$

Going back to the previous subchapter, Equation 18 can be rewritten as a function of the transformed water content, $\bar{\omega}$:

$$\bar{\omega} \cdot \frac{dS(\bar{\omega})}{d\bar{\omega}} - S(\bar{\omega}) = 0 \Leftrightarrow (1-\bar{\omega})^{n-1} \cdot (m \cdot (1-\bar{\omega}) - n \cdot \bar{\omega}) - (1-\bar{\omega})^n = 0 \Longrightarrow \bar{\omega} = \bar{\omega}_{opt} \quad [36]$$

Solving the equation, the optimum value of the optimum water content can be determined:

$$\omega_{opt} = \bar{\omega}_{opt} \cdot \frac{\omega_m}{\bar{\omega}_m} = \frac{m-1}{m+n-1} \cdot \frac{\omega_m}{\bar{\omega}_m} \quad [37]$$

And alongside with it will come the value of the maximum dry unit weight.

The compaction curve, given by Equation 17, can be expressed in a more compact format as a function of the ratio between the water content and the degree of saturation at the optimum point, ω_{opt}/S_{opt}, by letting:

$$\frac{\omega}{S} = \frac{\bar{S}_{opt}}{\bar{\omega}_{opt}} \cdot \frac{\bar{\omega}}{\bar{S}} \cdot \frac{\omega_{opt}}{S_{opt}} \quad [38]$$

Where:

$$\frac{\bar{\omega}}{\bar{S}} = \frac{1}{\bar{\omega}^{m-1} \cdot (1-\bar{\omega})^n - {\bar{\omega}_m}^{m-1} \cdot (1-\bar{\omega}_m)^{n-1} \cdot (m-(m+n) \cdot \bar{\omega}_m)} \quad [39]$$

And:

$$\frac{\bar{S}_{opt}}{\bar{\omega}_{opt}} = \frac{(m-1)^{m-1} \cdot n^n}{(m+n-1)^{m+n-1}} - \bar{\omega}_m{}^{m-1} \cdot (1-\bar{\omega}_m)^{n-1} \cdot (m-(m+n) \cdot \bar{\omega}_m) \quad [40]$$

Having $\bar{\omega}$ any real value between 0 and $\bar{\omega}_m$. The ratio $\bar{S}_{opt}/\bar{\omega}_{opt}$ assumes a constant value for a particular compaction curve. Hence, for any known values of ω_{opt}, S_{opt} and G_s the compaction curve becomes completely determined for any pertinent set of values of m, n and $\bar{\omega}_m$. Otherwise, the compaction curve can be kept expressed in terms of the original model parameters ω_m and S_m, letting:

$$\frac{\omega}{S} = \frac{\bar{S}_m}{\bar{\omega}_m} \cdot \frac{\bar{\omega}}{\bar{S}} \cdot \frac{\omega_m}{S_m} \quad [41]$$

Where:

$$\frac{\bar{S}_m}{\bar{\omega}_m} = \bar{\omega}_m{}^{m-1} \cdot (1-\bar{\omega}_m)^{n-1} \cdot \big((m+n-1) \cdot \bar{\omega}_m - m + 1\big) \quad [42]$$

And $\bar{\omega}/\bar{S}$ is equally given by Equation 39. The ratio $\bar{S}_m/\bar{\omega}_m$ assumes, as well, a constant value for a particular compaction curve.

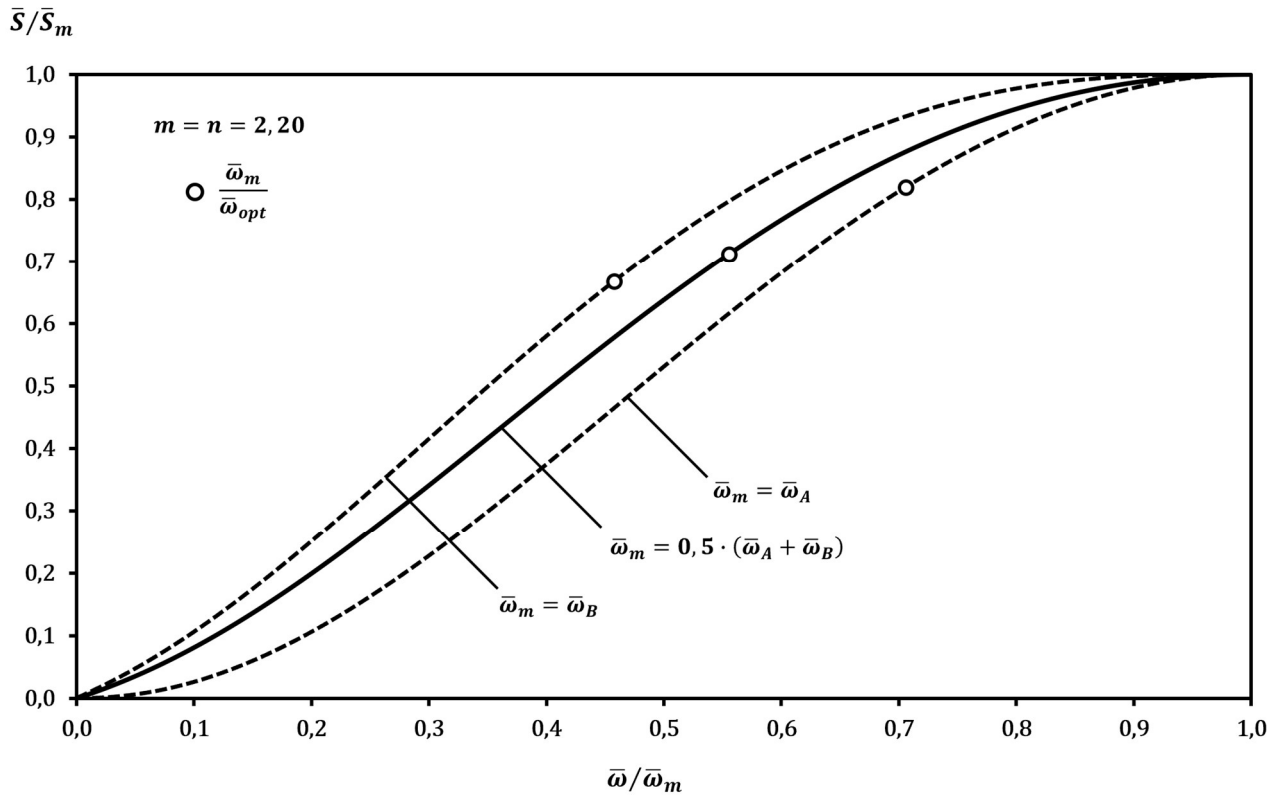

Figure 5

The role of the transformed maximum water content $\bar{\omega}_m$ is illustrated in Figure 5, keeping the value of the exponents n and m constant.

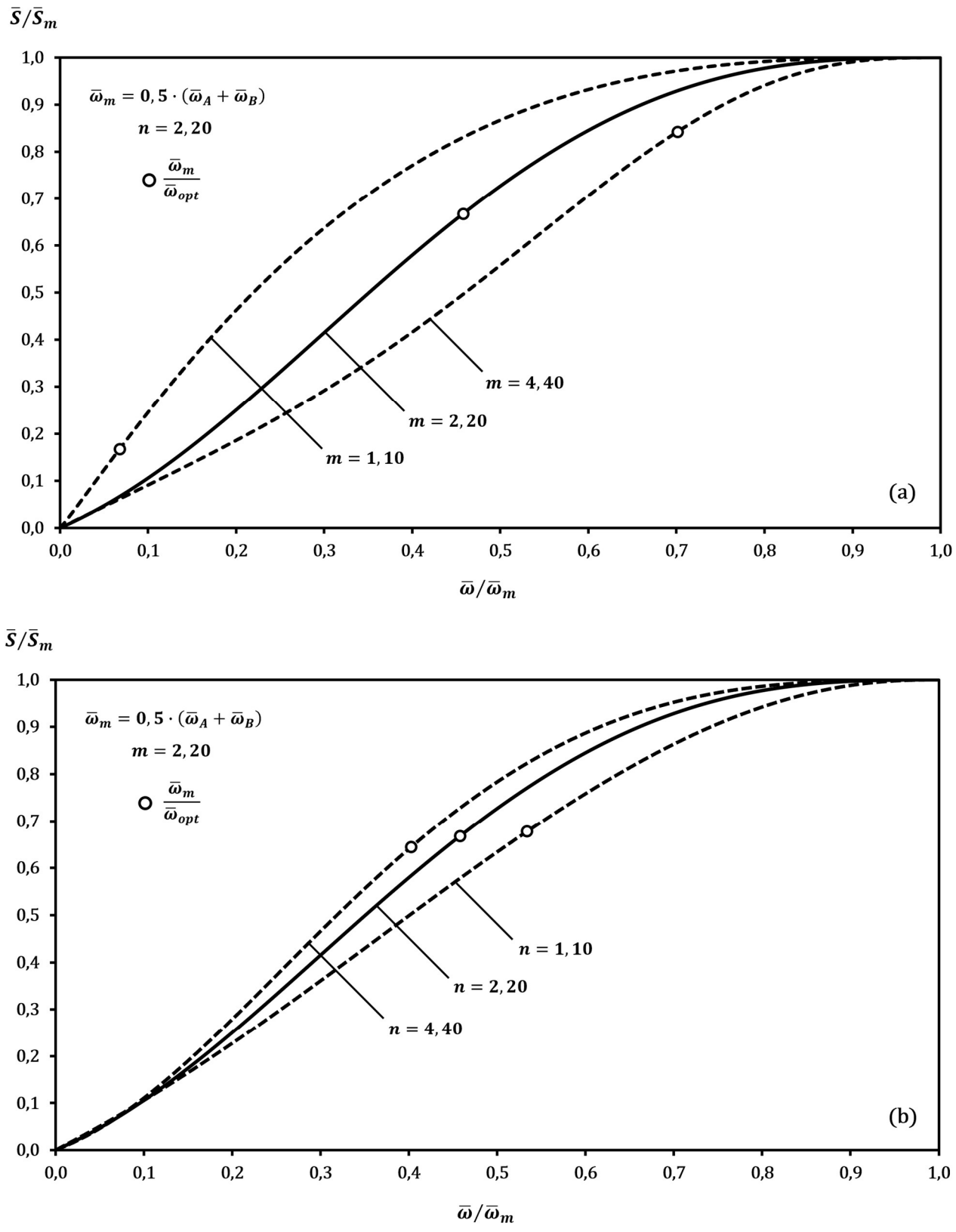

Figure 6

In turn, the role of the two function exponents n and m and their combination is illustrated in Figure 6, parts (a) and (b) respectively, letting one of the exponents to vary with the other one kept constant.

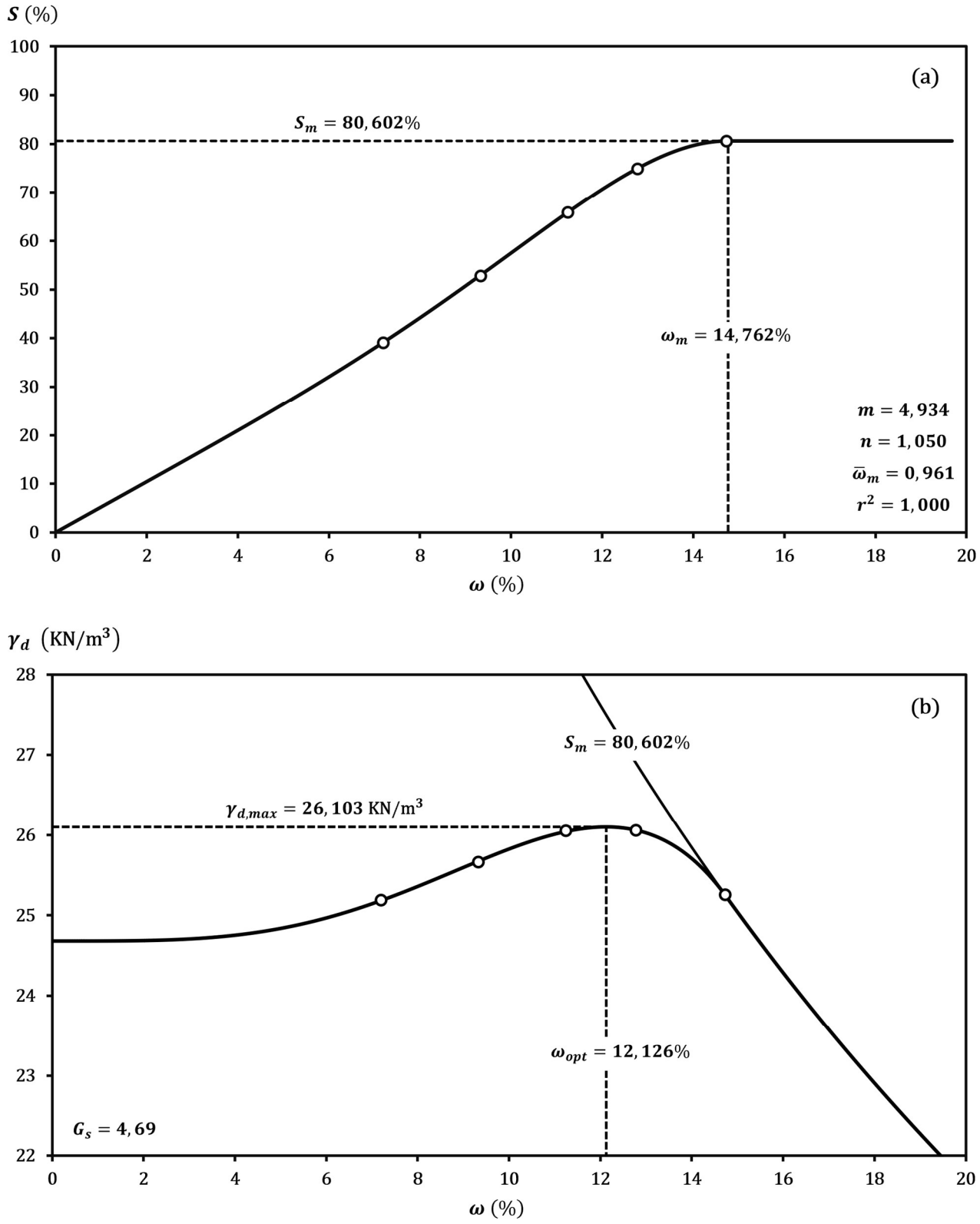

Figure 7

While exponents n and m are altogether responsible for providing curvature and asymmetry on any direction to the compaction curve, $\bar{\omega}_m$ is a more neutral parameter and, as a first simplification, one may simply take $\bar{\omega}_m = \bar{\omega}_B$ or a fraction of it. This $S(\omega)$ model is very flexible and, at the same time and because of it, very sensible to small variations of the test data it intends to mimic. Many combinations of the parameter values will

provide a very good fit with test data, and such flexibility is welcomed to allow a good discussion to flourish ahead on this booklet. Say we are constructing now what will be destroyed afterwards for the strength of any argument. This, rebuilding on the debris of what we built and destroy, is the way some men, divinely uninspired, can do get inspiration.

Figure 7, on the previous page, contains in part (a) an arbitrary example of application our $S(\omega)$ function to the data from a standard compaction 5-point test, performed on a filtered iron-ore mine tailings sample. On part (b) of the same figure, the resulting compaction curve is shown.

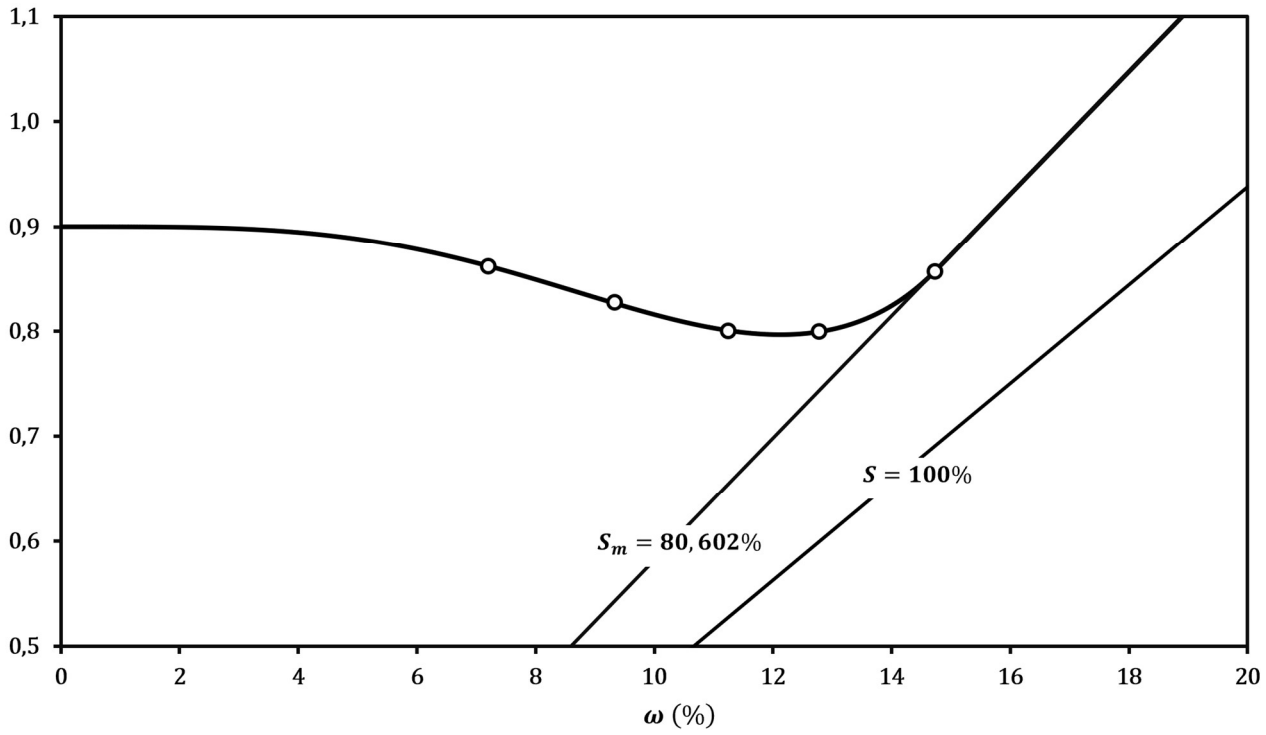

Figure 8

There are several other useful forms of representing the compaction curve of a soil and we will be using some of them indistinctly. The compaction curve can be drawn on the ω-e space, as applied to the same material sample used for Figure 7 and shown in Figure 8 or it can be drawn in relative terms, using the deviation of saturation degree in relation to the optimum, $S - S_{opt}$, and the degree of compaction R, as shown in Figure 9 at the beginning of next page. These alternative representation forms are particularly useful to superimpose the compaction curves of different samples, eventually from the same "unique" material. The specific gravity of solids is one of those variables whose noise we usually want to get rid of.

In principle, we have developed a mathematical model which is sufficiently flexible to describe the compaction curve of many soils, using a curve-fitting technique to derive its parameters from test data points. Obviously, 5-point standard tests, being restricted to a narrow range around the point of optimum, do not allow validating to full-extent all the hypothesis used to build the $S(\omega)$ function, but, anyway, it is around the point of optimum that we are interested to investigate. It might be questionable to develop a rich five parameters model and simultaneously "complain" about the variability of the test results data. As in life, it is easier to become poorer than getting richer and any further possible simplification is not just easy to implement but also welcomed.

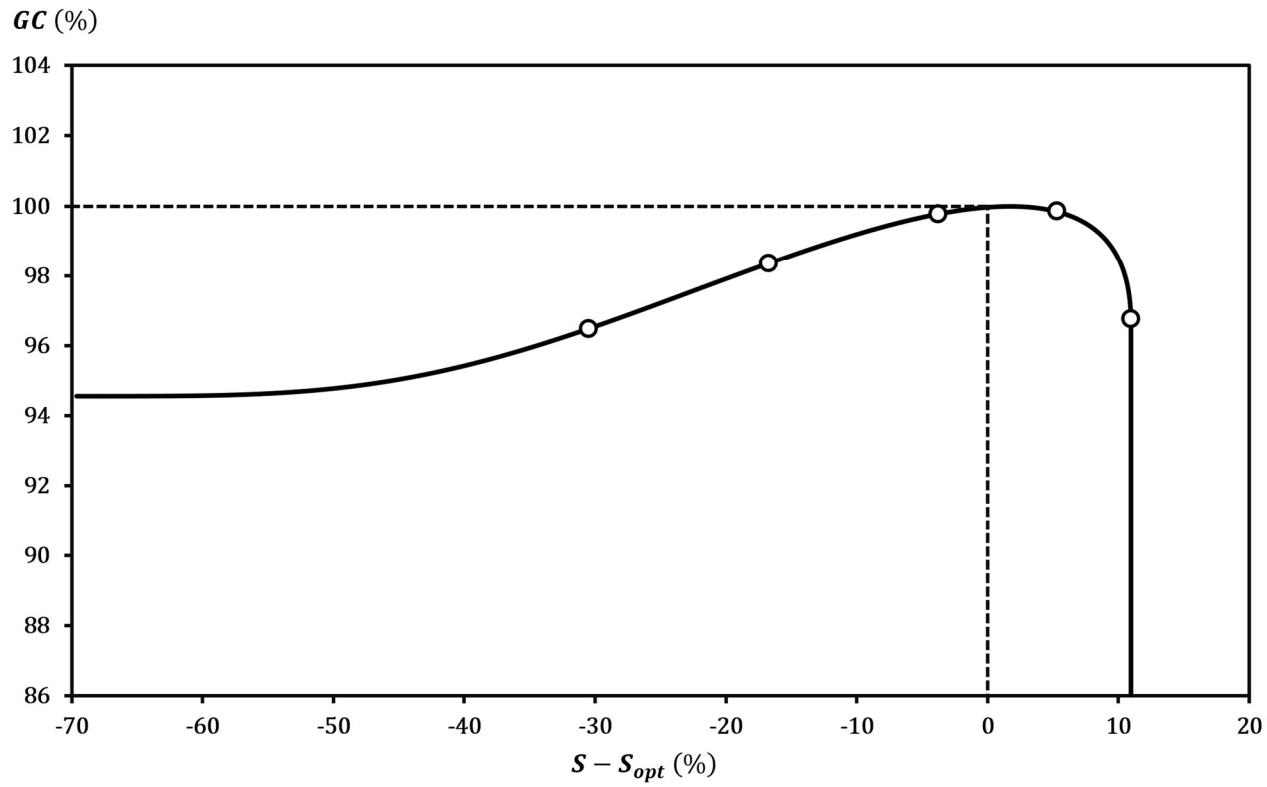

Figure 9

After testing the model on 250 different compaction tests, fortuitously or not as much, an application example with a perfect fit has been provided to start with. On that universe of tests, the coefficient of determination was 0,989±0,024. However, even if the model error was null, its accuracy would be seriously affected by measurement errors and acceptable reference values are unavailable to evaluate the closeness of agreement of test data. So far, our $S(\omega)$ function is just a mathematical preciousness, limited to single peak compaction curves or to a limited range of water contents around the optimum point of an irregular compaction curve. Nevertheless, with a simple adjustment, our $S(\omega)$ function is also able to simulate one-and-one half peak compaction curves. One subchapter down, we will be discussing the measurement errors and to what extent they affect any attempt of rationalising soil compaction.

At this moment of reading no one should be wondering what the author thinks about a statement declaring the inexistence of a relationship between the degree of compaction and the void ratio of a soil, even if it is called filtered tailings. About the “0,6 maximum void ratio” criterium, for now, in view of Figure 8, we just can repeat what was said before. Sometimes, when money is not a concern, is better to buy heavier rollers or place the mine waste elsewhere, not on a “0,6 maximum void ratio” non liquefiable tailings pile. And that was what happened on the case that motivated this booklet writing. At this point, we are far from understanding what the “0,6 maximum void ratio” criterium means exactly.

3.3. A short pause to pay tribute to Hilf

We wouldn't feel good about ourselves to be writing about compaction without at least mentioning Jack Hilf. Hilf’s “rapid method of construction control for embankments of cohesive soils” dates to the end of the fifty’s decade of last century and still is extensively used, as it was six decades later to obtain the data presented earlier on Chapter 2. The method, responding to the need of timesaving on the production pauses required on site to

validate the ongoing compaction quality, is one of those ingenious ideas that everyone finds obvious after getting knowledge of it. On this booklet we will not be addressing the quality control procedures on-site, even because our patient by those days seemed to somehow confuse the value of the enormous amount of testing data stored in some server with the value of information and preferred to keep data in secrecy. Perhaps is because of it that the windwards side of powder mountains are, as we write, being constructed with less voids than they are on the leeward side.

At some point of Hilf's method a second-degree polynomial function will have to be fitted to three determinations of wet unit weight, γ_h, and, after some conversion, the vertex of a parabola must be derived. The curve-fitting, analogous to what we will be using, is what justifies this pause at this moment, although being the less shinning part of Hilf's method. The expedite method allows to estimate the degree of compaction and the deviation of water content from optimum, $\Delta\omega = \omega_{opt} - \omega$, without knowing the maximum dry unit weight or the optimum water content. It goes as briefly follows. Let ω_f be the field water content of a test specimen and z the weight of water added (or removed) on the laboratory to two equal specimens sampled around the field-testing point, expressed in percentage of the weight of the initial sample:

$$z(\omega) = \frac{\Delta W_w}{(W_w + W_s)_f} \times 100\% = \frac{\omega \cdot W_s - \omega_f \cdot W_s}{(1 + \omega_f) \cdot W_s} \times 100\% = \frac{\omega - \omega_f}{1 + \omega_f} \times 100\% \Longrightarrow$$
$$\Longrightarrow 1 + z = \frac{1 + \omega}{1 + \omega_f} \quad [43]$$

A function called converted wet unit-weight, $g(z)$, can be defined as follows:

$$g(z) = \frac{\gamma_h}{1 + z} = \frac{\gamma_d \cdot (1 + \omega)}{\frac{1 + \omega}{1 + \omega_f}} = \gamma_d \cdot (1 + \omega_f) \quad [44]$$

After converting the three measurements of unit wet weight and even just having one measurement of ω_f we have got three points, (z_1, g_1), (z_2, g_2) and (z_3, g_3), from where a maximum value of converted wet unit-weight, g_{max}, can be derived. From the equation of a quadratic polynomial, $g = a \cdot z^2 + b \cdot z + c$, we know that the ordinate of the vertex of the parabola will be located at:

$$g_{max} = c - \frac{b^2}{4 \cdot a} \quad [45]$$

With:

$$a = \frac{z_1 \cdot (g_2 - g_3) + z_2 \cdot (g_3 - g_1) + z_3 \cdot (g_1 - g_2)}{(z_1 - z_2) \cdot (z_2 - z_3) \cdot (z_3 - z_1)} \quad [41]$$

$$b = -\frac{{z_1}^2 \cdot (g_2 - g_3) + {z_2}^2 \cdot (g_3 - g_1) + {z_3}^2 \cdot (g_1 - g_2)}{(z_1 - z_2) \cdot (z_2 - z_3) \cdot (z_3 - z_1)} \quad [42]$$

$$c = -\frac{z_1 \cdot z_2 \cdot (z_1 - z_2) \cdot g_3 + z_2 \cdot z_3 \cdot (z_2 - z_3) \cdot g_1 + z_3 \cdot z_1 \cdot (z_3 - z_1) \cdot g_2}{(z_1 - z_2) \cdot (z_2 - z_3) \cdot (z_3 - z_1)} \quad [43]$$

Having g_{max}, the field degree of compaction is immediately calculated:

$$R = \frac{\gamma_d}{\gamma_{d,max}} \times 100\% = \frac{\gamma_h/(1+\omega_f)}{g_{max}/(1+\omega_f)} \times 100\% = \frac{\gamma_{h,F}}{g_{max}} \times 100\% \quad [44]$$

Also, letting z_{max} be the abscissa of the maximum converted wet unit weight, we also know that:

$$\omega_{opt} - \omega_f = \frac{z_{max}}{1 + z_{max}} \cdot (1 + \omega_{opt}) \times 100\% \quad [45]$$

Avoiding the determination of the optimum water content, ω_{opt}, to save time, its value may be estimated from empirical correlations with the maximum wet density (for example ASTM, 2017). Going back to Chapter 2, the values of the field degree of compaction shown on Figure 2, or Figure 3, were all of them obtained with the Hilf method and are referred to the normal Proctor energy. Values of the degree of compaction over 100%, faced with distrust by our friends, the mountain builders, meant simply that the tailings placed on the first stage were being over-compacted or compacted with an energy greater than the one used earlier to find the miraculous "0,6 maximum void ratio" limit. The best solution to over-compaction is over-over-compaction. So, on the second stage of construction, almost 50% of the material was placed with a degree of compaction greater than 104%. We may presume that filtered tailings are innocuous to the detrimental effect of over-compaction found on some soils. Other effects that not the production cost, naturally.

3.4. Testing our $S(\omega)$ function

To investigate the quality of the model, we will be starting this subchapter with an attempt of curve-fitting to the results of compaction tests performed on samples of two different iron-ore filtered tailings, each of them submitted to four different levels of energy (2 materials × 4 energies × 1 test). At all, eight compaction curves were individually simulated making use of a total of $N = 42$ determinations ω-γ_d. As the objective of the exercise is not to find some meaning for the model parameters, curve-fitting was carried without imposing any constraint on the values of the parameters from one individual curve to another, including those of the same material.

For both tailings samples simultaneously, Figure 10, on next page, compares, point by point, the values measured or directly derived from measurements, y, with the values predicted with the model, $\hat{y}$, respectively on part (a) for the degree of saturation and on part (b), for the dry unit weight. The absolute percentage error ε and its mean value $\bar{\varepsilon}$ for the whole data set can be used as the evaluation metrics of the accuracy of the model and are defined as follows:

$$\bar{\varepsilon} = \frac{1}{N} \cdot \sum_{i=1}^{N} \varepsilon_i = \frac{1}{N} \cdot \sum_{i=1}^{N} \frac{|y_i - \hat{y}_i|}{y_i} \times 100\% \quad [46]$$

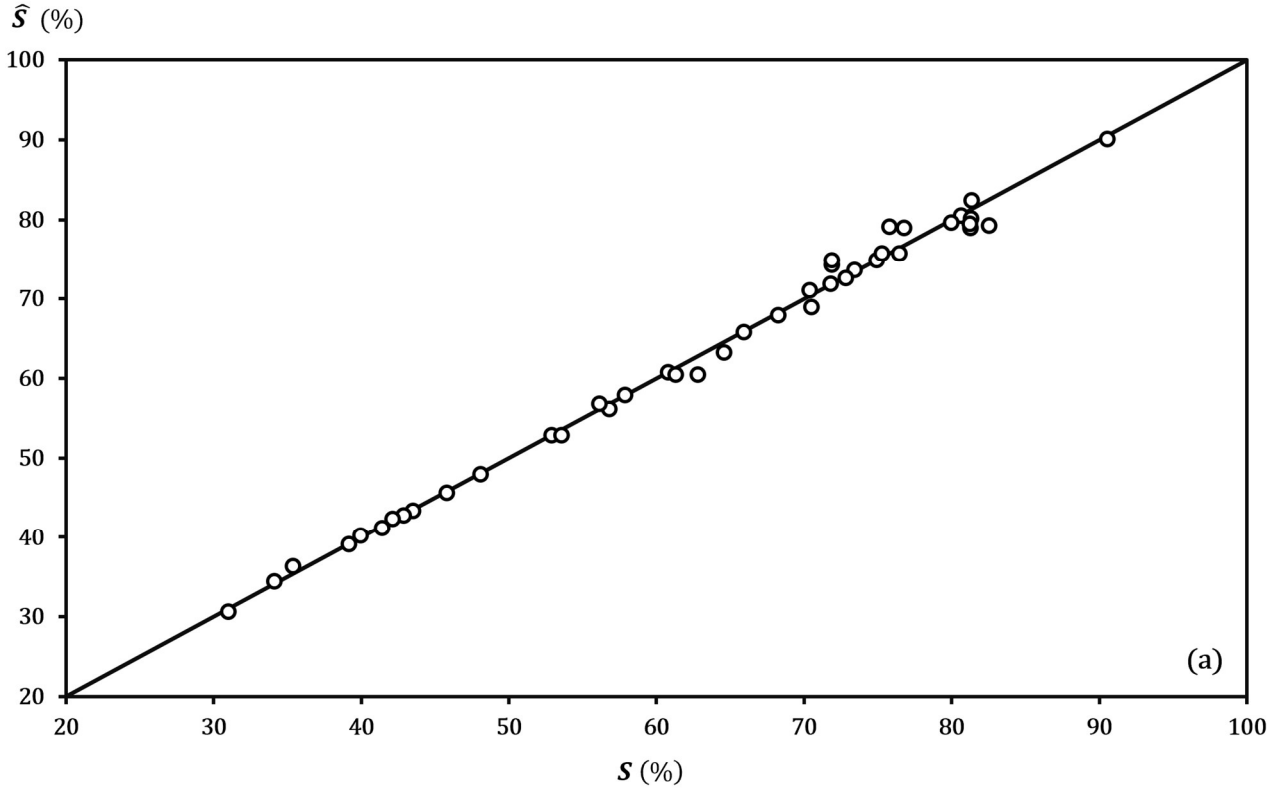

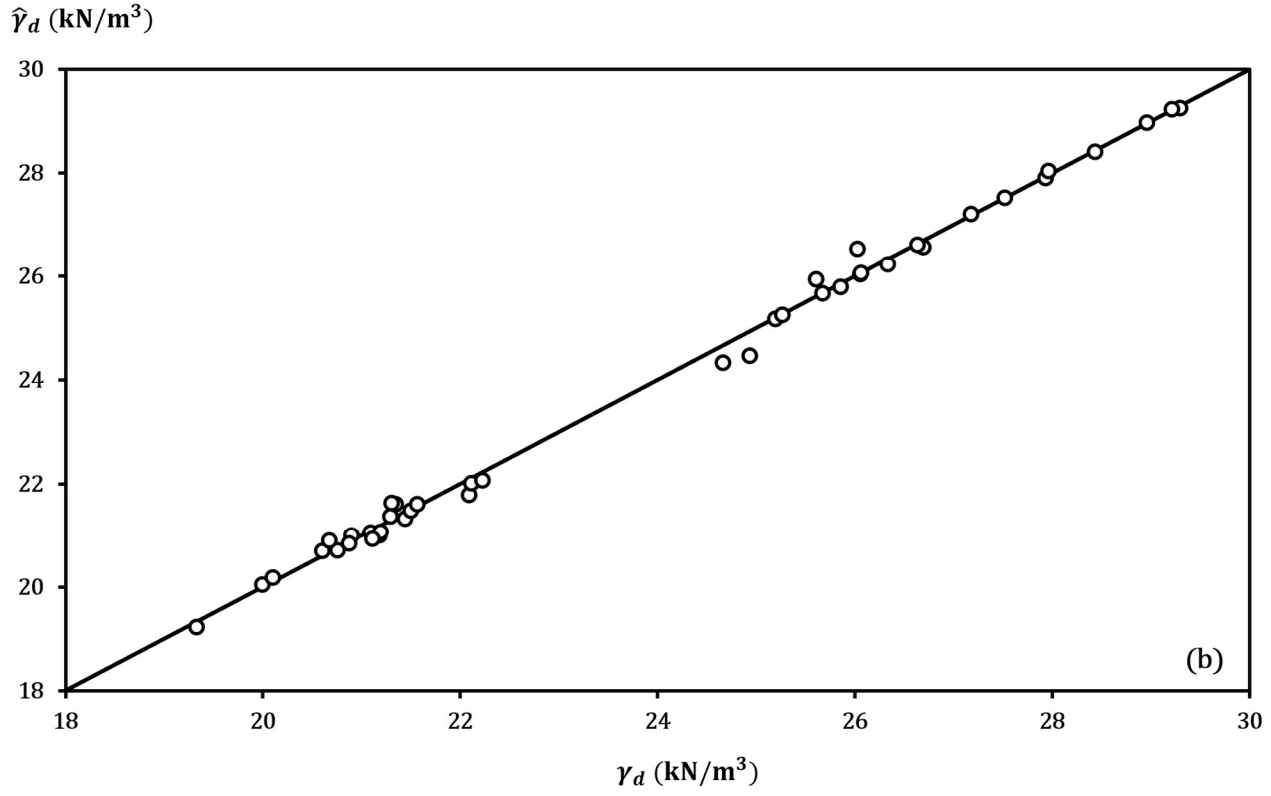

Figure 10

For this same evaluation exercise, Figure 11, one page down, shows the absolute percentage error point by point and the mean absolute percentage error value of all data, respectively for the degree of saturation in part (a) and for the dry unit weight on part (b). Dashed lines correspond to the 95th percentile of measurements. The

resulting mean absolute percent error is 1,22% for the saturation degree and 0,49% for the dry unit-weight. On 95% of the determinations, the absolute percent error is lower than 4,20% for the saturation degree and lower than 1,81% for the dry unit-weight, suggesting that the model error is not greater than the measurement one.

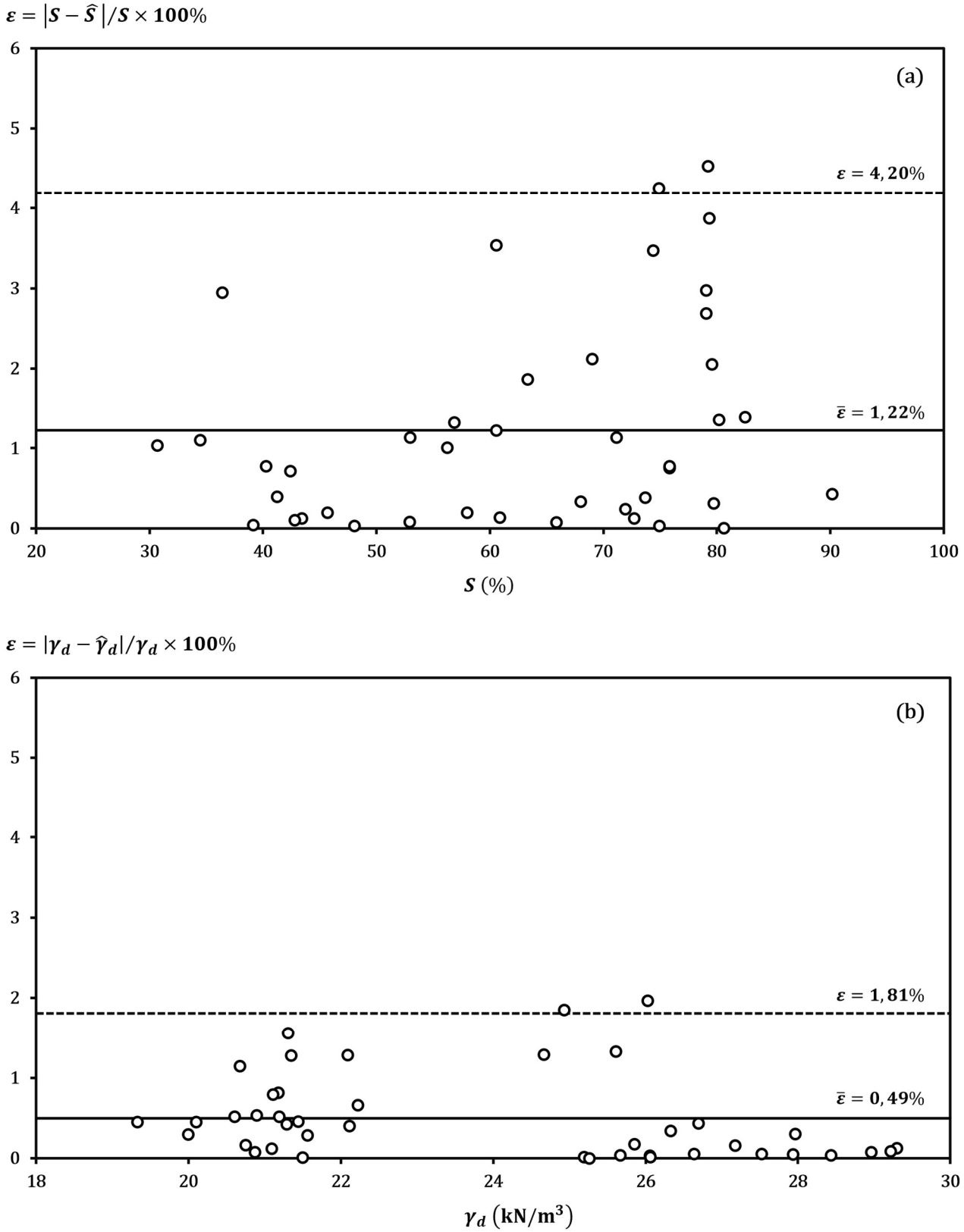

Figure 11

For instance, a similar metrics is used on the Australian compaction test standard, 1289.5.1.1:2017, to evaluate the precision of laboratory test data, either in terms of repeatability or reproducibility. The limit of acceptance of each two determinations of dry unit weight is 2% in what concerns to repeatability and 4% in what concerns to reproducibility, in accordance with that standard. The North American standard, ASTM D698-12(2021), also gives information about the measurement errors, although a little more stringent acceptance criteria is provided.

On a second model evaluation exercise, results of compaction tests done on samples of two other iron-ore filtered tailings were used, each of them having been subjected to one-time repeated tests under two different compaction energies (2 materials × 2 energies × 2 tests). At all, this second data set also comprises $N = 42$ determinations ω-γ_d. The mean absolute percent error $\bar{\varepsilon}$ resulting from curve-fitting individually to each of the 8 compaction curves is 0,50% for the saturation degree and 0,20% for the dry unit-weight. On 95% of the determinations, the absolute percent error is less than 2,70% for the saturation degree and less than 1,18% for the dry unit-weight. Compared with the results obtained on the previous exercise, a better curve-fitting was obtained with this new set of data. Everything is different on the data used for this second exercise, not just the material itself but also the laboratory where tests were performed.

Using alternately the compaction curves simulated individually for each member of the 4 pairs of tests available, the distances relatively to the measurement points of the pairing test were then calculated, providing some sense on the repeatability errors of testing. The number of points in comparison is obviously the same ($N = 42$). Now the resulting mean absolute percent error is 2,09% for the saturation degree and 0,82% for the dry unit-weight, nearly four times greater than the modelling error alone reported on the precedent paragraph. On 95% of the determinations, the absolute percent error is lower than 6,08% for the saturation degree and lower than 2,23% for the dry unit-weight, nearly the double of the modelling error on its own. Exceptionally the errors committed on the prediction, we may believe, will not exceed 50% of those acceptable for repeated testing.

Still using the simulated curves to measure the error between each pair of test measurements, the same analysis was done but this time separately for each different compaction energy. The number of points in comparison is $N = 21$ for each of the two different energies. The laboratory measurement error committed on the test repetition is greater for the heavier compaction energy. The mean absolute percent error for the saturation degree is 1,65% under the normal Proctor energy and 2,48% under the modified Proctor energy. The mean absolute percent error for the dry unit weight is 0,69% under the normal Proctor energy and 0,94% under the modified Proctor energy. On 95% of the determinations of the saturation degree, the absolute percent error is lower than 4,45% under the normal Proctor energy and lower than 6,34% under the modified Proctor energy. For the dry unit weight, on 95% of the determinations, the absolute percent error is lower than 2,00% under the normal Proctor energy and lower than 2,33% under the modified Proctor energy. The greater the compaction energy is, the greater seem to be the measurement errors.

Finally, a single curve was simultaneously fitted to all the points of each pair of repeated tests done on the same soil under the same energy. The total number of modelled curves is four and the number of points in comparison is again $N = 42$, being the errors on each test point measured in relation to the average curves obtained for the pair of repeated tests. The mean absolute percent error is 1,20% for the saturation degree and 0,48% for the dry unit-weight, around half of the values obtained when each data point from a pair member was compared to the curves simulated separately for the other pair member. On 95% of the determinations, the absolute percent error is lower than 2,99% for the saturation degree and lower than 1,18% for the dry unit-weight.

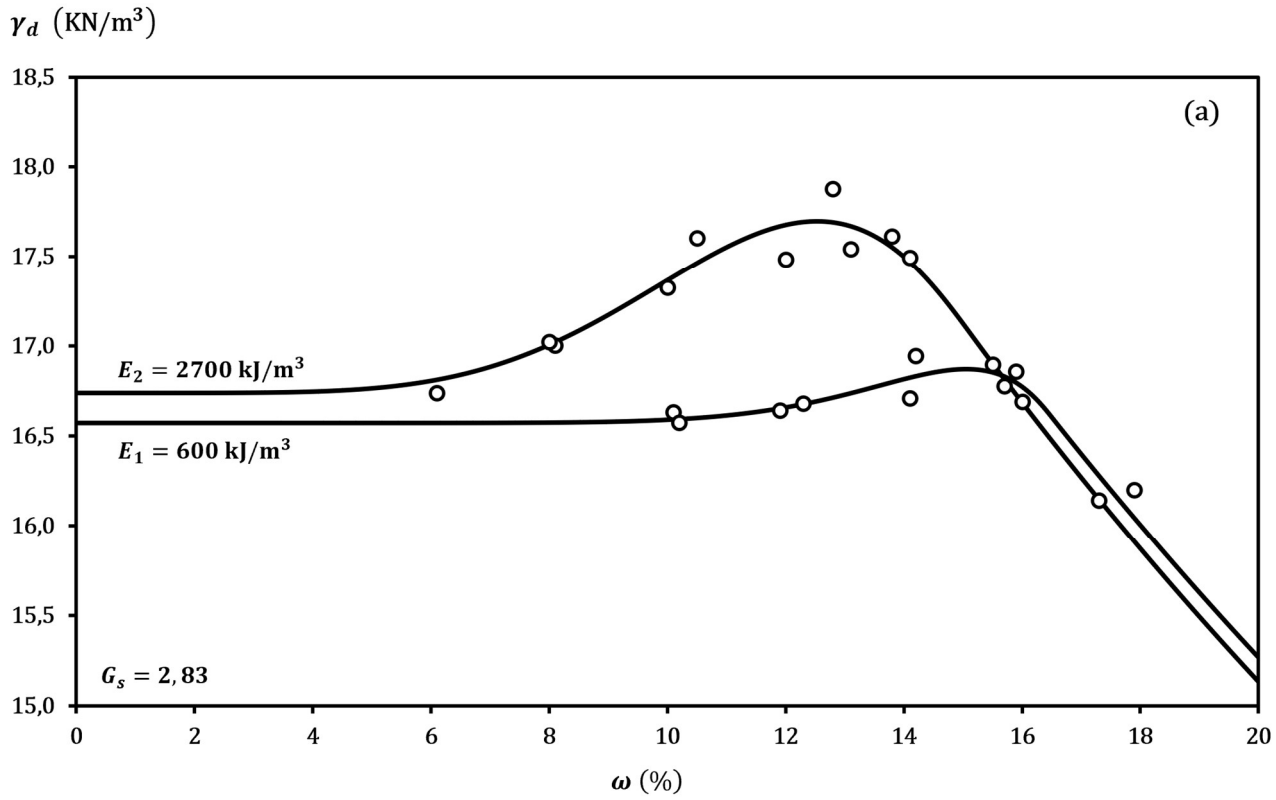

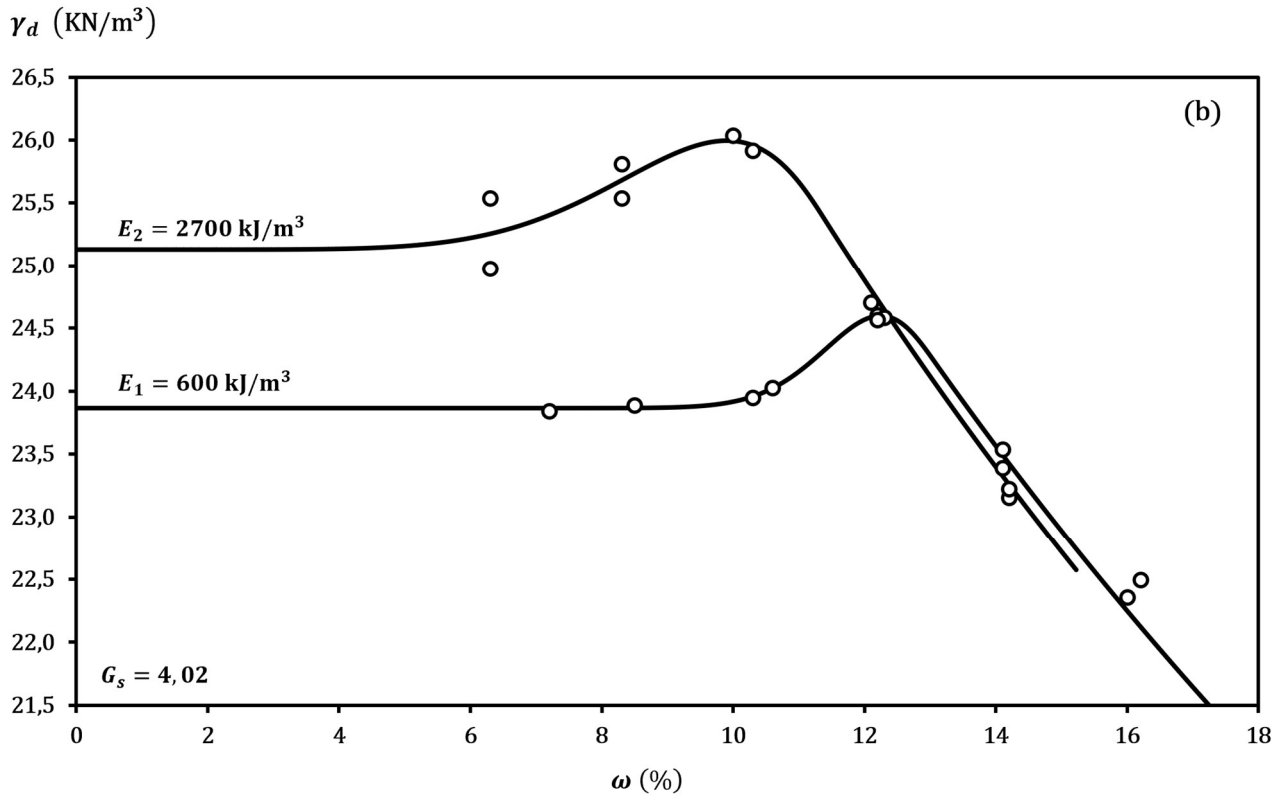

Figure 12

Figure 13 shows in part (a) the simulated compaction curves for one of the tailings samples and in part (b) for the other one, alongside with the two sets of repeated test data available for each compaction energy. It is worth noting that the parameter that most influences the absolute values of dry unit weight is the specific gravity of solids, which, for the latter set of tests, has a value of 2,83 for one of the tailings and 4,02 for the other one.

As we will see, the range of values of specific gravity of the dewatered tailings obtained from the same operation plant and destined for the same dry stacking pile is wider than on other type of earthwork material.

A third and last model validation exercise was done to ascertain the propagation of the measurement errors through the model. It is a simple and light legwork exercise. A perfect model fit to a five-points compaction test serves as the starting point, assuming that the resulting compaction curve is exempted of any error. On the previous exercise, we have quoted a standard that defines that two determinations, on the same laboratory, of the (maximum) dry unit weight will be acceptable if the absolute value of ratio between their difference and the average value of both measurements is no greater than 2%. The same standard finds acceptable that the same metrics apply to the (optimum) water content determination, with a limit of 10%. As neither the maximum dry unit weight nor the optimum water content is as measurement, we enlarged the application of these acceptance criteria to any point (ω, γ_d) obtained on a compaction test. We have assumed that those precision limits mean that 95% of all measurements will differ no more than 1,96× $\sqrt{2}$ standard deviations from each other and the respective coefficients of variations were estimated from there.

Assuming that the specific gravity of solids is an exact quantity, the uncertainty (the standard deviation) on the calculation of the void ratio δe from test measurements would be:

$$\delta e \cong \sqrt{\left(\frac{\partial e}{\partial \gamma_d}\right)^2 \cdot \delta {\gamma_d}^2} = \frac{\gamma_w \cdot G_s}{\gamma_d} \cdot \frac{\delta \gamma_d}{\gamma_d} = (1+e) \cdot \frac{\delta \gamma_d}{\gamma_d} \qquad [47]$$

And the uncertainty on the calculation of the degree of saturation δS would be:

$$\delta S \cong \sqrt{\left(\frac{\partial S}{\partial e}\right)^2 \cdot \delta e^2 + \left(\frac{\partial S}{\partial \omega}\right)^2 \cdot \delta \omega^2} = \sqrt{\left(-\frac{\omega \cdot G_s}{e^2}\right)^2 \cdot \delta e^2 + \left(\frac{G_s}{e}\right)^2 \cdot \delta \omega^2} = S \cdot \sqrt{\left(\frac{\delta e}{e}\right)^2 + \left(\frac{\delta \omega}{\omega}\right)^2} \qquad [48]$$

Producing repeated random 5-point arrays of ω and γ_d, each of them with an expectation given by our initial mean compaction curve, would allow to confirm on the long run the propagated errors δe and δS given by the above equations. The long run could be after thousands of arrays, but our objective is not to confirm the error propagation equations. We are interested to know how affected by the model the measurement errors are and for that we have produced 200 random 5-point arrays of ω and γ_d and fitted our model to each of them. The difference on the errors due solely to measurements and those resulting from the simulated curves in relation to the expected values should provide a good feel on the modelling errors alone.

If we insist on the absolute percentage error as the evaluation metrics, the mean value of the error attributable to measurements alone is of 1,65% and 1,63% for the calculated values of saturation degree and void ratio, respectively. The mean value of the total error, including that due to modelling, is of 1,46% and 1,45% for the calculated values of degree of saturation and void ratio, respectively. This means that the model has some corrective effect on most cases, being the mean value of the modelling error of (−) 0,19% for either the calculated values of degree of saturation or void ratio. Just like the expert eye of the laboratory technician would detect them, the model penalises measurements that are seemingly outliers.

On 80% of the calculated values, the maximum error attributable to measurements is of 2,61% and 2,59% for the degree of saturation and void ratio, respectively. For the same percentile, the maximum total error is of 2,32% and 2,28% for the calculated values of degree of saturation and void ratio, respectively. The error attributable to modelling alone is on 80% of the calculations of (−) 0,35% or (−) 0,36% for the degree of saturation and void ratio, respectively. On 95% of the calculated values, the maximum error attributable to measurements alone is of 4,27% and 4,33% for the calculated values of saturation and degree and void ratio, respectively. For the same percentile, the mean total error is of 3,75% and 3,69% for the calculated values of degree of saturation and void ratio, respectively. The error attributable to modelling alone is on 95% of the calculations of (−) 1,18% or (−) 1,14% for the degree of saturation and void ratio, respectively. So, effectively, just exceptionally the error committed on a simulation will be as high as 50% of that considered acceptable for the measurements.

In terms of uncertainty, which is centered on each single value of ω, the relative error (the coefficient of variation) obtained for the simulated degree of saturation is $\delta S/S =$ 0,033 to 0,045 and the relative error obtained for the simulated void ratio $\delta e/e =$ 0,013 to 0,016. According to Equation 47 and Equation 48, the relative error for the values calculated from measurements directly would be $\delta S/S =$ 0,035 to 0,042 and $\delta e/e =$ 0,012 to 0,015. 200 random 5-point arrays of ω and γ_d was the number necessary to bring the numerical results of the measurement uncertainty within these latter values.

Now it should be the moment to say how good our model is, even if none of the previous testing exercises shine for statistical erudition. We do not need to say it beyond evidence, so we will limit ourselves to say this is the best model we know about. And the only one also. One is better than none. We will return to this subject on Chapter 5, where the application of a compaction curve model on the real world is discussed.

4. THE THIRD DIMENSION

4.1. Compaction energy

On a standard laboratory compaction test, a soil with a known water content is placed in N_L layers on a mould with volume V, being each layer compacted with N_B blows of a rammer with weight W dropped from a height H. The compaction energy per unit volume is:

$$E = \frac{W \cdot H \cdot N_L \cdot N_B}{V} \quad [49]$$

Being any of the variable's values standardised. Compaction curves determined with other laboratorial method, and on field as well, are not necessarily equal to those obtained following the standard test. In any case, as already could be seen on Figure 12, increasing the compaction effort forces a point corresponding to a certain degree of compaction in the space ω - γ_d to displace upwards, on the sense of increasing dry weights and leftwards, on the sense of decreasing water contents. Basically, a greater density at cost of less moulding water. Despite the general trend, the displacement of the compaction curves does not evolve linearly with the applied energy, nor the shape of the compaction curves is maintained on the travel.

Furthermore, even for a "unique" soil, as the filtered tailings could be, the efficiency of compaction not just decreases with an increasing effort, as it is highly variable. To some extent Figure 4 shows that an increase on the compaction energy resulted on a spreading of the end-product properties, not on a simple translation towards a denser status with the same dispersion. Figure 13, on the next page, corroborates either the general trend or the practical difficulty of predicting the effect of an energy increase on a large mass of compacted soil. The data on this figure was obtained from compaction tests on 24 different iron ore tailings, from which 2 were subjected to 4 different compaction efforts, 13 were subjected to 3 different compaction efforts and 9 were subjected to 2 different compaction efforts, from which 2 were subjected to one-time repeated tests.

All the 24 different materials were subjected to a compaction effort equivalent to that of the normal Proctor, which is herein taken as the reference, E_R. It can be seen in part (a) of the referred figure that increasing the energy to $E/E_R = 4{,}5$, leading to the modified Proctor energy, results on a decrease on the required optimum water content to $\omega_{opt}(E)/\omega_{opt}(E_R) \times 100\% = 84{,}5 \pm 4{,}2\%$. In part (b) of the same figure, for the same increase on the energy, an increase of the maximum dry unit weight to $\gamma_{d,max}(E)/\gamma_{d,max}(E_R) \times 100\% = 104{,}3 \pm 1{,}9\%$ results. These findings are appreciably in line with those obtained on the analysis of the statistical distribution of the field control tests results presented earlier on Chapter 2, for a particular dry stacking tailings pile.

Going back to Figure 2 or Figure 3, we can roughly conclude that moving all the compaction points, including those with a void ratio of 0,72, below the "0,6 maximum void ratio" limit would be equivalent to raise the maximum dry weight by about 8%. According to Figure 13, the compaction energy required to fulfil the requirement would have to be around five times greater than the one being applied earlier. That means thinner layers, more compactor passes and heavier rollers. Just like it was done for the second stage of construction of the tailings pile introduced on Chapter 2.

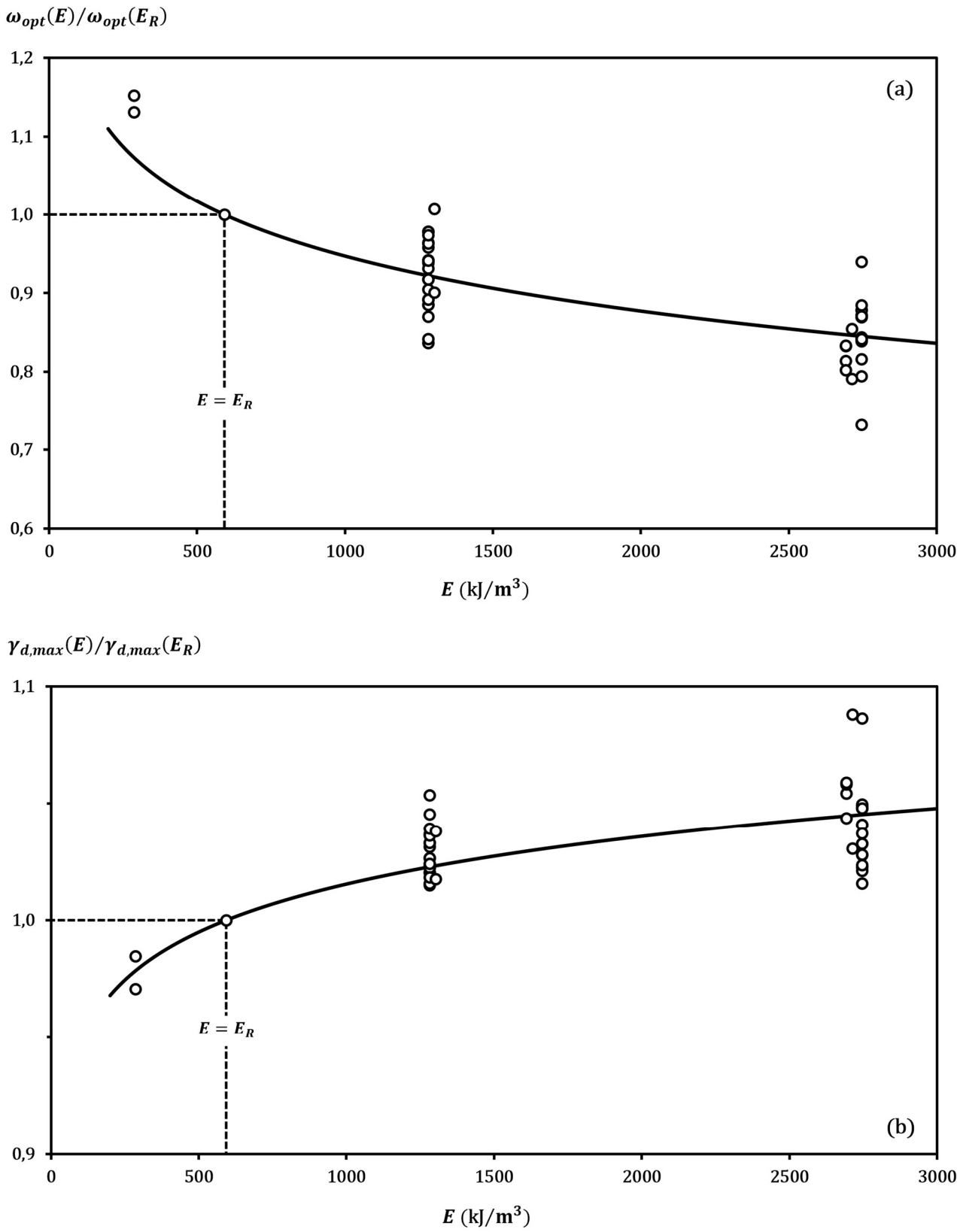

Figure 13

Having observed, as in Figure 12, that the maximum water content and the saturation degree upon which a material no longer can be dynamically compacted both decrease with increasing compaction energy, the

following relationships between the model parameters ω_m and S_m and the compaction energy E are put forward:

$$\frac{\omega_m}{\omega_{mR}} = 1 + k_1 \cdot \log\left(\frac{E}{E_R}\right) \quad [50]$$

And:

$$\frac{S_m}{S_{mR}} = 1 + k_2 \cdot \log\left(\frac{E}{E_R}\right) \quad [51]$$

Being ω_{mR} and S_{mR} the maximum water content and respective saturation degree obtained for a reference energy E_R. We will be calling the ratio E/E_R as the relative energy. Coefficients k_1 and k_2, expectably with negative values, are determined from experimental data and allow defining a family of compaction curves for the same material from a single compaction curve, that we will call the reference one. Inversely, the compaction energy for any point on the ω-γ_d space, or any other space correlated with these variables, can be found by the following equality:

$$\log\left(\frac{E}{E_R}\right) = \frac{\omega_{mR} \cdot S_m - \omega_m \cdot S_{mR}}{k_2 \cdot \omega_m \cdot S_{mR} - k_1 \cdot \omega_{mR} \cdot S_m} \quad [52]$$

As the shape of the compaction curve also changes with the applied energy, the same approach can be used for the remaining model parameters m, n and $\bar{\omega}_m$. A line connecting all the points of limiting compaction water content is readily available using:

$$\frac{\omega_m}{S_m} = \frac{1 + k_1 \cdot \log\left(\frac{E}{E_R}\right)}{1 + k_2 \cdot \log\left(\frac{E}{E_R}\right)} \cdot \frac{\omega_{mR}}{S_{mR}} = \left(\frac{k_2 - k_1}{k_2 \cdot \left(k_2 \cdot \log\left(\frac{E}{E_R}\right) + 1\right)} + \frac{k_1}{k_2}\right) \cdot \frac{\omega_{mR}}{S_{mR}} \quad [53]$$

Any reference energy compaction curve will be dragged on space with the displacement of the point of maximum water content (ω_m, S_m) along this common place line, according to any other applied compaction energy. If a family of compaction curves was to displace along the same saturation line, coefficient k_2 would have to be null. Also, a line of optimums, that is a line connecting all the points of optimum water content, can be obtained from:

$$\frac{\omega_{opt}}{S_{opt}} = \left(\frac{\bar{\omega}_{opt}}{\bar{S}_{opt}}\right) \cdot \left(\frac{\bar{S}_m}{\bar{\omega}_m}\right) \cdot \left(\frac{k_2 - k_1}{k_2 \cdot \left(k_2 \cdot \log\left(\frac{E}{E_R}\right) + 1\right)} + \frac{k_1}{k_2}\right) \cdot \frac{\omega_{mR}}{S_{mR}} \quad [54]$$

Where the first term of the product chain on the right hand-side member is given by Equation 40 and the second term is given by Equation 42. However, these two terms, which are uniquely functions of the model parameters

m, n and $\bar{\omega}_m$, can be themselves functions of the relative compaction energy as required to change the shape of the compaction curve within the family of the same material.

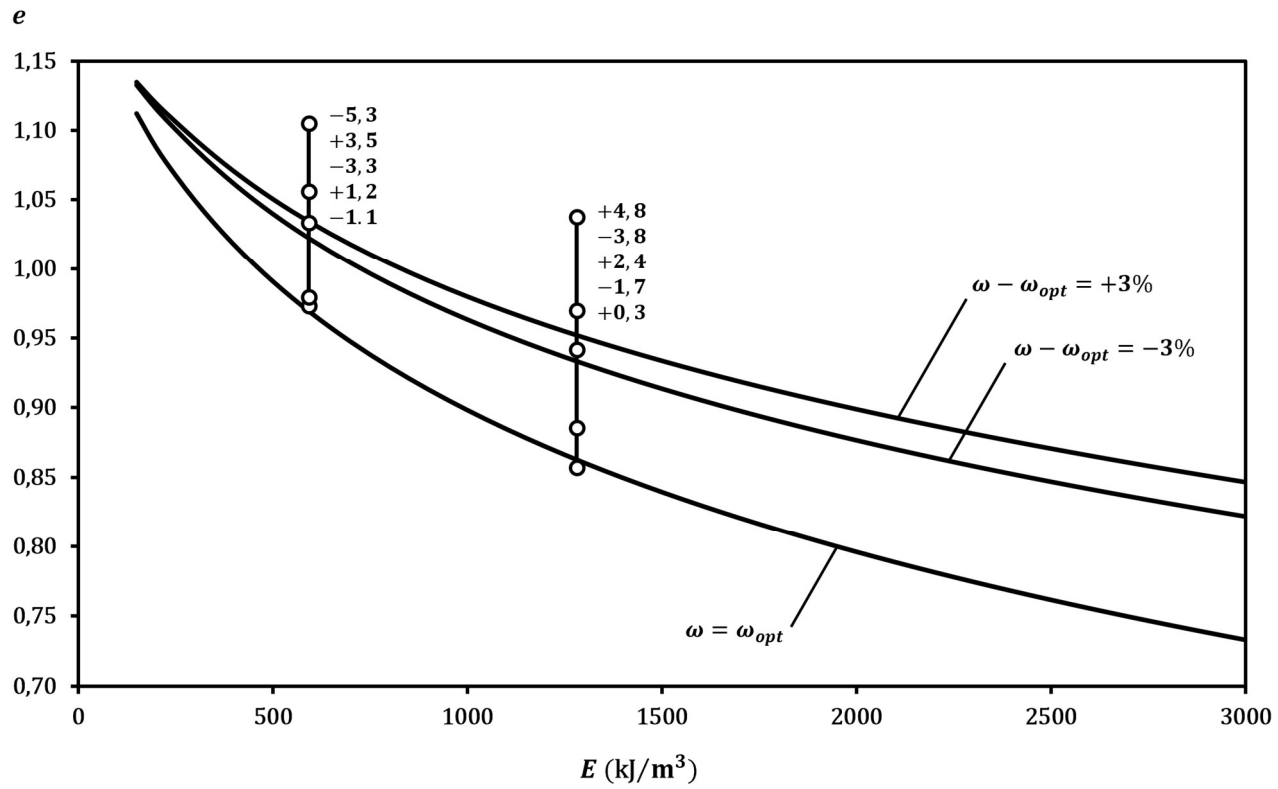

Figure 14

To further illustrate the predictive ability that is incorporated to our model by Equation 50 and Equation 51, it is shown on Figure 14 how the void ratio varies with the compaction energy for three different deviations of water content from optimum, $\omega - \omega_{opt}$. The curves were derived from two compaction tests on the same sample of an iron ore filtered tailings, one using the normal proctor energy, $E = E_R$, and the other one using a higher energy, $E/E_R = 2{,}16$. The 5-points of each compaction test are represented on the figure as dots, labelled with the respective deviation of water content from optimum. For this example, model parameters m and n were not constrained, but their ratio was kept constant. Data from this example will continue to be used throughout the next section.

Figure 15, on next page, shows the transformed space curves $\bar{\omega}$ - $\bar{S}$, in part (a) for one iron-ore tailings sample and on part (b) for the other one, that are the basis of a family of compaction curves for each material under different compaction energies. For each material sample, four compaction tests under different energies were done, providing a series of 21 points each. The model was simultaneously fitted to the four compaction curves data series of each material and the test results presented on the figure have been brought back to the transformed space, where the model fitting to data can be appreciated over a single non-dimensional curve. For this testing exercise, the values of the model parameters m, n and $\bar{\omega}_m$ were kept constant for the same material, what allows presenting all data on the same graph, and the values of the remaining parameters, ω_m and S_m, were allowed to vary with respect to the relative energy in accordance with the previously proposed relationships.

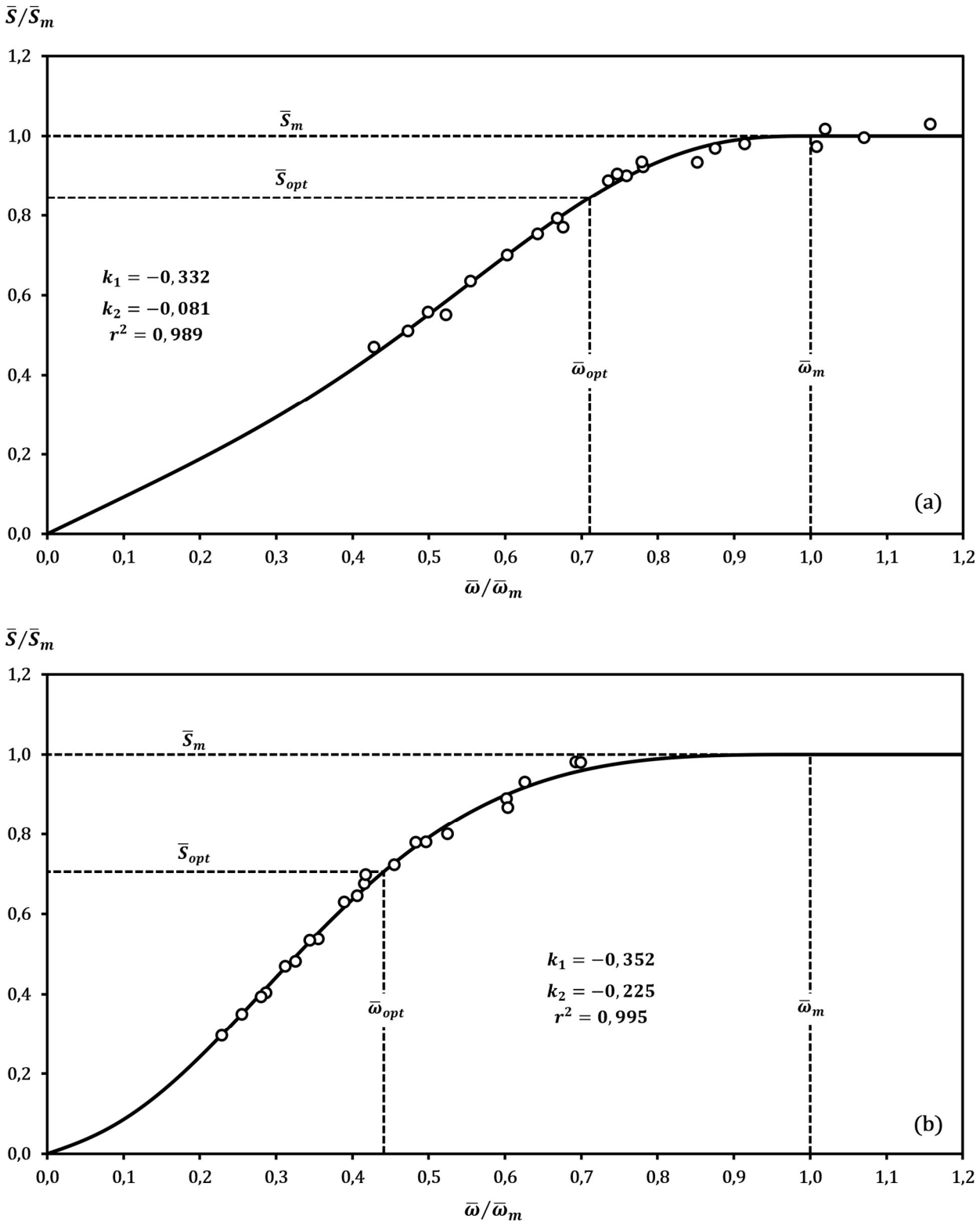

Figure 15

At cost of two additional parameters, k_1 and k_2, which now become 7 in total, it seems that we can expand the model predictive capacity to a three-dimensional space, ω-e-E, with a very reasonable agreement with test data. The third dimension, now added, is crucial to link the compaction state of a soil to its relevant geotechnical properties, like compressibility or shearing resistance. It is crucial or could be crucial, depending on the test data available.

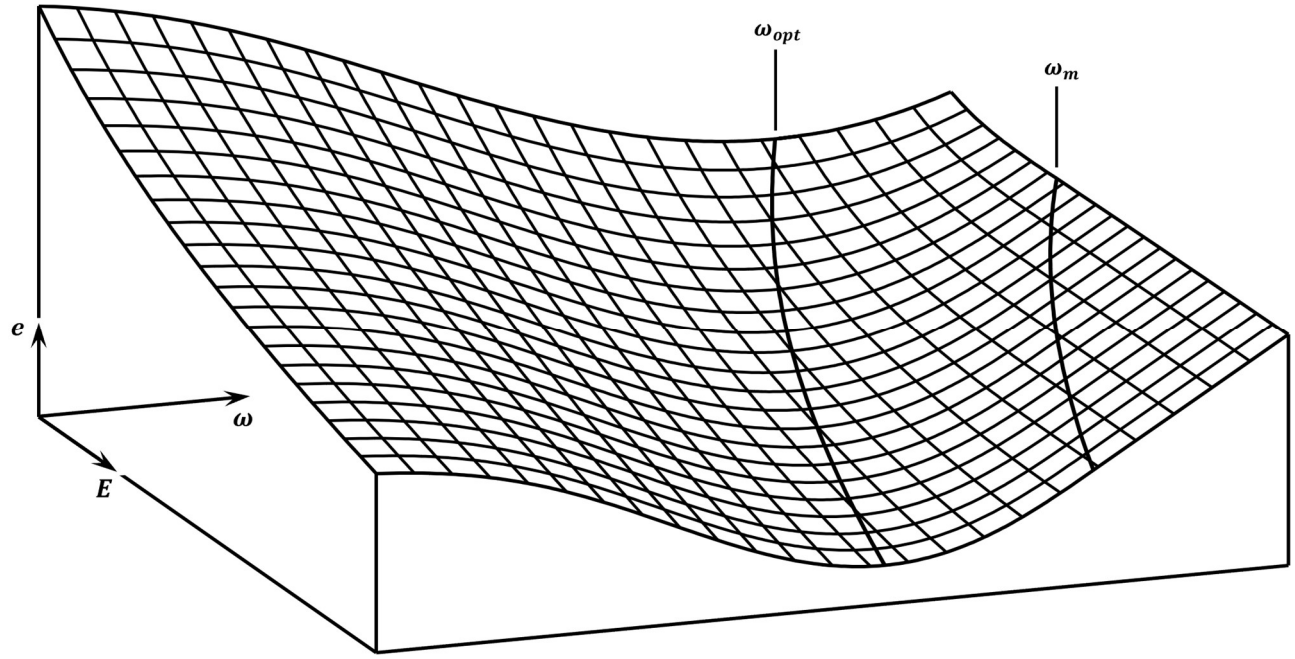

Figure 16

Figure 16 shows, in perspective, a rigorous box-cut through the three-dimensional space ω-e-E, orientated perpendicularly to the direction of the ω-E planes. Orthogonal lines of equal water content and equal energy are used to represent the compaction state surface of a material in terms of its void ratio. The projection of lines of equal energy on the same ω-e plane are the compaction curves on their true magnitude. This surface was created from the two compaction tests already mentioned earlier on this section and used to produce Figure 14.

The lower level of testing energy ($E = E_R$) constitutes the vertical boundary plane, ω-e, on the rear of box-cut and simulations at higher energies were taken up $E = 4{,}5 \times E_R$, which constitutes the vertical boundary plane on the front of the box-cut. Therefore, each step between two lines of equal energy represents the increment of dynamic compaction energy δE required to cause a certain decrement of the void ratio δe, for the same initial moulding water content ($\delta\omega = 0$). One can also interpret that each step between two lines of equal water content represent the increment of the moulding water content $\delta\omega$ required to achieve a certain increment of the void ratio δe, without changing the applied energy ($\delta E = 0$). But one should not infer that each step between two lines of equal water content represent the increment of water $\delta\omega$ required to produce a certain increment of the void ratio δe, on a material that was previously compacted under certain energy.

4.2. Compaction prestress

Compaction prestress is a technical term of our predilection whose origin we could trace back to the fifties of last century and was used, for instance, by T. William Lambe. Nowadays, perhaps a term like the yielding stress of compacted soil seems more scientific, but its relevance is the same and the attention that deserves today on the context of unsaturated soils constitutive modelling is no less than it was sixty years ago on the grounds of the most practical, and no less scientific, engineering. Compaction is an old business and some of its secrets may be lost within hundreds of uncolorful studies forgotten on the shelves of some university repository.

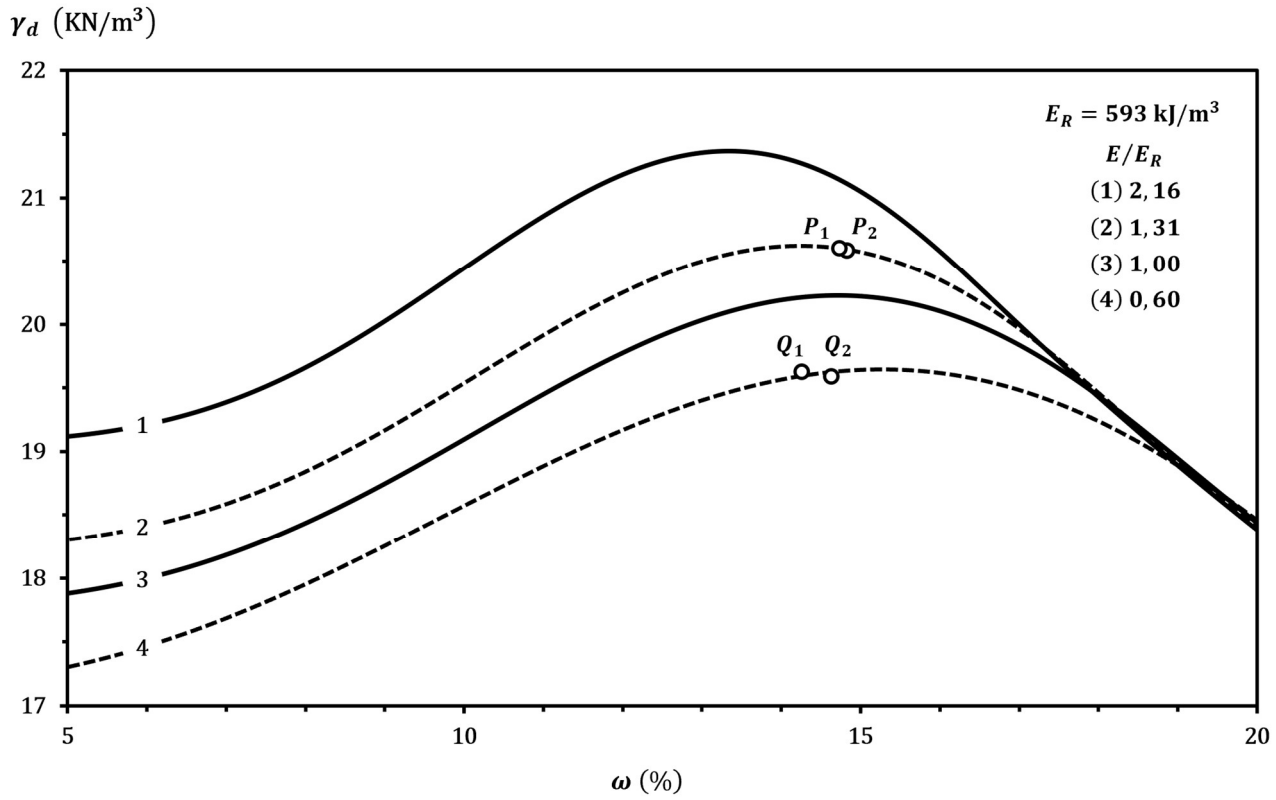

Figure 17

The exercise that follows makes use of the previous relationships between the model parameters and the compaction energy but attempts to go somehow beyond it by discussing the strain energy effectively stored in the soil after being compacted. Two compaction tests on a sample of the same iron ore tailings, under two different energies, $E/E_R = 1$ and $E/E_R = 2{,}16$, were first used to define the values of the compaction curve model parameters. The compaction curves obtained directly from test data are shown in continuous line in Figure 17. The test data is the same behind Figure 14 and Figure 16.

Further to the compaction tests, two pairs of oedometric tests were done on the same sampled material, each pair on samples compacted with a different energy. We do not know what energy was used on the compaction, but will be admitting, as we were told, that the specimens for the one-dimensional consolidation tests were trimmed from the Proctor test mould, where each pair of samples had been compacted with the same unknown effort. The water content and the dry unit weight of the specimens at the beginning of the consolidation test are represented on Figure 17 by points P_1 and P_2 for one level of energy and by points Q_1 and Q_2 for the other level of energy.

Seeking within the family of compaction curves of this same material for those passing through the as-compacted pair of points, it is concluded that the relative compaction energy used to prepare the specimens was $E/E_R = 1{,}31$ for points P_1 and P_2 and $E/E_R = 0{,}60$ for points Q_1 and Q_2, having as reference the energy value of $E_R = 593$kJ/m^3. The pair of points P_1 and P_2 correspond to specimens compacted on the wet branch of their respective compaction curve, with a water content deviation from optimum of $\omega - \omega_{opt} \cong +0{,}5\%$ and the pair of points Q_1 and Q_2 correspond to specimens compacted on the wet branch of their respective compaction curve, with a water content deviation from optimum of $\omega - \omega_{opt} \cong -0{,}8\%$. The guessed compaction curves corresponding to the energy presumably used on the preparation of each pair of specimens are represented on Figure 17 with dashed lines.

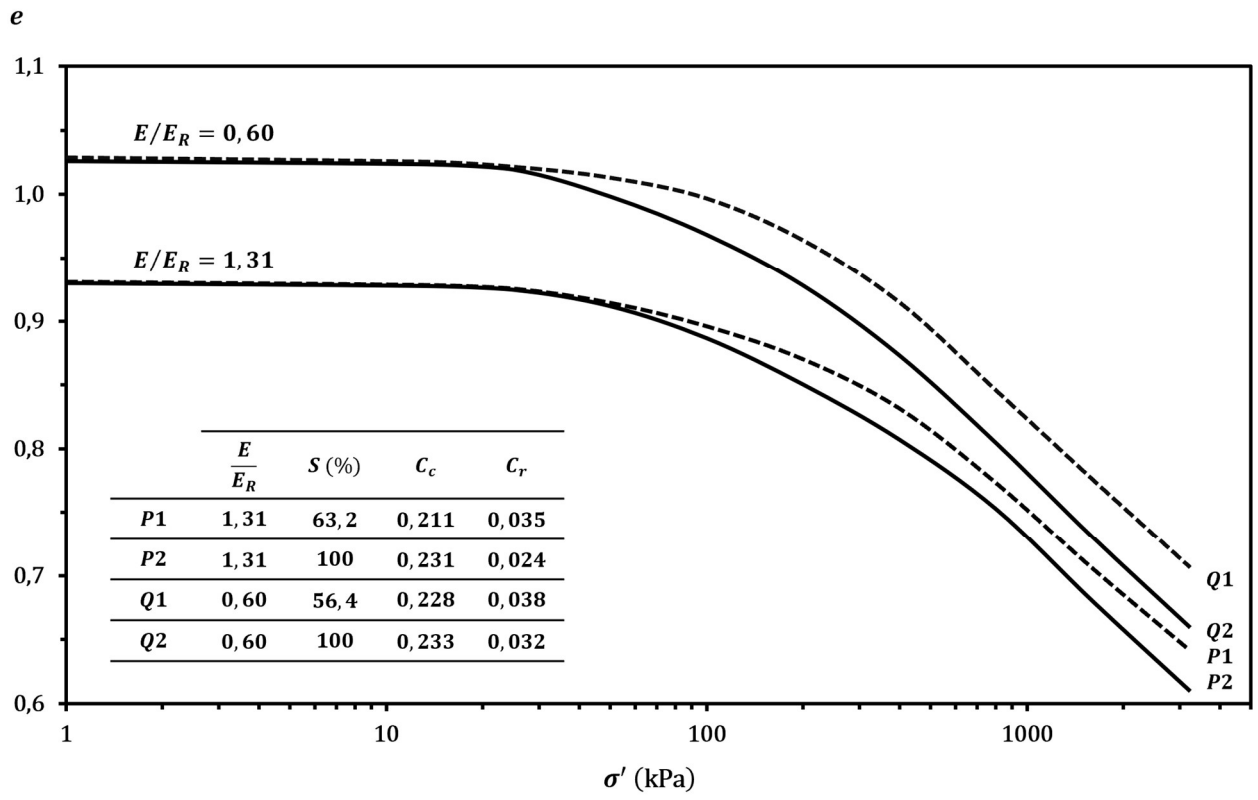

	$\frac{E}{E_R}$	S (%)	C_c	C_r
P1	1,31	63,2	0,211	0,035
P2	1,31	100	0,231	0,024
Q1	0,60	56,4	0,228	0,038
Q2	0,60	100	0,233	0,032

Figure 18

For each pair of specimens compacted with the same energy, one oedometric test was done maintaining the as-compacted moulding water content (P_1 or Q_1), and the other test was done after saturating the material (P_2 or Q_2). The compression curves resulting from each of the four oedometric tests are shown in Figure 18 on the usual e-$\log \sigma'$ space. To start with, we will be admitting that either for the unsaturated and the saturated specimens corrected compression curves can be approximated by two straight lines, one for the virgin compression branch with slope C_c (compression coefficient) and one for unloading-reloading branch with slope C_r (recompression coefficient). The interpreted results are tabulated on the figure.

We may observe that this tailings sample was far from having a void ratio of 0,6, even after being compacted on laboratory with an energy 30% greater than the normal Proctor one. Furthermore, even if compacted under a static load of 3200KPa and then unloaded, the void ratio would still be much greater than 0,6. We may also observe that the compressibility on the virgin branch decreases very modestly with an increase of the compaction effort (compare curves for points P_1 or P_2 with curves for points Q_1 or Q_2). The postulate of a single virgin compression curve regardless of the initial state is put into question. Anytime the advantages of soil compaction are casted, the reduction of compressibility is among them. However, any of those times when the reduction of compressibility is pointed as an advantage, those who point it have in mind some utilisation of the earthwork and for the case of the mountains of powder treated here the only utility is getting rid of mining waste.

If one just looks at the values of the compression indexes indicated on the figure's table may be tempted to think that compaction, in terms of reducing soil compressibility, is a fuss about nothing. But it is not so as we will straight away see. The volumetric strain ε_v relates to a change on the void ratio:

$$\varepsilon_v = -\frac{e - e_0}{1 + e_0} \quad [55]$$

Being e_0 the initial void ratio of the specimen. The total volumetric strain can be decomposed into an elastic ${\varepsilon_v}^e$ and a plastic component ${\varepsilon_v}^p$. Let us suppose a specimen recompressed from its initial stress (σ'_0, e_0) to the maximum past stress experienced by the material (σ'_y, e_y), then compressed to new maximum stress (σ'_{y1}, e_{y1}) and finally unloaded to an arbitrary stress (σ', e). Also, let us consider that e^p is the void ratio that the soil would have if completely unloaded from the new maximum stress σ'_{y1} to the initial stress σ'_0 ($\sigma' = \sigma'_0$), so that the irrecoverable change of the void ratio was $e^p - e_0$. This path describes the oedometric tests. Under such conditions, the total strain and its two components would be:

$$\begin{aligned} \varepsilon_v &= {\varepsilon_v}^e + {\varepsilon_v}^p = \left(-\frac{e - e^p}{1 + e_0}\right) + \left(-\frac{e^p - e_0}{1 + e_0}\right) = \\ &= \left(-\frac{C_r}{1 + e_0} \cdot \log\left(\frac{\sigma'}{\sigma'_0}\right)\right) + \left(-\frac{C_c - C_r}{1 + e_0} \cdot \log\left(\frac{\sigma'_{y1}}{\sigma'_y}\right)\right) \end{aligned} \quad [56]$$

Analogously to the pre-consolidation stress in natural soils, σ'_y is the compaction prestress and reflects the fraction of the applied energy released at cost of plastic deformation. For the one-dimensional compression problem, the strain energy density u, in differential form, is defined as:

$$du = \sigma' \cdot d\varepsilon_v \quad [57]$$

Which may also be decomposed into and elastic and plastic component:

$$du = du^e + du^p = \sigma' \cdot d{\varepsilon_v}^e + \sigma' \cdot d{\varepsilon_v}^p \quad [58]$$

Noting that:

$$d\varepsilon_v = -\frac{C}{1 + e_0} \cdot \frac{\partial(\log \sigma')}{\partial \sigma'} \cdot d\sigma' = -\frac{C}{1 + e_0} \cdot \frac{1}{\sigma' \cdot \ln(10)} \cdot d\sigma' \quad [59]$$

Being C indistinctly any of the coefficients C_c or C_r, the total strain energy per unit volume during one-dimensional compression up to the compaction prestress threshold will be given by:

$$u = u^e + u^p = \left(\frac{C_r}{(1 + e_0) \cdot \ln(10)} \cdot \sigma'\right) + (0), \quad \sigma' \leq \sigma'_y \quad [60]$$

And beyond that stress level:

$$u = u^e + u^p = \left(\frac{C_r}{(1+e_0)\cdot\ln(10)}\cdot\sigma'\right) + \left(\frac{C_c - C_r}{(1+e_0)\cdot\ln(10)}\cdot\left(\sigma' - {\sigma'}_y\right)\right), \quad \sigma' \geq {\sigma'}_y \qquad [61]$$

All this is applicable to saturated soils without violating excessively the sensitivity of the most purist loyalists of thermomechanics' laws and theorems. According to the above formulation, the unrecoverable strain energy varies linearly with stress and, on a σ'- u^p plot, the negative ordinate at origin will be the strain energy dissipated during the compaction work and the abscissa at null energy will be the compaction prestress. Test data can be transformed from the e-$\log\sigma'$ space to the σ'-u^p space:

$$u^p\left({\sigma'}_j\right) = \sum_{i=0}^{j}\Delta{u^p}_i \cong \sum_{i=0}^{j}\left[\left(\frac{{\sigma'}_i + {\sigma'}_{i-1}}{2}\right)\cdot\left(\varepsilon_i - \varepsilon_{i-1}\right)\right] - \frac{C_r}{(1+e_0)\cdot\ln(10)}\cdot{\sigma'}_j \qquad [62]$$

And a linear regression over the test data points at higher stress levels, i to j, will simultaneously provide the compaction prestress and the respective irrecoverable strain energy. For the saturated sample prepared with a relative energy $E/E_R = 1{,}31$ (Point P_2), the estimated compaction prestress is ${\sigma'}_y \cong 315$KPa and the dissipated strain energy is $u^p = 15{,}5$kJ/m^3. For the saturated sample prepared with a relative energy $E/E_R = 0{,}60$ (Point Q_2), the estimated compaction prestress is ${\sigma'}_y \cong 191$KPa and the dissipated strain energy is $u^p = 9{,}7$kJ/m^3.

If compacted at the optimum point, the saturated unit weight of the material subjected to a relative compaction energy $E/E_R = 0{,}60$ would be $\gamma_{sat} = \gamma_w + \gamma_{d,max}\cdot(1 - 1/G_s) \approx 24{,}7$kN/m^3. For a tailings element loaded by a column of overlying material with a height of 250m, the vertical stress would be in the order of 6,2MPa. Admitting that it rained so much that each compacted layer of a tailings pile got saturated before the subsequent layer was placed and forgetting the generation of excess pore pressures, the total volumetric strain of that element would be of $\varepsilon_v = 17{,}4\%$. A similar material, with the same saturated unit weight and the same compressibility index, would suffer a total volumetric strain of $\varepsilon_v = 43{,}5\%$ if no compaction energy had been dissipated. This already seems relevant, although, as said before, a good reason should exist for reducing the construction settlements of a useless mountain of mining waste. We know of none. On reality the filtered tailings from which the tested samples were taken will be, one day, subjected to stress levels of around 6,2MPa, on the base of a pile currently under construction. After less than a dozen of meters of cover, the compacted tailings will be again over the virgin compression line.

Applying the same methodology to the unsaturated specimens, for the sample prepared with a relative energy $E/E_R = 1{,}31$ (Point P_1), the estimated compaction prestress is $\bar{\sigma}_y \cong 294$KPa and the dissipated strain energy is $u^p = 12{,}4$kJ/m^3. For the unsaturated sample prepared with a relative energy $E/E_R = 0{,}60$ (Point Q_1), the estimated compaction prestress is $\bar{\sigma}_y \cong 227$KPa and the dissipated strain energy is $u^p = 9{,}7$kJ/m^3.

However, from a theoretical perspective, equation 57 cannot be used for the unsaturated specimens (points P_1 or Q_1). According to Alan Bishop´s definition of effective stress, we have:

$$\sigma' = \sigma - \left(u_a - S\cdot(u_a - u_w)\right) = \bar{\sigma} + S\cdot s \qquad [63]$$

Where σ is the total stress, u_a and u_w the pore pressures on the air and water phases and s is suction. $\bar{\sigma}$ is called the net stress and, for the unsaturated specimens, that is the stress that can be read on the abscissa of the graph presented on Figure 18. Starting from above on the thermomechanics hierarchy, as Guy Houlsby taught us, the total strain energy density (or the work input per volume unit), for an unsaturated soil obeying Bishop's effective stress definition, is:

$$du = \bar{\sigma} \cdot d\varepsilon_v + s \cdot \left(-\frac{e}{1+e} \cdot dS + S \cdot d\varepsilon_v\right) = \sigma' \cdot d\varepsilon_v - \frac{s \cdot e}{1+e} \cdot dS \quad [64]$$

From which we can see that equation 57 is a particular case of this last equation for a saturated soil or, more generally as the equation say, for any soil compressed while its saturation degree is maintained ($dS = 0$). For that case, the compression index in equation 61, instead of a material constant, would be a function of the saturation degree, $C_c = C_c(S)$. Naturally, on our oedometer tests, the saturation degree was increasing with the application of stress, as volumetric strains were also growing. Equation 64 can be manipulated in different forms. Letting:

$$dS = \frac{\partial}{\partial \omega}\left(\frac{G_s \cdot \omega}{e}\right) \cdot d\omega + \frac{\partial}{\partial e}\left(\frac{G_s \cdot \omega}{e}\right) \cdot de = \frac{G_s}{e} \cdot d\omega - \frac{G_s \cdot \omega}{e^2} \cdot de \quad [65]$$

And replacing dS on equation 64:

$$\begin{aligned} du &= \sigma' \cdot d\varepsilon_v - s \cdot \left(\frac{G_s}{1+e} \cdot d\omega - \frac{G_s \cdot \omega}{e} \cdot \frac{de}{1+e}\right) = \\ &= \sigma' \cdot d\varepsilon_v - \frac{s \cdot G_s}{1+e} \cdot d\omega + s \cdot S \cdot d\varepsilon_v = \bar{\sigma} \cdot d\varepsilon_v - \frac{s \cdot G_s}{1+e} \cdot d\omega \end{aligned} \quad [66]$$

Meaning that the saturation degree can be indifferently replaced by water content as a state variable. If a soil sample had been compressed under constant water content ($d\omega = 0$), the total volumetric strain could, by hypothesis, be estimated as:

$$\varepsilon_v = -\frac{\bar{C}_c(\omega)}{1+e_0} \cdot \log(\bar{\sigma}) \quad [67]$$

And the respective total differential:

$$-d\varepsilon_v = \frac{\partial \bar{C}_c(\omega)}{\partial \omega} \cdot \frac{1}{1+e_0} \cdot \log(\bar{\sigma}) \cdot d\omega + \frac{\bar{C}_c(\omega)}{(1+e_0) \cdot \ln(10)} \cdot \frac{1}{\bar{\sigma}} \cdot d\bar{\sigma} \quad [68]$$

Which is perfectly compatible with the strain energy differential given before. Assuming that the recompression coefficient is not affected by the water content, the plastic strain component would be:

$$\varepsilon_v{}^p = -\frac{\bar{C}_c(\omega) - C_r}{1 + e_0} \cdot \log(\bar{\sigma}) \quad [69]$$

Or similarly, using the saturation degree as variable:

$$\varepsilon_v{}^p = -\frac{\bar{C}_c(S) - C_r}{1 + e_0} \cdot \log(\sigma') \quad [70]$$

On the e-$\log \bar{\sigma}$ space equation 69 becomes:

$$e = e_0(\omega) - \bar{C}_c(\omega) \cdot \log(\bar{\sigma}) \quad [71]$$

Each point of a compaction curve reveals a plastic strain, or, equivalently, an irreversible void ratio change (Δe^p) from the loosest state ($e = e_0, E_R = 1$), which according to our model is:

$$e^p = e_0 - \Delta e^p = \varepsilon_v{}^p \cdot (1 + e_0) = G_s \cdot \frac{\omega}{S} = G_s \cdot \frac{\bar{S}_m}{\bar{\omega}_m} \cdot \frac{\bar{\omega}}{\bar{S}} \cdot \frac{\omega_m}{S_m} = G_s \cdot \mathcal{S}_1 \cdot \mathcal{S}_2 \cdot \frac{\omega_{mR}}{S_{mR}} \quad [72]$$

Being, from equations 39 and 42:

$$\mathcal{S}_1 = \frac{\bar{S}_m}{\bar{\omega}_m} \cdot \frac{\bar{\omega}}{\bar{S}} = \frac{(1-m) \cdot (1 - \bar{\omega}_m) - n \cdot \bar{\omega}_m}{\left(\frac{\bar{\omega}}{\bar{\omega}_m}\right)^{m-1} \cdot \left(\frac{1-\bar{\omega}}{1-\bar{\omega}_m}\right)^{n-1} - (m \cdot (1 - \bar{\omega}_m) - n \cdot \bar{\omega}_m)} \quad [73]$$

And, from equation 53:

$$\mathcal{S}_2 = \frac{k_2 - k_1}{k_2 \cdot \left(k_2 \cdot \log\left(\frac{E}{E_R}\right) + 1\right)} + \frac{k_1}{k_2} \quad [74]$$

On the previous chapter we have seen that we can relate both ω_m and S_m, and therefore ω and S, to a relative energy E/E_R. If some correlation between compaction energy and compaction prestress (or yield net stress) could be experimentally established, a yield surface on the e-ω-$\bar{\sigma}_y$ space could be obtained, without ever needing to evaluate the suction stress installed on soil samples compacted dynamically on the Proctor mould.

In terms of plastic strain, equation 72 can be eventually rewritten as:

$$\Delta\varepsilon_v{}^p = -\frac{e^p - e^p{}_R}{1 + e_0} = \frac{\mathcal{S}_1(E) \cdot \mathcal{S}_2(E) - \mathcal{S}_1(E_R)}{\frac{S_{mR}}{G_s \cdot \omega_{mR}} + \mathcal{S}_1(E_R)} \cdot \left(1 + \varepsilon_v{}^p{}_R\right) + \varepsilon_v{}^p{}_R \quad [75]$$

Which represents the increment of plastic strain produced by increasing the compaction energy from E_R to E at constant water content. The reference strain ${\varepsilon_v}^p{}_R$ would be the one produced previously by applying the reference compaction energy to a soil element on its loosest state ($e = e_0$). If the shape parameters of the compaction curve model were the same regardless of the compaction energy, then $\mathcal{S}_1(E) = \mathcal{S}_1(E_R) = S_1$. So far, all testing required to consubstantiate the model comes from the Proctor test, with a minimum required of two tests under different energies. But the more, the better.

Making an analogy between the Proctor test and the oedometric test, there will be a net stress that under constant water content produces the same plastic strain as that of a dynamically compacted specimen. On the hypothesis of equation 69 validity, equalling the strain energy density and the compaction energy:

$$E = u^p = \frac{C_c - C_r}{(1 + e_0) \cdot \ln(10)} \cdot \bar{\sigma}_y \Longrightarrow E = {\varepsilon_v}^p \cdot \frac{\bar{\sigma}_y}{\ln \bar{\sigma}_y} \quad [76]$$

The compaction prestress $\bar{\sigma}_y$ can be extracted from the above equation using the Lambert W function:

$$\frac{\ln \bar{\sigma}_y}{\bar{\sigma}_y} \cdot \frac{E}{{\varepsilon_v}^p} = 1 \Longrightarrow -\ln \bar{\sigma}_y \cdot e^{-\ln \bar{\sigma}_y} = -\frac{{\varepsilon_v}^p}{E} \Longrightarrow \bar{\sigma}_y = e^{-W(-{\varepsilon_v}^p/E)} \quad [77]$$

The value of the Lambert function can be calculated by letting:

$$x = W\left(-\frac{{\varepsilon_v}^p}{E}\right) = W(x \cdot e^x) \Longrightarrow -\frac{{\varepsilon_v}^p}{E} = x \cdot e^x \Longrightarrow f(x) = x \cdot e^x - \frac{{\varepsilon_v}^p}{E} = 0 \quad [78]$$

And iteratively finding the root of the equation with the Newton-Raphson method:

$$x_{i+1} = x_i - \frac{x_i \cdot e^{x_i} + {\varepsilon_v}^p/E}{e^{x_i} \cdot (x_i + 1)} \quad [79]$$

This way we would have changed the E axis on the ω-e-E tri-dimensional space into a $\bar{\sigma}_y$ axis on a new transformed space ω-e-$\bar{\sigma}_y$, where the relationship e-$\log \bar{\sigma}_y$ is linear as postulated initially. To avoid losing at this stage any of the information contained on the ω-e-E surface, a different approach is preferable, as explained further down. Above all, there is a reason for not using the above equations and that reason was already evinced when stating the values of the plastic strain energy density deduced from the oedometer test, that is:

$$u^p \ll E \quad [80]$$

Before continuing, it may be useful to illustrate the information that is contained on the compaction curves and the compaction state surface that results from their collation.

Figure 19, on next page, shows the projection of constant water content curves on the ${e_v}^p$- E plane, namely in part (a) for curves on the dry side of optimum and in part (b) for curves on the wet side of optimum. We are still

working with the data from compaction tests presented on the previous section and that originated Figure 14. The curves presented on this figure are the bidimensional version of the ones presented in three dimensions on Figure 16.

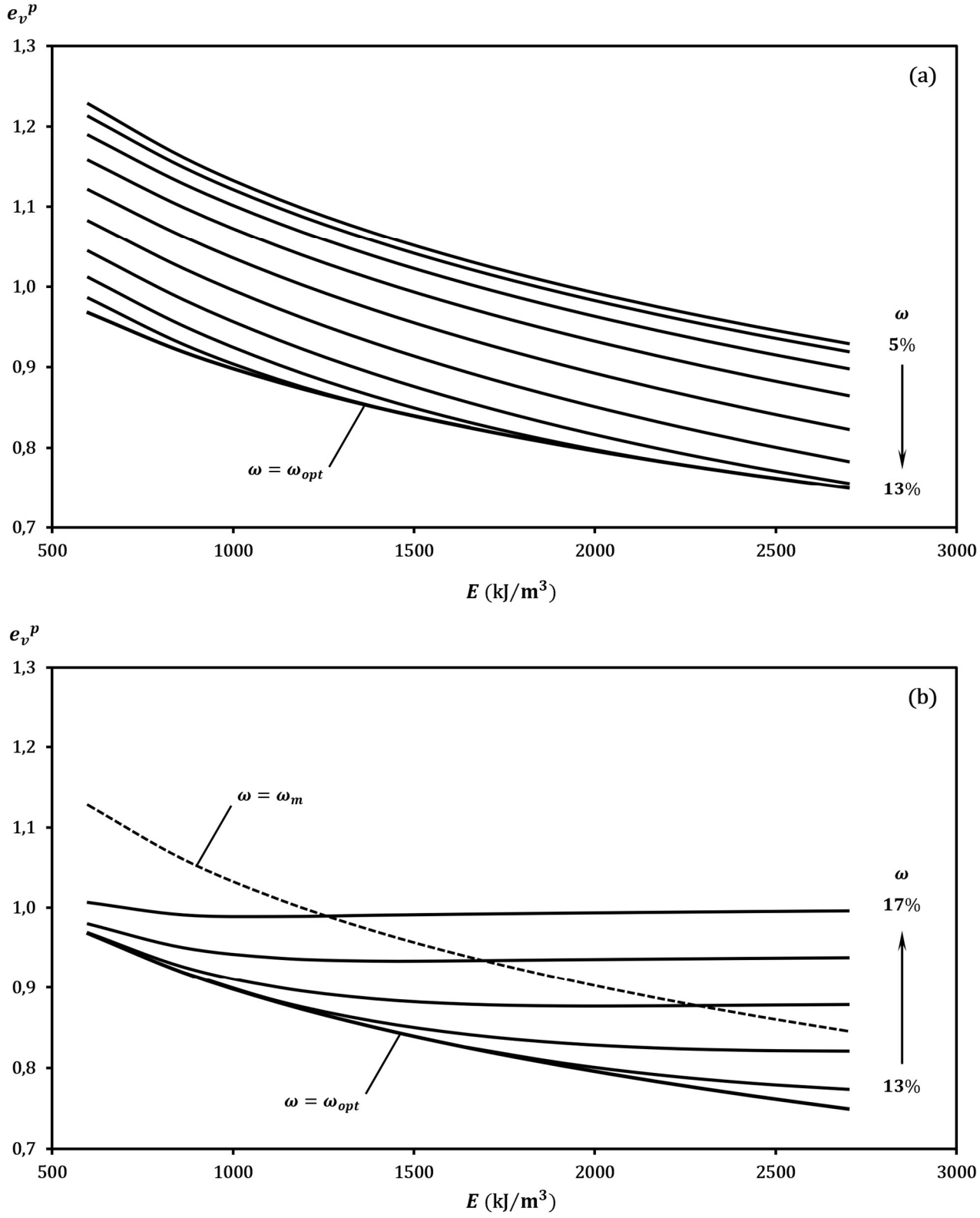

Figure 19

Curves corresponding to water contents of 13% and 14% cross the line of optimums, meaning that, for the energy levels in cause, the optimum water content lies around those values. On the dry side, resemblance with one-dimensional static compression curves is obvious, but not as much when moving to the wet side. We must remember that the Proctor test is done at constant water content and there is no drainage.

Equation 69 may be regarded as a particular case of a compression curve with non-linear tangent modulus:

$$\frac{d\bar{\sigma}_y}{d{\varepsilon_v}^p} = D \cdot {\bar{\sigma}_y}^{1-a} \quad [81]$$

If the exponent $1-a$ is taken to be unitary (a =0):

$$d{\varepsilon_v}^p = \frac{1}{D} \cdot \frac{d\bar{\sigma}_y}{\bar{\sigma}_y} \Longrightarrow {\varepsilon_v}^p = \int_{\varepsilon^p} \frac{1}{D} \cdot \frac{1}{\bar{\sigma}_y} \cdot d\bar{\sigma}_y = \frac{1}{D \cdot \ln 10} \cdot \log\left(\bar{\sigma}_y\right) = -\frac{\bar{C}_c(\omega) - C_r}{1 + e_0} \cdot \log\left(\bar{\sigma}_y\right) \quad [82]$$

The statement about the particularity is demonstrated. If the exponent $1-a$ is taken as a real number between 0 and 1, the plastic strain will be:

$${\varepsilon_v}^p = \frac{1}{a \cdot D} \cdot {\bar{\sigma}_y}^a \quad [83]$$

And the plastic strain energy density:

$$u^p = \int_{{\varepsilon_v}^p} \bar{\sigma}_y \cdot d{\varepsilon_v}^p = \int_{\bar{\sigma}_y} \bar{\sigma}_y \cdot \left(\frac{1}{D} \cdot {\bar{\sigma}_y}^{a-1}\right) \cdot d\bar{\sigma}_y = \frac{1}{(a+1) \cdot D} \cdot {\bar{\sigma}_y}^{a+1} = \frac{a}{(a+1)} \cdot {\varepsilon_v}^p \cdot {\bar{\sigma}_y}^a \quad [84]$$

Multiplying the plastic strain energy density by a strain infinitesimal and integrating the product:

$$\int_{{\varepsilon_v}^p} u^p \cdot d{\varepsilon_v}^p = \frac{a^2}{(a+1) \cdot (2 \cdot a + 1)} \cdot \bar{\sigma}_y \cdot ({\varepsilon_v}^p)^2 = \frac{a^2 \cdot (a \cdot D)^{1/a}}{(a+1) \cdot (2 \cdot a + 1)} \cdot ({\varepsilon_v}^p)^{(2 \cdot a + 1)/a} \quad [85]$$

Where d is a constant that assumes the value of 6 for $a = 1$ and approaches $+\infty$ as a tends to zero. This integral corresponds to the area below the curves $E(\varepsilon)$ derived with our model, hence:

$$\int_{{\varepsilon_v}^p} E({\varepsilon_v}^p) \cdot d{\varepsilon_v}^p = I_1({\varepsilon_v}^p) \quad [86]$$

Although an analytical solution can be found for the integral $I_1({\varepsilon_v}^p)$ on the previous formula, numerical integration has been used. Succinctly (letting ${\varepsilon_v}^p = \varepsilon$ for simplicity), we retain the first terms of a Taylor series expansion around a generic point ε_i:

$$
\begin{aligned}
I_1(\varepsilon_i) &= \int_{\varepsilon_i-\Delta\varepsilon_{i-1}}^{\varepsilon_i+\Delta\varepsilon_{i+1}} E(\varepsilon)\cdot d\varepsilon = I(\varepsilon_i+\Delta\varepsilon_{i+1}) - I(\varepsilon_i-\Delta\varepsilon_{i-1}) = \\
&= \left[I(\varepsilon_i) + \frac{dI(\varepsilon_i)}{d\varepsilon}\cdot\Delta\varepsilon_{i+1} + \frac{1}{2}\cdot\frac{d^2I(\varepsilon_i)}{d\varepsilon^2}\cdot{\Delta\varepsilon_{i+1}}^2 + \frac{1}{6}\cdot\frac{d^3I(\varepsilon_i)}{d\varepsilon^3}\cdot{\Delta\varepsilon_{i+1}}^3 + \cdots\right] - \\
&\quad - \left[I(\varepsilon_i) - \frac{dI(\varepsilon_i)}{d\varepsilon}\cdot\Delta\varepsilon_{i-1} + \frac{1}{2}\cdot\frac{d^2I(\varepsilon_i)}{d\varepsilon^2}\cdot{\Delta\varepsilon_{i-1}}^2 - \frac{1}{6}\cdot\frac{d^3I(\varepsilon_i)}{d\varepsilon^3}\cdot{\Delta\varepsilon_{i-1}}^3 - \cdots\right] \cong \\
&\cong \frac{dI(\varepsilon_i)}{d\varepsilon}\cdot(\Delta\varepsilon_{i+1}+\Delta\varepsilon_{i-1}) + \frac{1}{2}\cdot\frac{d^2I(\varepsilon_i)}{d\varepsilon^2}\cdot\left({\Delta\varepsilon_{i+1}}^2 - {\Delta\varepsilon_{i-1}}^2\right) + \\
&\quad + \frac{1}{6}\cdot\frac{d^3I(\varepsilon_i)}{d\varepsilon^3}\cdot\left({\Delta\varepsilon_{i+1}}^3 + {\Delta\varepsilon_{i-1}}^3\right) = \\
&= E(\varepsilon_i)\cdot(\Delta\varepsilon_{i+1}+\Delta\varepsilon_{i-1}) + \frac{1}{2}\cdot\frac{d\left(E(\varepsilon_i)\right)}{d\varepsilon}\cdot\left({\Delta\varepsilon_{i+1}}^2 - {\Delta\varepsilon_{i-1}}^2\right) + \\
&\quad + \frac{1}{6}\cdot\frac{d^2\left(E(\varepsilon_i)\right)}{d\varepsilon^2}\cdot\left({\Delta\varepsilon_{i+1}}^3 + {\Delta\varepsilon_{i-1}}^3\right)
\end{aligned}
\qquad [87]
$$

Being the derivates of $E(\varepsilon)$ approximated by central differences:

$$
\frac{d\left(E(\varepsilon_i)\right)}{d\varepsilon} \approx \frac{\left(E(\varepsilon_{i+1}) - E(\varepsilon_i)\right)\cdot{\Delta\varepsilon_{i-1}}^2 + \left(E(\varepsilon_i) - E(\varepsilon_{i-1})\right)\cdot{\Delta\varepsilon_{i+1}}^2}{\Delta\varepsilon_{i-1}\cdot\Delta\varepsilon_{i+1}\cdot(\Delta\varepsilon_{i-1}+\Delta\varepsilon_{i+1})} \qquad [88]
$$

And:

$$
\frac{d^2E(\varepsilon_i)}{d\varepsilon^2} \approx 2\cdot\frac{\left(E(\varepsilon_{i+1}) - E(\varepsilon_i)\right)\cdot\Delta\varepsilon_{i-1} - \left(E(\varepsilon_i) - E(\varepsilon_{i-1})\right)\cdot\Delta\varepsilon_{i+1}}{\Delta\varepsilon_{i-1}\cdot\Delta\varepsilon_{i+1}\cdot(\Delta\varepsilon_{i-1}+\Delta\varepsilon_{i+1})} \qquad [89]
$$

And finally:

$$
I_1\left(\varepsilon_j\right) = \sum_{\substack{i=2 \\ \Delta i=2}}^{j\le N-1} I_1(\varepsilon_i) \qquad [90]
$$

On our case, backward and forward finite differences are unequal:

$$
\Delta\varepsilon_{i-1} = \varepsilon_i - \varepsilon_{i-1} \neq \Delta\varepsilon_{i+1} = \varepsilon_{i+1} - \varepsilon_i \qquad [91]
$$

And equations 87 to 89 cannot be further simplified. If the integral function $I_1({\varepsilon_v}^p)$ is multiplied by an infinitesimal strain and reintegrated numerically as before we arrive at:

$$I_2({\varepsilon_v}^p) = \int_{{\varepsilon_v}^p} I_1({\varepsilon_v}^p) \cdot d{\varepsilon_v}^p = \frac{a^3 \cdot (a \cdot D)^{1/a}}{(a+1) \cdot (2 \cdot a + 1) \cdot (3 \cdot a + 1)} \cdot ({\varepsilon_v}^p)^{(3 \cdot a + 1)/a} \quad [92]$$

From equation 86 and equation 92, we have:

$$I_2({\varepsilon_v}^p) = \frac{2 \cdot a + 1}{3 \cdot a + 1} \cdot \frac{\left(I_1({\varepsilon_v}^p)\right)^2}{E({\varepsilon_v}^p)} \quad [93]$$

From where the parameters of the power law constitutive relationship can be obtained:

$$a = \frac{E({\varepsilon_v}^p) \cdot I_2({\varepsilon_v}^p) - \left(I_1({\varepsilon_v}^p)\right)^2}{2 \cdot \left(I_1({\varepsilon_v}^p)\right)^2 - 3 \cdot E({\varepsilon_v}^p) \cdot I_2({\varepsilon_v}^p)} = a(\omega) \quad [94]$$

And:

$$D = \frac{(1+a)^a}{(1+2 \cdot a)^{a+1}} \cdot \frac{\left(E({\varepsilon_v}^p)\right)^{2 \cdot a + 1}}{\left(I_1({\varepsilon_v}^p)\right)^{a+1}} = D(\omega) \quad [95]$$

As illustrated on Figure 20, on next page, extending the above integrations up to the strain that corresponds to the optimum water content ω_{opt} results on a fair match between the strain energy associated with the latter constitutive relationship and that contained on the compaction curves. The continuous lines on the figure result from the derived two-parameter constitutive relationship and the points result solely from the compaction model as explained on the previous section. A better fit is possible by retrogressively constraining the values of the shape parameters of the compaction model, m and n. Otherwise, a richer constitutive relationship would have to be used, but its experimental proof with laboratory test results would have to be feasible, as the power-law type is to a sufficient extend.

In contrast with the previous figure, Figure 21, also on next page, shows that as soon as the line of optimum water content is reached from the dry side, the ${\varepsilon_v}^p$-E lines abruptly change their curvature and tend to a point of tangency with the vertical direction at the point of maximum water content, ω_m.

By the definition of derivate, the tangency point corresponds to an infinite equivalent static yield stress, which logically means that no matter how much further compaction effort is statically applied beyond that point, the volumetric plastic strain will not increase further. The same is expected to be observed on an oedometric test on a nearly saturated specimen, if water drainage is not allowed. On the wet-side region of compaction, air bubbles occluded on the water phase will no longer be freely and independently expelled and the yield stress will not increase. A separated treatment of the problem is required on the wet side, leading to a discontinuous energy efficiency function, broken along the line of optimums.

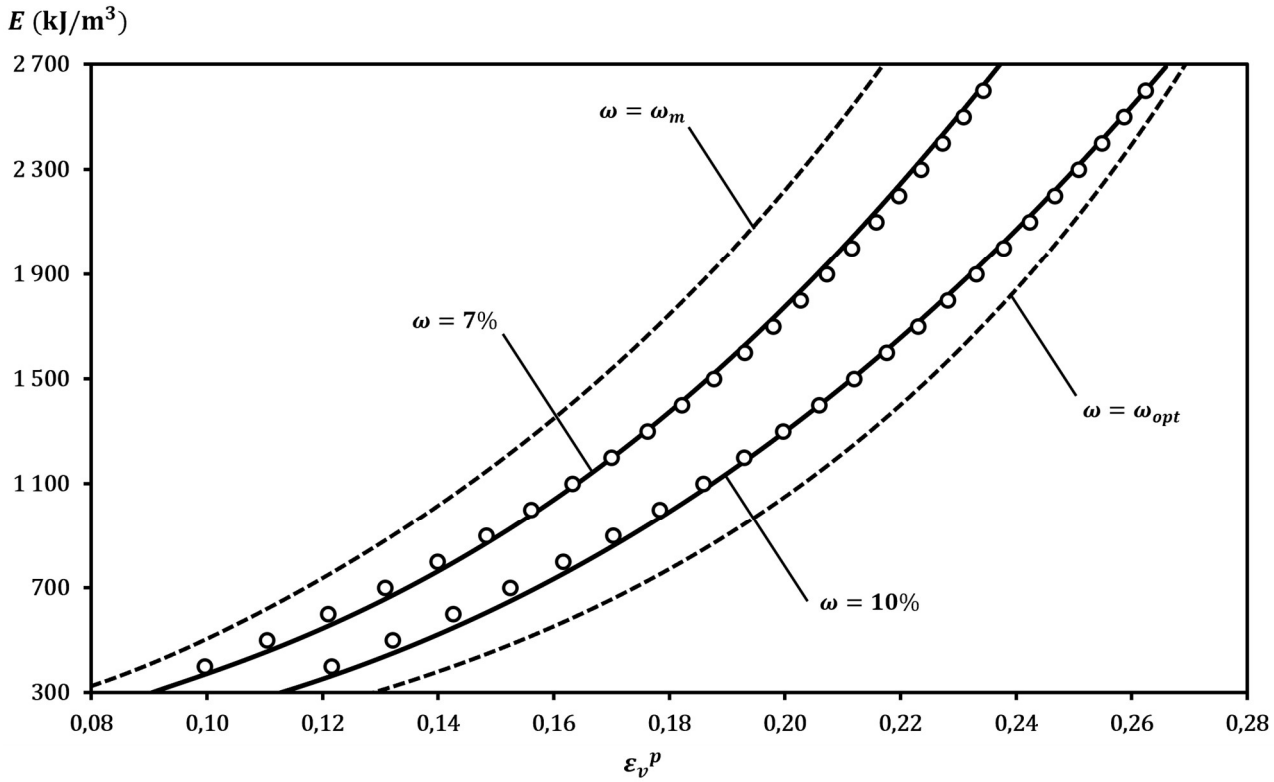

Figure 20

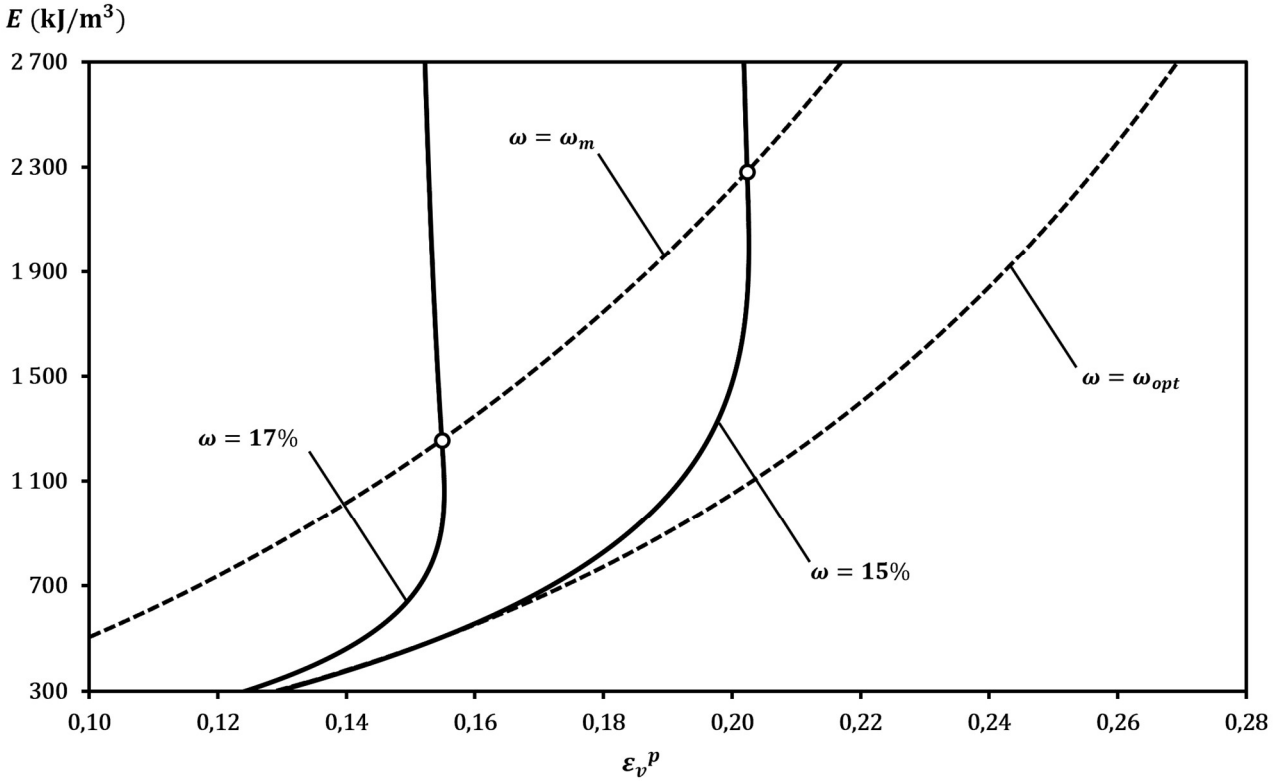

Figure 21

The compaction prestress as presented so far presuppose that all the dynamic compaction work input was transformed into strain energy, from which a substantial part, the one that we are interested on, is irrecoverable and preserved as information to be collected from the Proctor compaction curves. The compaction prestress

obtained from the compaction test nominal energy would traduce a 100% energy efficiency. We have seen at the beginning of this section that plastic strain energy u^p deduced from the oedometer tests is small fraction of the compaction work input E and we will call the ratio $\eta = u^p/E \times 100\%$ the energy efficiency, replacing on the previous formulation E by a fraction of it, $\eta \times E$, as obtained on a oedometric test.

From experience, we can expect the energy efficiency to decrease as the moulding water content increases and as well as the level of compaction energy increases. If enough test results were available, those expectations could be traduced by:

$$\eta = \alpha_1 - \alpha_2 \cdot \left(\frac{\omega}{\omega_{opt}}\right) - \alpha_3 \cdot \log\left(\frac{E}{E_R}\right) \qquad [96]$$

Where the values of the α coefficients would be such that the calculated compaction prestress equalled the yield stress derived from one-dimensional static compression tests. On the most innocent thinking, the energy efficiency function is supposed to be derived solely from the results of oedometric tests on compacted specimens, from which we can determine either E or u^p. The third term of the second member, expressing the dependency of the energy efficiency on the relative energy may be redundant in some cases, as the second term, expressing the dependency of the energy efficiency on the moulding water content, already incorporates a component of energy dependency, once the optimum water content is itself dependent on the compaction effort.

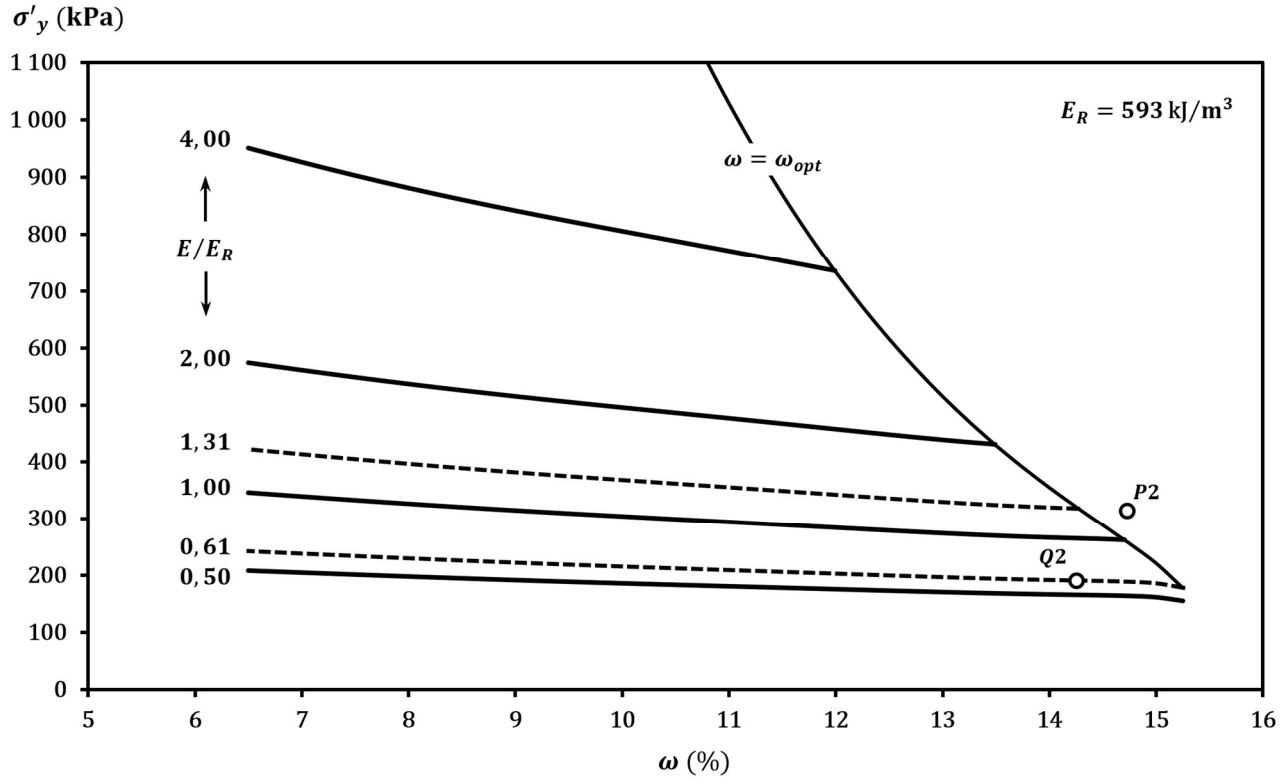

Figure 22

For our case study, we have just two oedometric tests results to work with (points Q_1 and P_1 on unsaturated specimens or points Q_2 and P_2 on saturated specimens), just being one of them on the dry-side region of

compaction. So, we have two points $(S/S_m, E/E_R, \eta)$ to compose a plane, namely point $Q_2 = (0{,}800, 0{,}613, 0{,}028)$ and point $P_2 = (0{,}917, 1{,}315, 0{,}020)$. Three points would be the minimum necessary the define a planar surface. Therefore, with enough good will, we may be speculatively led to the ω-$\bar{\sigma}_y$ curves shown on Figure 22, on the previous page, for different relative compaction energies, including those used to prepare the oedometric tests specimens. They may be right, or they may be wrong, and the best part is that nobody knows. If someone wanted to know, the cost of a couple more of oedometric tests would be the price to pay.

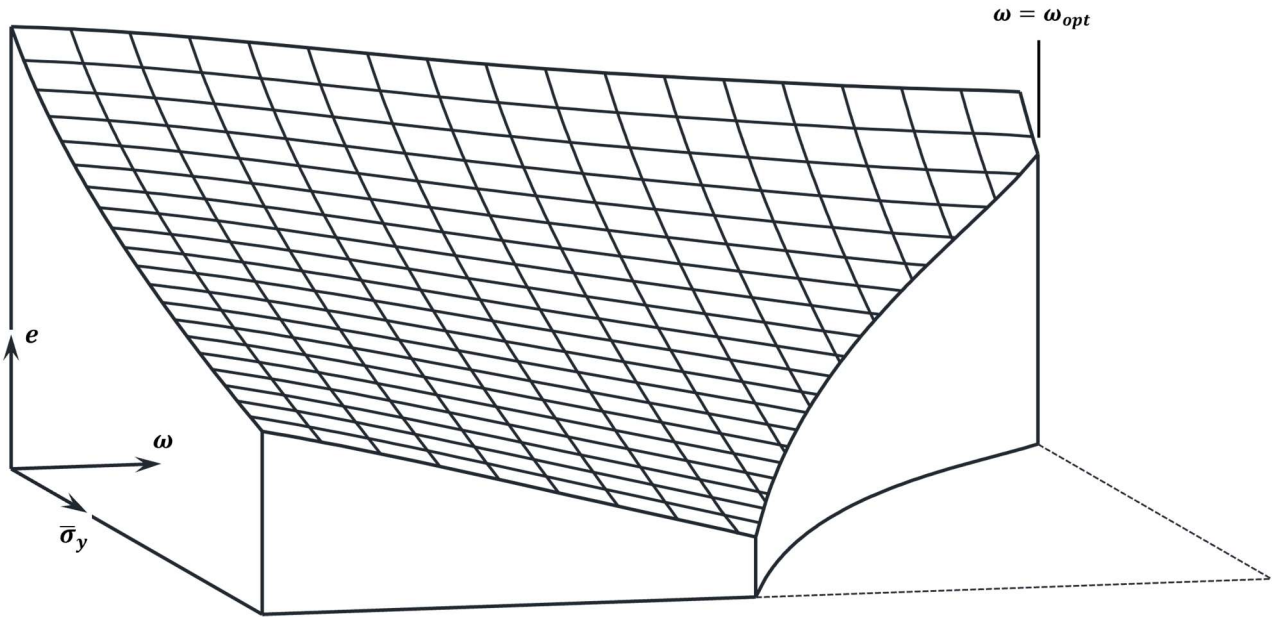

Figure 23

The ω-e-E surface illustrated earlier on Figure 16 can now be transformed into a ω-e-$\bar{\sigma}_y$ surface as illustrated on Figure 23, noting that the compaction curves do not lie anymore on ω-e planes, although their projection on a ω-e plane is still the same. Therefore, a single compaction curve, corresponding to a single compaction energy, will not correspond to a single compaction prestress. Curves with constant $\bar{\sigma}_y$ can be projected to a common ω-e plane and the values of the compaction prestress can be readily mapped over the initial compaction curves, as initially intended.

On Figure 23, water content varies from 6,5% to 15,0% with 17 increments of 0,5% and the compaction prestress varies from 150kPa to 1.150kPa with 19 increments of 50kPa. The box cut is truncated by the vertically ruled surface that contains the line of optimum water content and represents the compaction state boundary of the tailings soil used on the example, when the water content is lower or equal to the optimum. The reference horizontal plane is located at a 0,6 void ratio and the maximum represented value is 1,3. On the wet-side region, we may understand that the compaction prestress is lower, for the same water content, than the one obtained along the line of optimums and likely to decrease as the full saturation degree is approached. Based on these assumptions, a second state boundary surface, pinned on the line of optimums, can be freely derived for the wet-side region.

Figure 24, on next page, shows what happens when the surface shown in Figure 23 is cut by a vertically ruled surface having a compaction curve (constant E) on the ω-$\bar{\sigma}_y$ plane as its directrix. The initial compaction curves

are integrally preserved on this new surface and the energy efficiency function simply changes the compaction energy axis into a more meaningful compaction prestress axis.

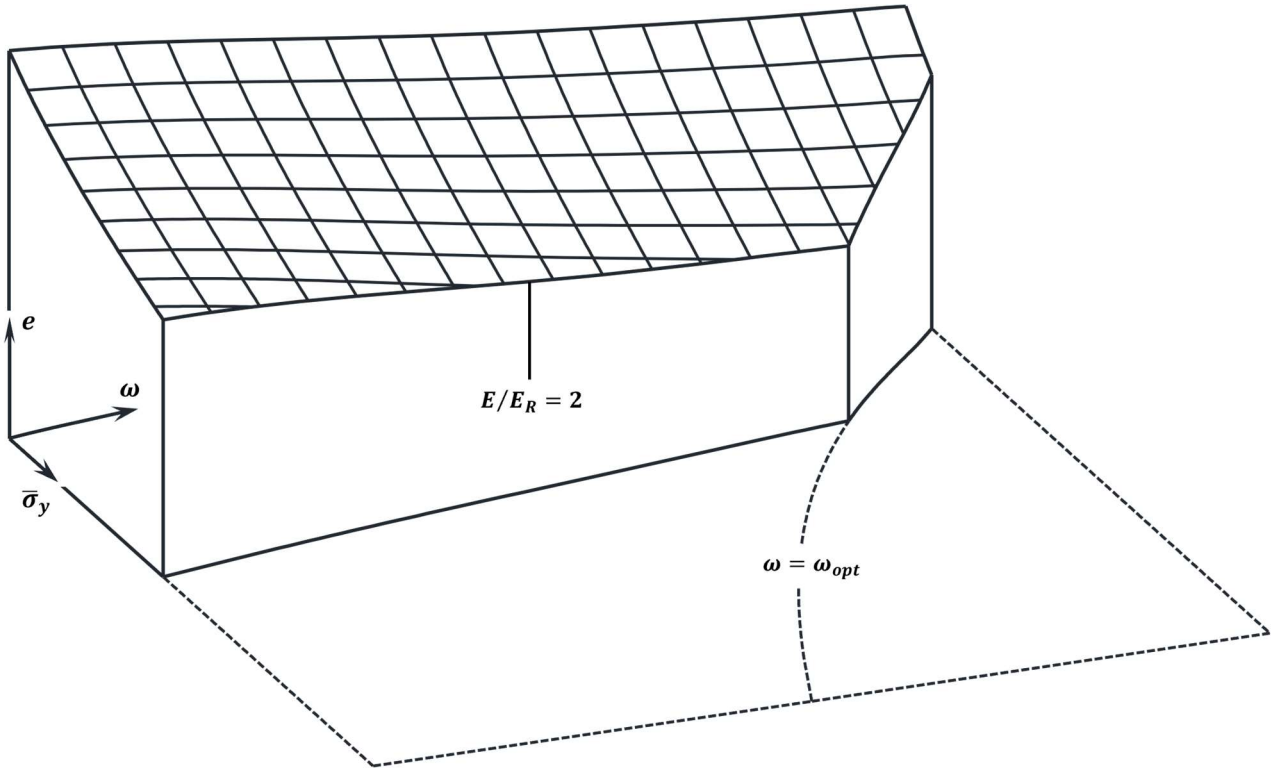

Figure 24

We have seen before that the oedometric tests can be one source of the true values of the compaction prestress preserved on compacted specimens, in respect to which the energy efficiency function can be calibrated. Eventually, constant water content tests would be ideal, but not necessarily. There is nothing that precludes the use of saturated specimens and obtain from them the values of the compaction prestress in terms of effective stress (σ'_y instead of $\bar{\sigma}_y$), once it is in terms of effective stress, with the role of suction eliminated, that intrinsic soil properties are manifested. In this, there is no unwillingness of the author against unsaturated soil mechanics, pretty much the contrary. Nothing is as important as suction to understand what happens when suction evanishes.

However, despite willing to set unsaturated soil mechanics aside, we will have to admit that the effect of saturating the as-compacted specimens, designedly the induced swelling or collapse, is independent of the sequence in which loading and wetting tales place. Saturation causes plastic deformations, and the problem of collapse is another one to be aware of. For now, we will retrieve the oedometric tests results presented earlier on this section (Points Q_2 and P_2), for which the specimens were saturated ahead of load application, even noting that no swelling was reported as one could expect. This would be a condition like that experienced by an earthwork constructed under prolonged rainy weather.

We may have deceived the readers that could be expecting for more, as an uncontroversial proof that going through all this works pays the effort and provides the best-ever definition of compaction state boundary surfaces. Indeed, a point or two perfectly lying on a surface say very little about the geometry of that surface. There are infinite surfaces that could pass through two points and many of them would be conforming to our expectations. How we understand it… We know a thing or two about deception. Others, like our friends the

mountain builders, are less demanding and perhaps would be sufficiently pleased to be informed that the oedometric tests from upon which the "0,6 minimum void ratio" criterium was build were done on specimens compacted with an arbitrary energy and no one realise it.

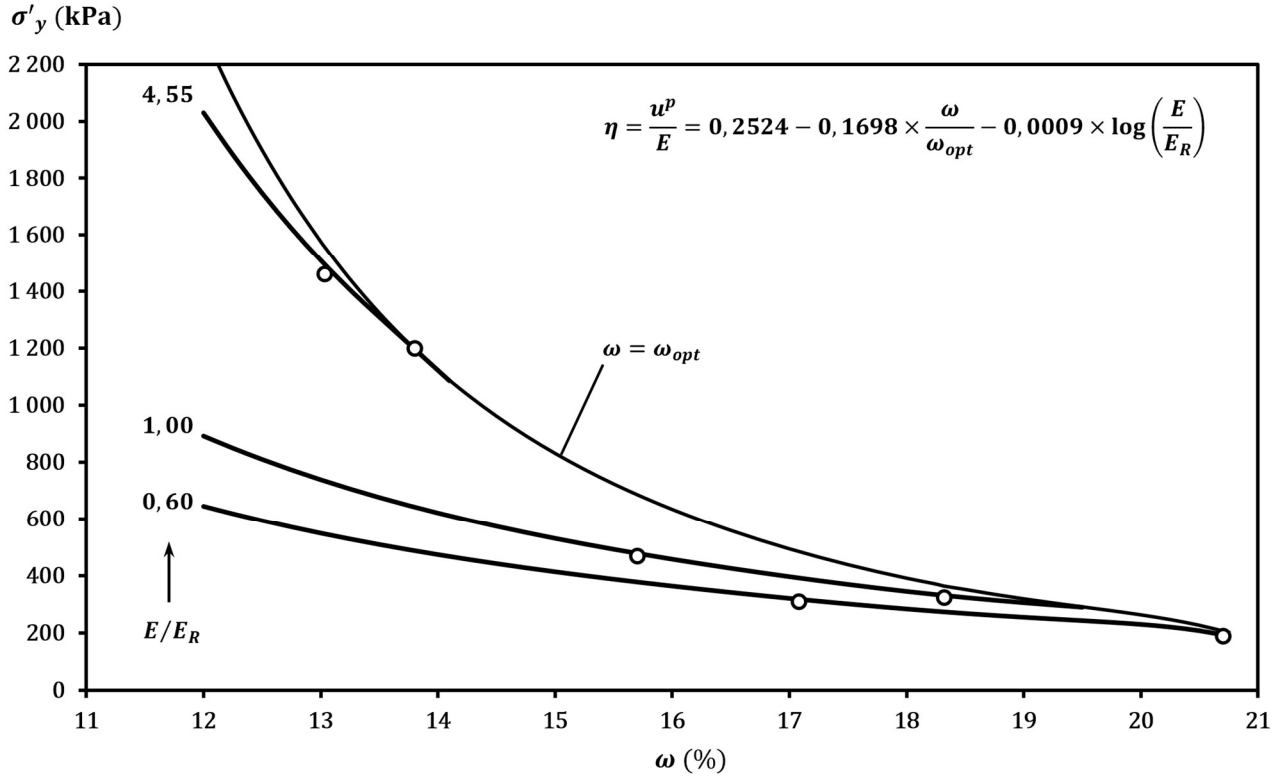

Figure 25

Nevertheless, not wishing to be absolutely deceiving, we present on Figure 25 the results of the application of this same methodology to a plastic clay, for which a judicious set of oedometric tests was performed. For this clay, our friend the Client put to disposal three pairs of oedometric test results, each done on saturated specimens prepared with two different moulding water contents on the dry-side region and compacted with the same effort. And guess what? The six points lie almost exactly on the derived compaction state surface.

The results are satisfactory even for the most demanding minds and we must emphasise that the coefficients of equation 96 are not supposedly obtained by trial and error, but the result of comparing the plastic strain energy contained on the oedometric test samples with the nominal dynamic energy used for their preparation. The curves ω-σ'_y presented on this last figure are supposed to be a mere consequence of the energy efficiency function derived from the oedometric tests, although no one would be punished by any moral law for going beyond and adjusting whatever needs to be adjusted to reach perfection or something else suitable. In fact, the passage from compaction energy to compaction prestress, in terms of effective stress, could be done without any theoretical background.

Figure 26, on next page, illustrates, as a mere curiosity, the energy efficiency function associated with the high plasticity clay compaction, being clear the dependency of the plastic strain energy dissipated on one-dimensional static compression on both moulding water content and intensity of compaction energy. Curiously, extending the ω-σ'_y lines over the line of optimums and into the compaction wet-region will provide a good

estimate of the compaction prestress achieved on specimens compacted with excessive water content. That completes the circle, and no more tedious equations are needed.

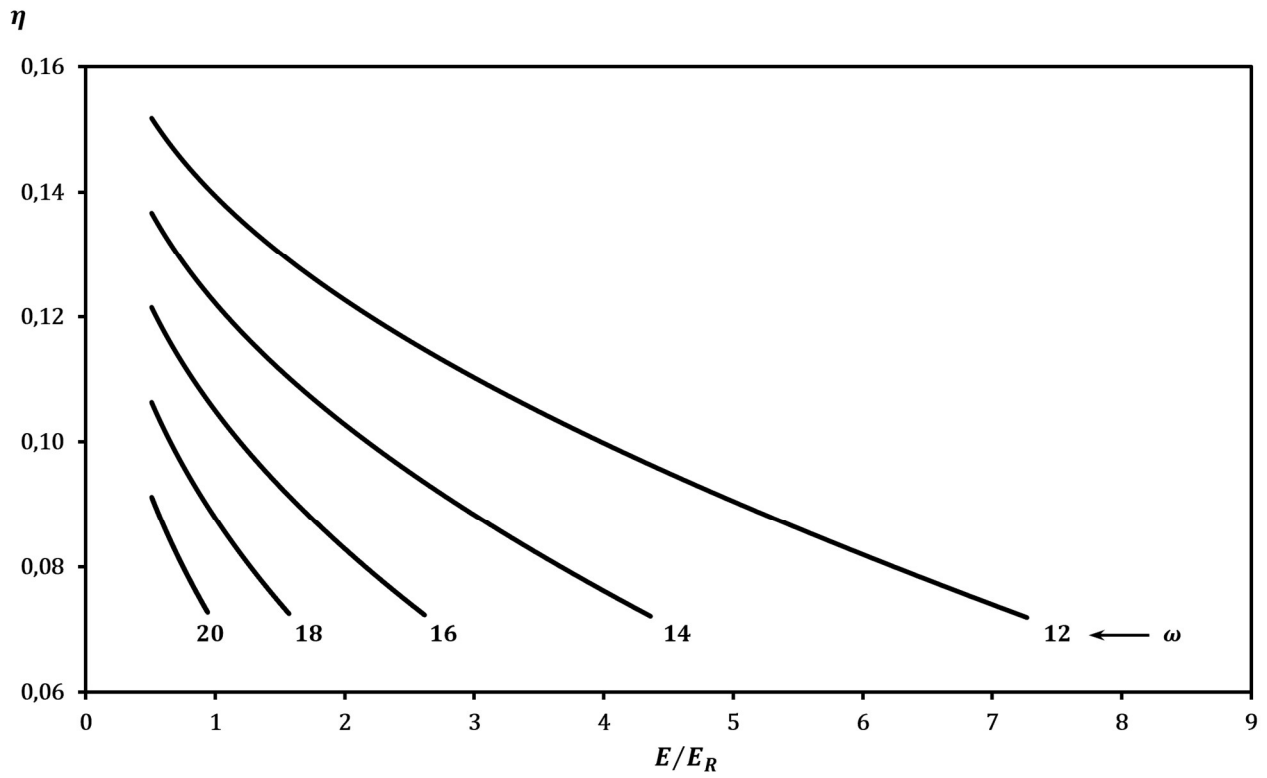

Figure 26

On some climates, mountains of powder constructed with dry material will end up getting wet. This is so true, or not, that the mountain builders we know are as obsessed today with static liquefaction as they were on those times where water transported tailings were stored in dams' reservoirs. They are expecting their mountains to get saturated bottom-up or top-down or both. But, at the same time, they do not seem too worried with removing conventional restraints on the minimum moulding water content, allowing it to fall behind a deviation of -3% from the optimum, for water-saving environmental reasons, they say. Collapsibility of tailings placed with a significant water deficiency and subjected to wetting under high stresses is a theme that should and would deserve all our attention, if we had something palpable to grab on to.

Above all, this chapter may be useful to bring back compaction prestress as an entity with physical meaning and capable of quantifying the mechanical benefits of compaction and, as such, of exposing its limitations. There is a limit on the prestressing that we can currently impose to a soil, which seems to be modest on the case of powder like tailings, and that limit dictates the behaviour of the material when placed in an earthwork, depending on its size and shape.

5. MOUNTAIN BUILDER'S REAL WORLD

5.1. State of play

Our quest is for understanding why, on the minds of real builders of compacted powder mountains, a "0,6 maximum void ratio" criterium constitutes the assurance of eternal life. Instead of digressing, for example to unsaturated soil mechanics, we need to refocus on our goal and this chapter is dedicated to the mountain builders day-by-day, when points do not lie on lines but are dispersed on diffuse clouds. At this incipient stage, we have seen that "0,6 maximum void ratio" may be just a funny way of saying "bring heavier rollers" or "these tailings are not suitable, take them somewhere else". These days everyone says whatever comes to his mind, and we are a good example of it, although we do not charge a penny for our sayings.

So far, no significant advance has been made on the "otherwise your tailings pile will liquefy" fable. On Chapter 2, we told of a case where heavier rollers were brought to action, and a denser end-product was achieved. We have also seen that the respective mountain builders did not show a true believe on the fable, because they left the base of their mountain as it was, supposedly susceptible to the terrifying phenomenon, and kept building piles elsewhere unconcerned with "0,6 maximum void ratio". Pure smartness.

On the previous chapter, we have seen that compressibility per se is unlikely to be the explanation. If a pile settles too much or too little during the years it takes to build will not hinder its serviceability, because its serviceability is none. If the material is heavily compacted, then it is likely that the structure settlements are lower and the cost of construction greater. For those whose money grows like grass, the cost is not an issue. A variable, the compaction prestress, has been introduced and will necessarily be recovered latter, while discussing the shearing resistance of the material. Collapsibility will also have to be addressed in any way, because not everything resumes to the heaviness of compaction, but also to how it is achieved. And now, to the clouds where compaction inhabits.

5.2. Quality control issues

The case introduced in Chapter 2 is an example of the application of the single result method for evaluation of test data. The earthworks specification for the first construction stage demanded the degree of compaction to be:

$$104\% \geq R \geq 98\% \qquad [97]$$

Having the standard compaction effort for reference. This means that any test result falling outside the acceptance limits was considered non-conforming and the compaction control strip where the single test was done was simply rejected without further consideration. Curve 1 on Figure 4, from Chapter 2, illustrates the overall result of the adopted quality control procedure for the first construction stage, pre "0,6 maximum void ratio" criterium. The cumulative distribution, a normal type one, of the degree of compaction is based on 74,6% of a total of $n = 3894$ control test results done during the first construction stage, corresponding that percentage to the quantity of compaction strips considered to be conforming to the specification and therefore accepted. Figure 27, on the next page, sheds some light about the overall problem, showing the percentages of rejected compaction works in accordance with the dual acceptance criteria (R and $\omega - \omega_{opt}$).

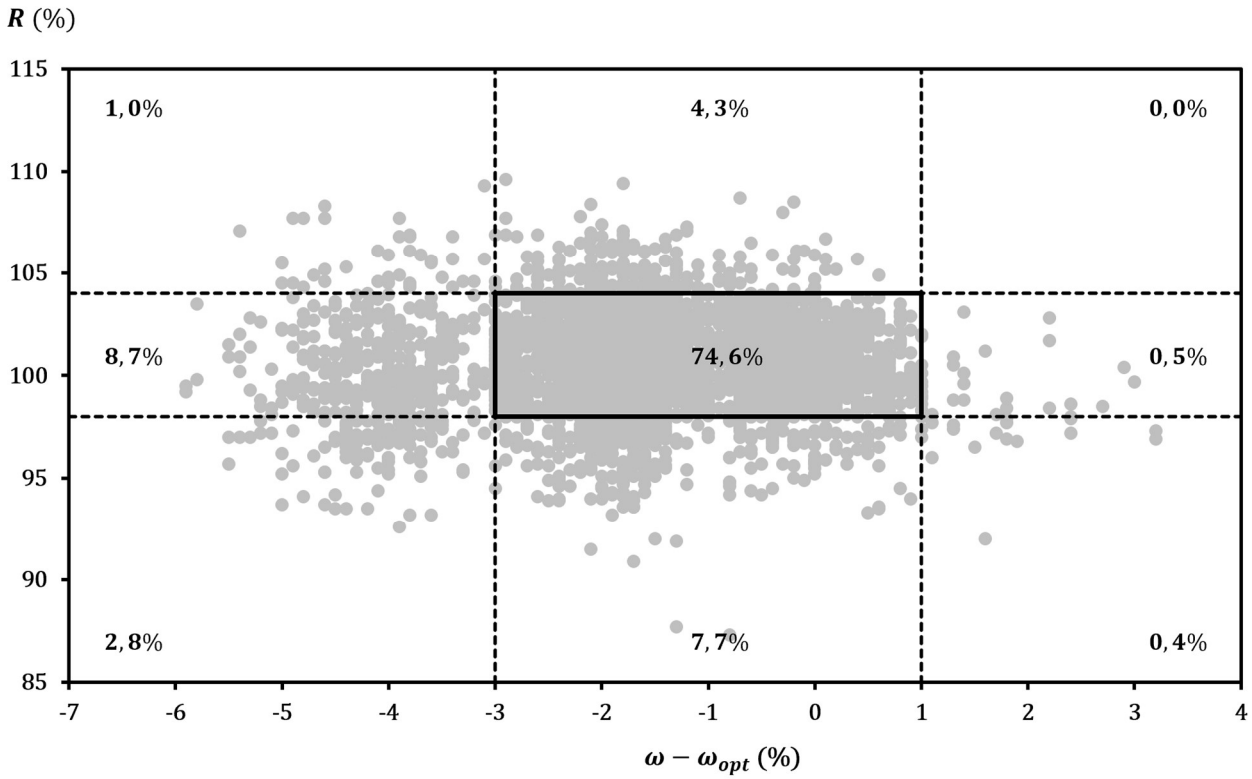

Figure 27

We may observe, in this figure, that, for half of the strips that were rejected (12,5% of total), compaction was attempted with the material too dry. The lower acceptance limit of -3% for the water content deviation was already generous in common standards. The low water content of the dewatered tailings and their subsequent drying during transportation and stocking could be one of the main sources of low productivity. Nevertheless, material complying with the water content criterium gave rise to a significative percentage (12,0% of total) of rejected works. For the following, we will concentrate our attention on the central division (74,6% of total) and try to discuss alternative forms to deal with the variability of the dry unit weight.

However, looking back at Figure 18, we can observe that a 1,5% volumetric collapse strain would result upon wetting of the material compacted slightly wet of optimum with a relative energy $E/E_R = 1{,}31$. For the second construction stage, with the "0,6 maximum void ratio" criterium in force, the lower limit of the water content deviation from optimum was alleviated, meaning that, eventually, material placed with a -6% deviation could have been accepted. We may wonder, and the mountain builders should, how much the collapse potential increased in consequence of that liberating decision. Unfortunately, for those who are subjected to fortune, we do not have test data to make alarming statements regarding the need to control compaction water contents to avoid the malefic effect of collapsibility.

Returning to the dry unit weight and concentrating only on the approved material, the mean value of our sampling is $\bar{R} = 100{,}7\%$ and its standard deviation is $S_R = 1{,}65\%$. The $1 - \alpha = 95\%$ confidence interval of the earthworks mean degree of compaction, μ_R, that is:

$$Pr(\bar{R}_L \leq \mu_R \leq \bar{R}_U) = 1 - \alpha \Leftrightarrow \quad [98]$$

$$\Leftrightarrow Pr(\bar{R} - k \cdot S_R \leq \mu_R \leq \bar{R} + k \cdot S_R) = 1 - \alpha \Leftrightarrow$$

$$\Leftrightarrow Pr\left(\left| t = \frac{\bar{R} - \mu_R}{S_R/\sqrt{n}} \right| \leq k\right) = 1 - \alpha$$

Can be calculated knowing that the random variable t follows a Student *t*-distribution with $f = n - 1$ degrees of freedom:

$$k = \frac{{F_t}^{-1}(1 - \alpha/2\,|f)}{\sqrt{n}} \quad [99]$$

Where ${F_t}^{-1}$ denotes the respective *t*-distribution quantile function. From here, we may state, with 95% confidence, that 100,7% $\leq \mu_R \leq$ 100,8%. Also, the upper one-sided confidence limit R_U for the 95th quantile ($p = 95\%$) of the earthwork's degree of compaction, meaning that:

$$Pr\big(R_U = \bar{R} + k \cdot S_R \geq \mu_R + K_p \cdot \sigma_R\big) = 1 - \alpha \Leftrightarrow$$

$$\Leftrightarrow Pr\left(t = \frac{-\frac{\bar{R} - \mu_R}{\sigma_R} \cdot \sqrt{n} + K_p \cdot \sqrt{n}}{\sqrt{n-1} \cdot \frac{S_R}{\sigma_R}} \cdot \sqrt{n-1} \leq k \cdot \sqrt{n} \right) = 1 - \alpha \quad [100]$$

Can be calculated knowing that the random variable t follows a non-central *t*-distribution with $f = n - 1$ degrees of freedom and a non-centrality parameter $\delta = K_p \cdot \sqrt{n}$, where $K_p = \Phi^{-1}(p)$ and Φ^{-1} denotes the quantile function of the standard normal distribution ($K_{0,95} = 1{,}64$ and $K_{0,90} = 1{,}28$):

$$k = \frac{{F_t}^{-1}(1 - \alpha | f, \delta)}{\sqrt{n}} \quad [101]$$

Where ${F_t}^{-1}$ denotes the respective *t*-distribution quantile function. Similarly, the lower one-sided confidence limit R_L for the 5th quantile ($p = 5\%$) of the earthwork's degree of compaction can be calculated substituting the numerator of equation 40 by ${F_t}^{-1}(\alpha|f, -\delta)$. Thereby, with $1 - \alpha = 95\%$ confidence, we may state that 95% of the earthwork has a degree of compaction lower than 103,5% and that 95% of the earthwork has a degree of compaction greater than 97,9% ($k = 1{,}70$). Alternatively, we may also state, with $1 - \alpha = 90\%$ confidence, that 90% of the earthwork has a degree of compaction lower than 102,9% and that 90% of the earthwork has a degree of compaction greater than 98,6% ($k = 1{,}32$).

If, for the sake of discussion, non-conforming tests with $R = 96\%$ were included, without necessarily meaning that the control strips where they were done needed to be rejected, plus 297 tests results can be integrated on the sample. The mean value of this new sample would be 100,7% and the standard deviation 1,65%. Now, with $1 - \alpha = 95\%$ confidence, we may state that 95% of the earthwork would have a degree of compaction lower than 103,6% and that 95% of the earthwork would have a degree of compaction greater than 97,2%. Alternatively, we can state, with $1 - \alpha = 90\%$ confidence, that 90% of the earthwork would have a degree of

compaction lower than 102,9% and that 5% of the earthwork would have a degree of compaction greater than 97,9%. If we compare the statistics of the two samples, we will probably be wondering if there was an effective necessity of rejecting all compaction strips where the (96% $\leq R <$ 98%) non-conforming tests where done.

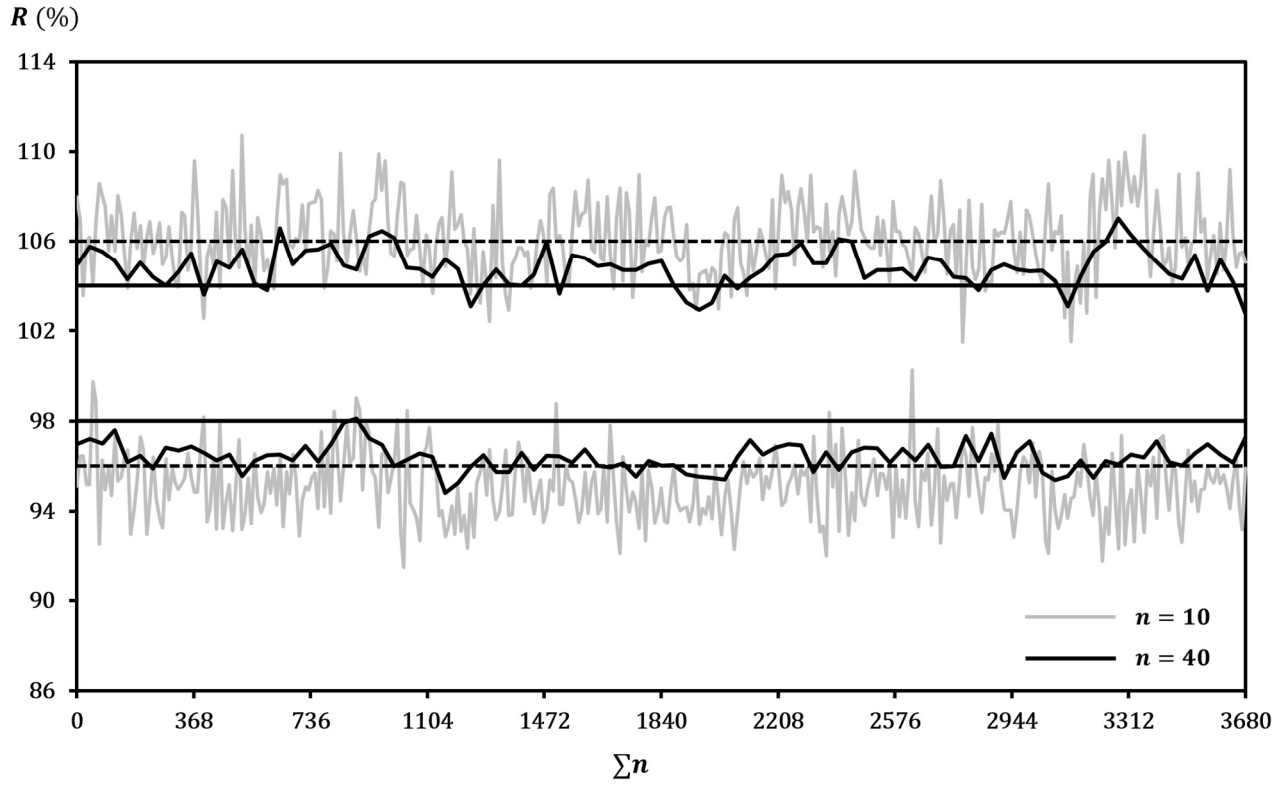

Figure 28

It is obvious that the above statistics are useful à posteriori to evaluate the quality of the whole earthwork or a substantial part of it, but not on a routine basis. This results from the fact that the mean value μ_R and the standard deviation σ_R of the population are not known from the start and better estimates of them just will become available as the cumulative number of tests available grows. This is illustrated in Figure 28, where estimates of the upper and lower 5th quantiles, with a level of confidence of 95%, are based on sequential sets of samples of different size, $n = 10$ and $n = 40$. On this case, we are admitting that no control strip where tests resulted on a degree of compaction within the interval 96% $\leq R \leq$ 106% were rejected. If the calculation had been done using the cumulative number of available samples, the estimates would progressively, and rapidly, tend to the statistics presented early on for the whole earthwork.

The European standard EN 16907, alongside the single result method, suggests the use of statistical methods for compaction quality control. Next, we will see with an example where we would be taken if applying one of these methods, the so-called method of variables for test evaluation, to our case study. Meanwhile it is worth bearing in mind that resuming quality control to the evaluation of single tests results represents time saving. For this exercise, we will include all tests resulting in a degree of compaction within the interval 90% to 109%, comprising a total of $n = 3885$ determinations ranging between 90,9% and 108,7%, with a mean value of 100,5% and a standard deviation of 2,39%. For statistical control, the specification of earthworks compaction requires the definition of an acceptance sampling plan, and we will start with one having a single specification limit, $R_L =$ 96%, a lower one on the case. To facilitate the exposition, we will be assuming that the standard deviation of

earthwork is known in advance, $\sigma_R = 2{,}39\%$, what allows us to work only with normally distributed statistics. The objective of this hypothetical plan is to assure that the fraction of non-conforming material will lie within tolerable limits.

For instance, we could require the probability of good-quality material being rejected to be as much as $\alpha = 5\%$ (the producer´s risk) and, simultaneously, require that the probability of poor-quality material being accepted to be as much as $\beta = 10\%$ (the consumer´s risk). We will define good material as that containing a non-conforming fraction $p_a = 1{,}8\%$ (the acceptance quality limit) and we will define poor quality material as that containing a non-conforming fraction $p_u = 20{,}2\%$. Any other definition would be possible. The respective acceptance criterium would be:

$$\frac{\bar{R} - R_L}{\sigma_R} \geq k \quad [102]$$

Being k the acceptance constant and $\bar{R}$ the average degree of compaction resulting from n tests per compaction control strip. If the statistics are normally distributed, there is a unique relationship between the mean degree of compaction and the non-conforming fraction. So, denoting $z_p = \Phi^{-1}(p)$ as the p quantile of the standard normal distribution, for the good-quality material we will have a mean degree of compaction:

$$z_{1-\alpha} = \frac{\mu_{R,a} - R_L}{\sigma_R} = 1{,}645 \Longrightarrow \mu_{R,a} = R_L + z_{1-\alpha} \cdot \sigma_R = 101\% \quad [103]$$

And for the poor-quality material:

$$z_{1-\beta} = \frac{\mu_{R,u} - R_L}{\sigma_R} = 1{,}282 \Longrightarrow \mu_{R,u} = R_L + z_{1-\beta} \cdot \sigma_R = 98\% \quad [104]$$

We also have the following z-scores:

$$z_{a=0{,}018} = 2{,}090 \quad [105]$$

And:

$$z_{u=0{,}202} = 0{,}836 \quad [106]$$

The design of an acceptance sampling plan according to these requirements requires the acceptance constant and the number of sample tests to be determined in accordance. For that, we can start with the following statistical statements:

$$Pr\left(\frac{\bar{R} - R_L}{\sigma_R} \geq k \middle| \mu_R = \mu_{R,a}\right) = 1 - \alpha \Leftrightarrow Pr\left(\frac{\bar{R} - \mu_{R,a}}{\sigma_R/\sqrt{n}} \geq k \cdot \sqrt{n} - \frac{\mu_{R,a} - R_L}{\sigma_R/\sqrt{n}}\right) = 1 - \alpha \Longrightarrow \quad [107]$$

$$\Longrightarrow z_{1-\alpha} = (k - z_a) \cdot \sqrt{n} \Longrightarrow k = z_a + z_{1-\alpha}/\sqrt{n}$$

And:

$$Pr\left(\frac{\bar{R} - R_L}{\sigma_R} \geq k \middle| \mu_R = \mu_{R,u}\right) = \beta \Leftrightarrow Pr\left(\frac{\bar{R} - \mu_{R,u}}{\sigma_R/\sqrt{n}} \geq k \cdot \sqrt{n} - \frac{\mu_{R,u} - R_L}{\sigma_R/\sqrt{n}}\right) = \beta \Longrightarrow$$
$$\Longrightarrow z_\beta = (k - z_u) \cdot \sqrt{n} \Longrightarrow k = z_u - z_{1-\beta}/\sqrt{n} \quad [108]$$

From where two equations with two unknowns can be solved to yield:

$$n = \left(\frac{z_{1-\alpha} + z_{1-\beta}}{z_a - z_u}\right)^2 = \left(\frac{1{,}645 + 1{,}282}{2{,}090 - 0{,}836}\right)^2 = 5{,}4 \quad [109]$$

And:

$$k = \frac{z_{1-\alpha} \cdot z_u + z_{1-\beta} \cdot z_a}{z_{1-\alpha} + z_{1-\beta}} \quad [110]$$

We will round the result of equation 109 to the closest integer, $n = 5$ and take k as the average of the values calculated separately by equation 107 and 108 with the rounded value of n, which results in $k = 1{,}382$.

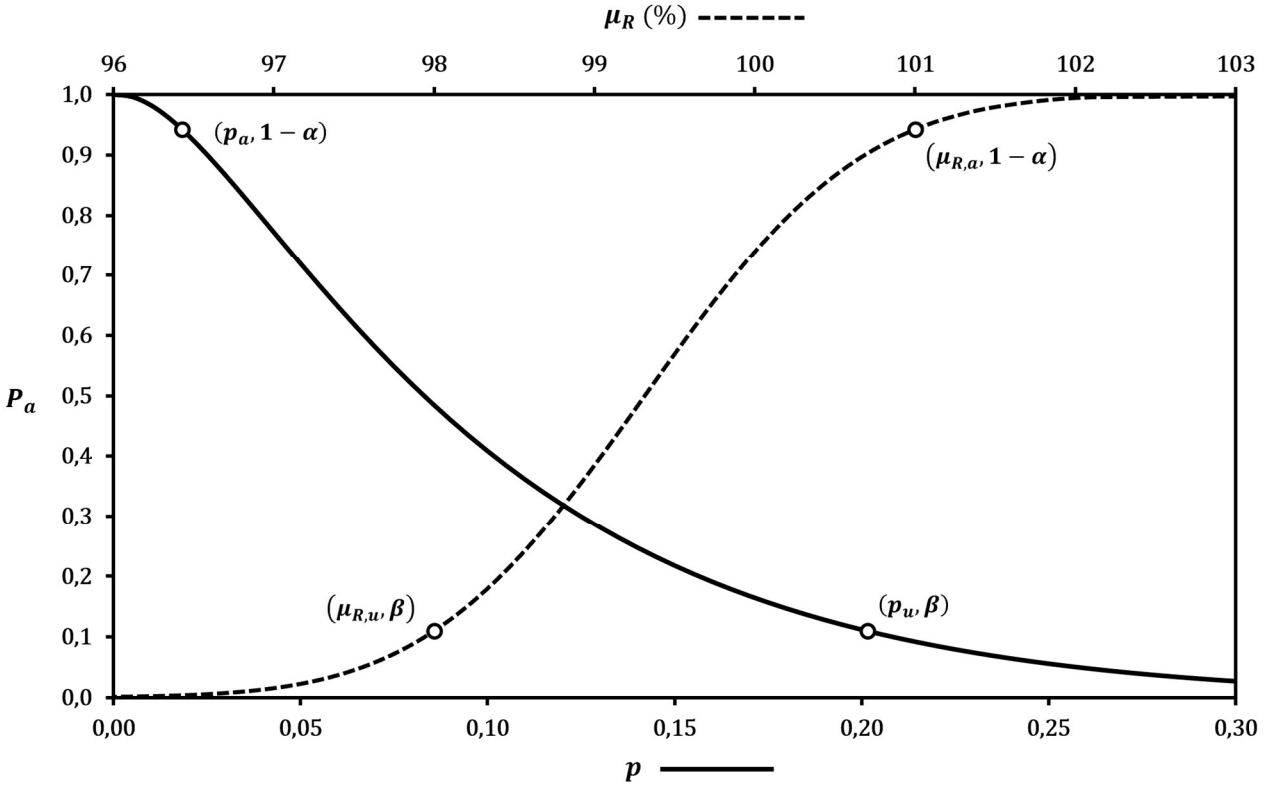

Figure 29

According to this plan, the probability of acceptance P_a of a compaction strip with a fraction non-conforming fraction p is given by:

$$P_a = 1 - \Phi\left(\left(k - z_p\right) \cdot \sqrt{n}\right) \quad [111]$$

The so-called operating characteristic curve of our intended sampling plan is represented in Figure 29, on the previous page.

To exemplify, our database of test results was subdivided sequentially in groups of 5, imagining that each group corresponded to the sampling on a same compaction control strip. At total we will be analysing 777 compaction strips. Performing the calculations, we end up with a total of 144 compaction strips being rejected, corresponding to 18,5% of the total production. The mean degree of compaction of the approved earthwork is 100,9% and for its rejected counterpart is 98,6%. Within the approved control strips, a fraction of 6,5% has a degree of compaction greater or equal to 104% and a fraction of 6,2% has a degree of compaction lower or equal to 98%. A fraction of 1,4% with a compaction degree lower or equal to 96% remains within the approved strips. The control strip with a greater non-conforming fraction that was still approved has an average degree of compaction of 99,3%.

Imagining now that each of the 777 compaction strips of the first sampling plan had been subjected to a single test and that the inspector in charge had a clinical eye to choose the location of the worst result test point from the same 5 possible, then 40% of the compaction strips would have been rejected for having a degree of compaction lower than 98%. Otherwise, if the inspector had a clinical eye to choose the location of the best result test point from the same 5 possible, no compaction strip would have been rejected. On this latter case, a fraction of 11% of the earthwork would have a degree of compaction lower or equal to 98%. For quality control with the single result method, the probability of acceptance of a compaction strip is simply the complementary of the non-conforming fraction within it, meaning that, for example, we have an 80% probability of accepting material containing a 20% non-conforming fraction.

If we considered that the standard deviation of the population is unknown a priori, the same procedure used for the known case can be followed, after replacing the denominator in Equation 102, σ_R, by the individual standard deviation of each n-sized sample, S_R. The resulting statistic, $(\bar{R} - R_L)/S_R$, will now follow a non-central t-distribution with $f = n - 1$ degrees of freedom and a non-centrality parameter $\delta = z_L \cdot \sqrt{n}$. Keeping the same z-scores of the previous plan, our new sampling plan will have the acceptance constant given by equation 110, $k = 1{,}385$, but the number of samples will have to be greater, as approximately given by:

$$n = \left(1 + \frac{k^2}{2}\right) \cdot \left(\frac{z_{1-\alpha} + z_{1-\beta}}{z_a - z_u}\right)^2 = \left(1 + \frac{1{,}385^2}{2}\right) \cdot \left(\frac{1{,}645 + 1{,}282}{2{,}090 - 0{,}836}\right)^2 = 10{,}7 \quad [112]$$

Which we will round to $n = 10$, the double of the sampling size of the previous plan.

This time our database of test results was subdivided sequentially in groups of 10, imagining that each group corresponded to the sampling on a same compaction control strip. At total we will be analysing 388 compaction strips. Performing the calculations, we end up with a total of 50 compaction strips being rejected, corresponding to 12,9% of the total production. The mean degree of compaction of the approved earthwork is 100,7% and for

its rejected counterpart is 99,2%. Within the approved control strips, a fraction of 5,6% has a degree of compaction greater or equal to 104% and a fraction of 8,4% has a degree of compaction lower or equal to 98%. A fraction of 1,8% with a compaction degree lower or equal to 96% remains within the approved strips. The control strip with a greater non-conforming fraction that was still approved has an average degree of compaction of 98,0% and a standard deviation of 1,2%.

A direct comparison with the results from the previous sampling plan is not immediate, as for this latter one nearly the double of tests would be required for the same volume of material compacted. In any case, the characteristic curve is the same for both plans. If a statistical quality control procedure was implemented starting with the assumption that the standard variation was unknown, it would be obviously advantageous switching to a new plan as soon as the test data accumulated until then allowed a good estimate of the standard deviation of the earthwork.

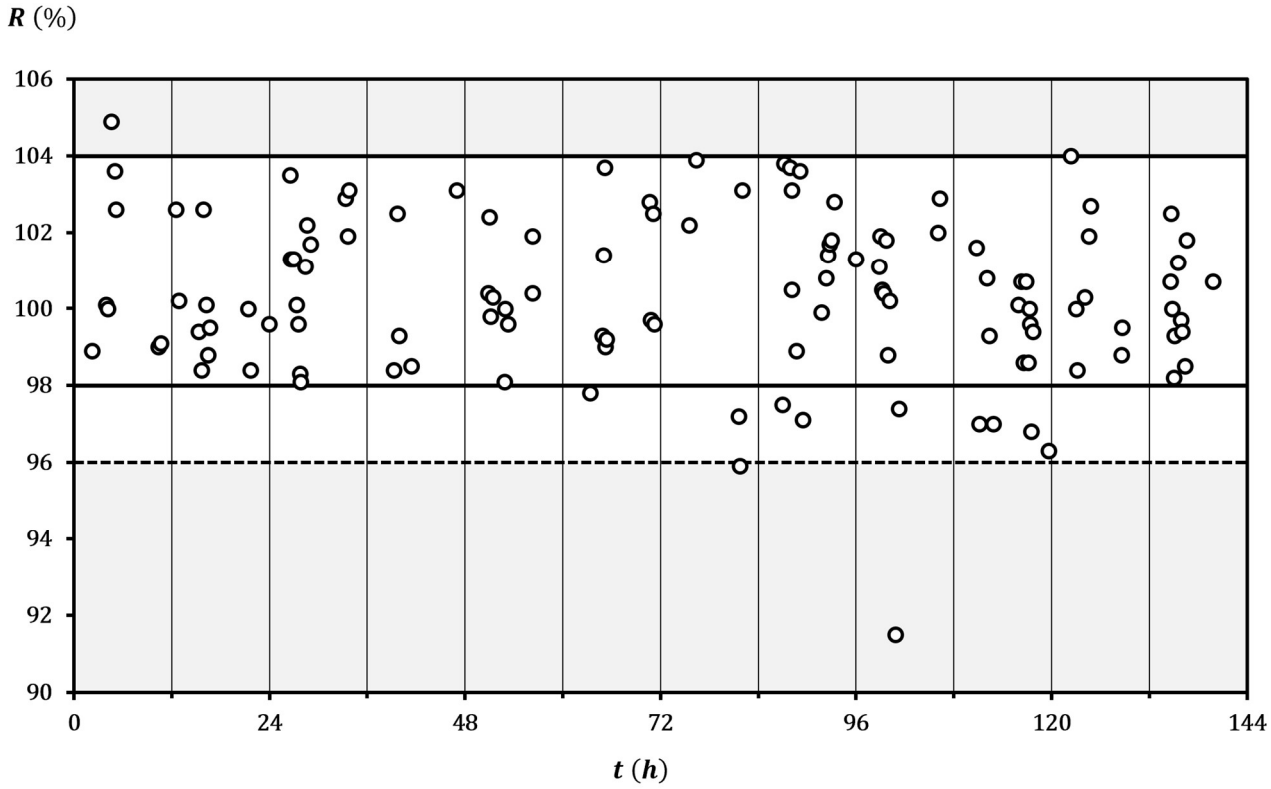

Figure 30

Albeit all the interest on the quality control subject, we would like to retain from this section that, within a control strip area, we will find material from the same source subject to the same compaction procedure, but with different degrees of compaction, most probably with some fraction of material non-conforming to the specifications. Figure 30 is a control chart containing the hourly results (degree of compaction by the Hilf method) of testing during a working week. Presuming that the tailings batch being placed each half day is from the same source and was compacted following the same procedure, we can observe that the variability of the determinations is as high on a half-day lapse as it is throughout the full week. A similar chart extending for months, apart from discernible and possibly explainable perturbations in some periods, as, for example, influenced by climacteric conditions, would lead us to the same conclusion. It seems that we cannot escape from treating filtered tailings compaction as a random construction process. Just like any other soil. Complementarily,

Figure 31 shows the evolution of the number of rejected compaction control strips during 52 consecutive calendar weeks.

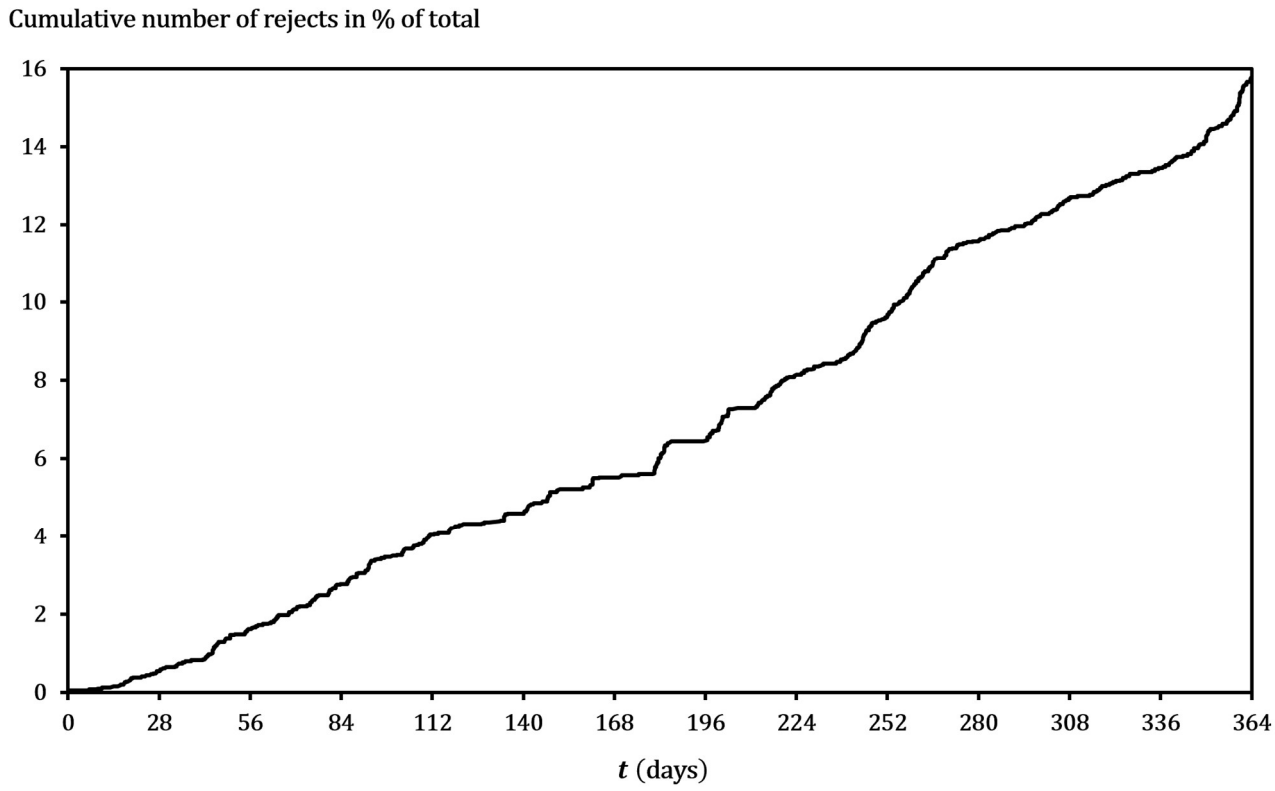

Figure 31

The nearly constant rate of rejections observed in the figure helps strengthen the idea that a relevant component of variability on the compaction of this material is related to variations in the production of each source lot and to a less extent related to variations among successive source lots. Our “unique” material is effectively “unique”, not unique. The geotechnical trauma.

5.3. Introducing the “55-70” tailings

Up until now, we have seen that, better or worse, we can aspire simulating the compaction curves of a soil subjected to different compaction energies and even to build a compaction state surface where the effects of compaction can be expressed in terms of relevant mechanical properties, like the as-compacted void ratio and prestress. All based on few routine geotechnical tests. We have given a couple of examples of quite successful application of the compaction curve model to different dry iron-ore mine tailings, however without ever addressing the index physical characteristics that differentiates them, as their granulometry. The challenging part starts now, inquiring if the model parameters can be related to basic physical properties in such a way that the former can be predicted from the latter.

We have gathered a database of 194 compaction tests, using the standard Proctor energy, all and which of them accompanied by the determination of the specific gravity of solids and grain size analysis. All these iron-ore tailings are non-plastic and were dewatered on treatment plants of the same mine and eventually placed on a same dry stacking pile, currently under construction. As “unique” as “unique” can be. The database includes material with fines content, FC (percentage of particles with dimension lower than 74μm, the opening of ASTM

sieve Nº200), ranging from 19% to 83%, but we will be concentrating our attention on a narrower range of material, having fines on the interval 55% $\leq FC \leq$ 70% and for which we have complete 105 sets of tests. This is our "55-70".

It will soon be understood the reason why it is preferable to study a narrower grading, but the previous chapter already provides some answer. Variability is astronomic in what concerns to this material compactability. The mean diameter of the "55-70" finer fraction, d_{50}, corresponding to a ponderal percentage $FC/2$, ranges between 0,010mm e 0,042mm and the mean diameter of the coarse fraction, corresponding to a ponderal percentage $50 + FC/2$, ranges between 0,107mm e 0,120mm. The ratio of the mean fraction's diameters ranges between 0,089 e 0,367. The material is as similar to powder as soil can be, despite the fine sand content still present. In technical terms, our powder is a lean silt (ML) according to the Unified Soil Classification System. The particle size distributions of the 105 samples of "55-70" are shown in Figure 32.

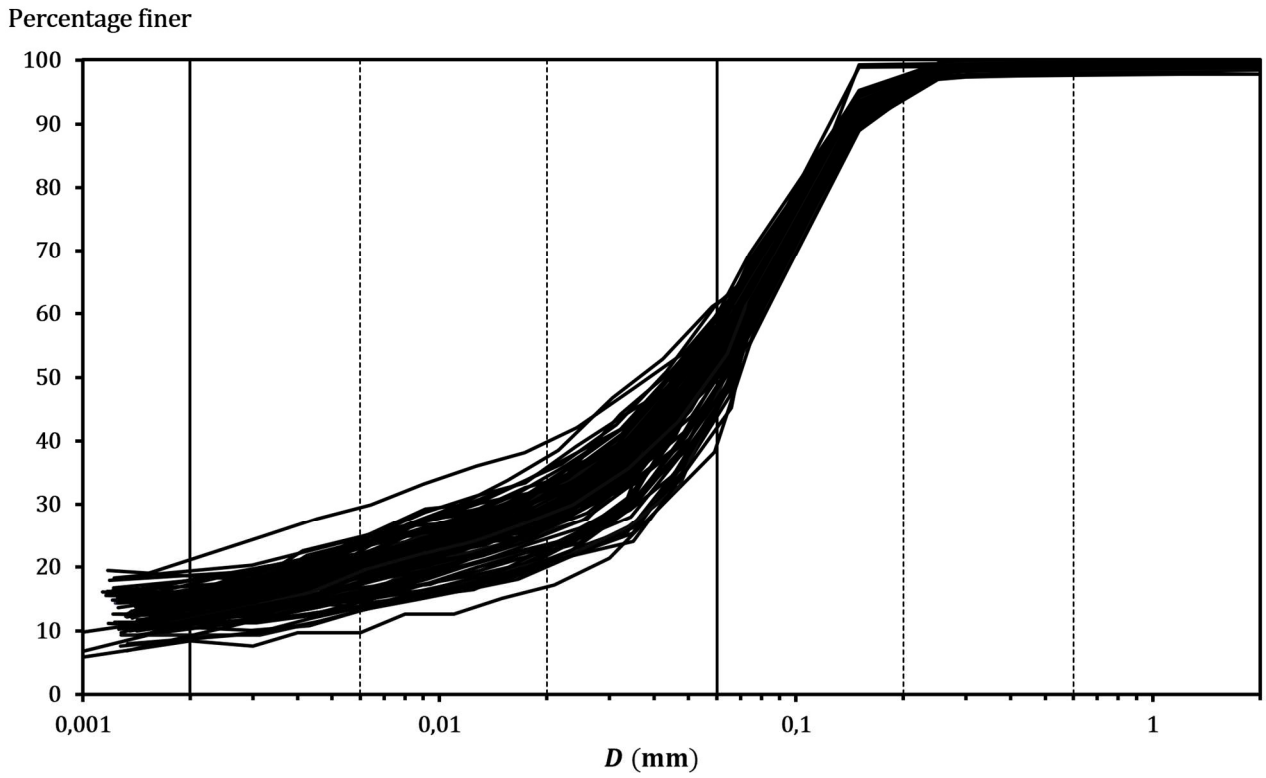

Figure 32

To illustrate conveniently the reach of our objective, Figure 33, on next page, shows simultaneously the $N =$ 525 points (ω, S) obtained on the 5-points compaction tests performed on each of the 105 samples. Is it possible to estimate the compaction curve model parameters (ω_m, S_m, m, n and $\overline{\omega}_m$) from the particle size analysis? The work of François de Larrard on concrete mixes would fit our goal as a glove, but we are limited to particle size distributions and the only void ratio that we know about is that of the mix called tailings. Therefore, conclusions, if any, will have to be reached with the information contained on a common particle size analysis. Also, our aim is not to come up with an endless and unappealing multivariable regression using a statistical software, rather finding a simple and intuitive correlation with a single variable that can describe, even if remotely, the different particle packings allowed by the tailings granulometries. We will make the omelette with the eggs we can break.

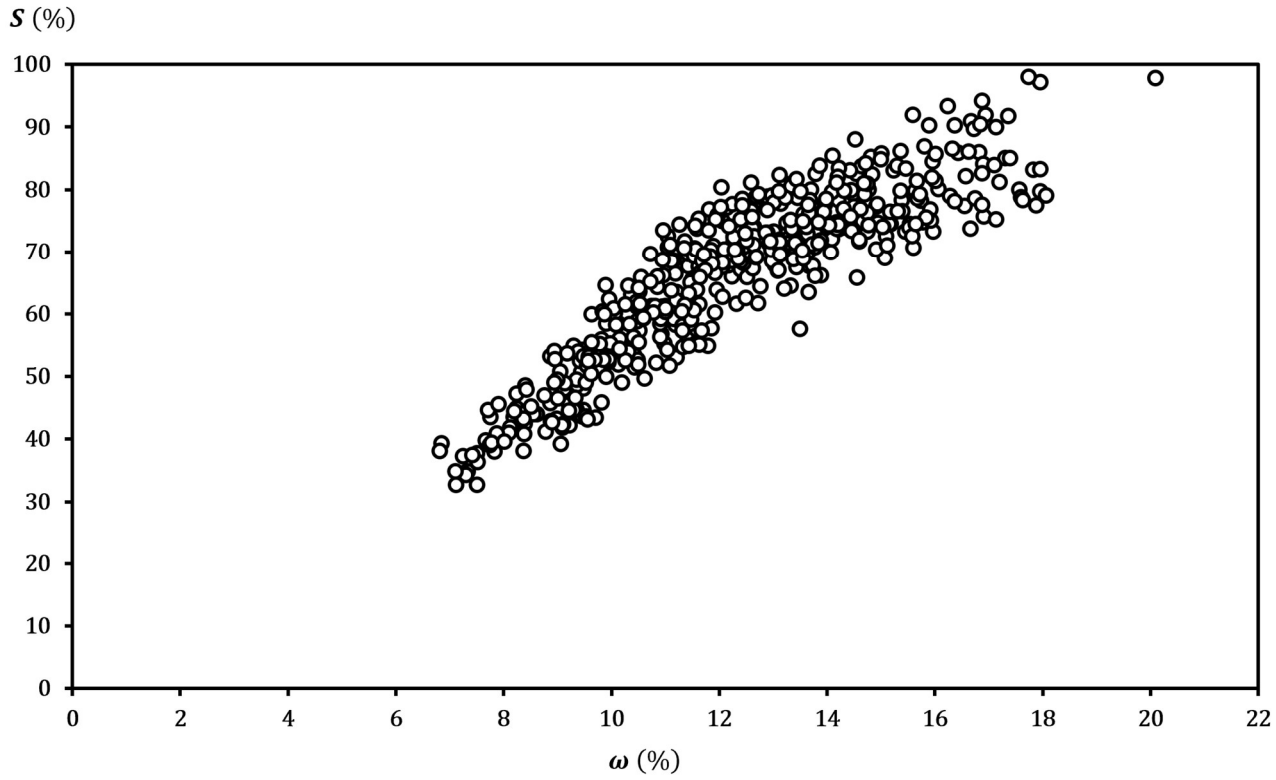

Figure 33

As referred, apart from the gradings, we have a determination of the specific gravity of solids for each sample. The mean value, for the 105 samples of "55-70", is 3,147 and the standard deviation is 0,072.

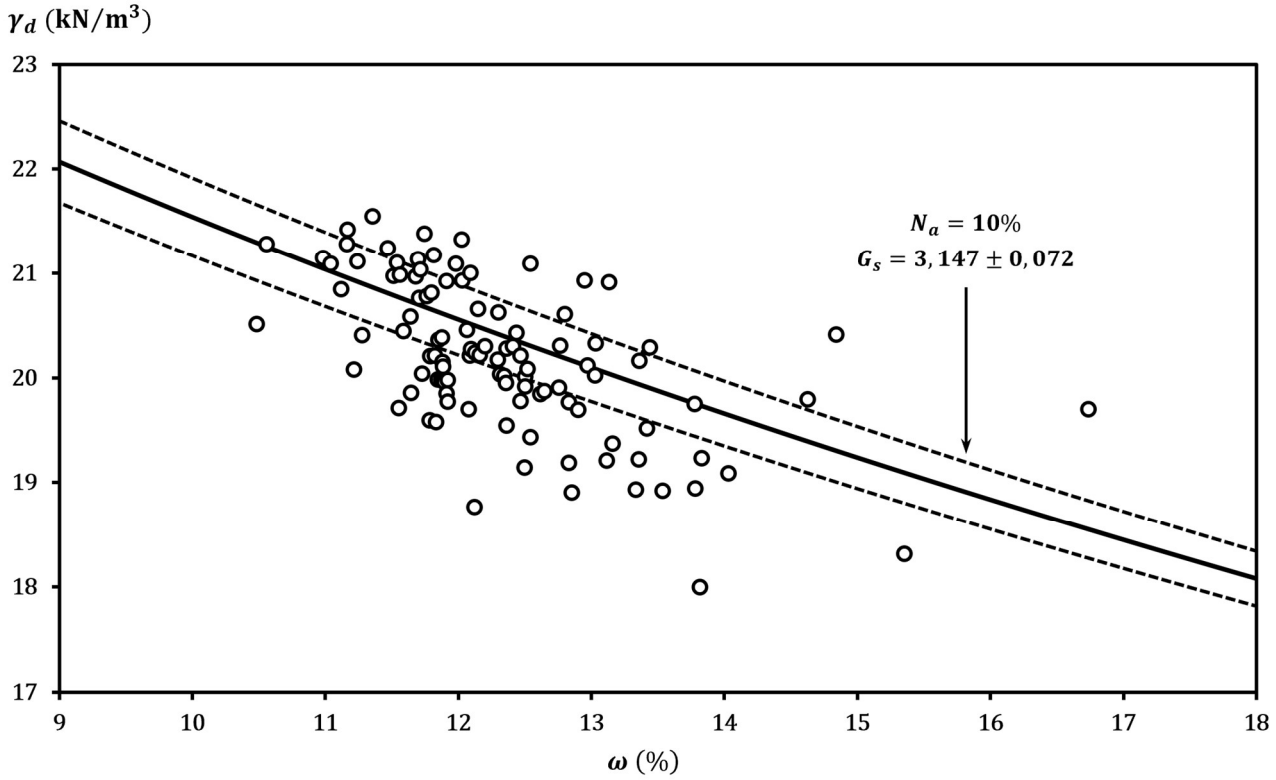

Figure 34

Figure 34, on the previous page, highlights the importance of the value of the specific gravity of solids used on calculations. On the figure, dots correspond to the optimum compaction point ($\omega_{opt}, \gamma_{d,max}$) of each of the 105 compaction tests and lines correspond to 10% of air voids, assuming three different values of specific gravity of solids spaced by one standard deviation around the mean. If the maximum percent of air voids was used as a compaction control parameter, as happens in some countries, we may observe the quantity of compaction works that would be differently rejected, depending on the value attributed to the specific gravity of solids. In rigorous terms, the mean value of the percent of air voids at the optimum compaction point is 10,9 and the standard deviation is 2,9%. Also, at same optimum point, the degree of saturation has a mean value of 69,6% and a standard deviation of 5,3%. In general terms, two observations seem pertinent regarding these statistics. On one hand, the typical reference value of 85% saturation degree expected to lead to the maximum dry weight does not apply to the filtered tailings. On the other hand, especially if a tight control is not exerted on the lower limit of the moulding water content, compacted tailings like the "55-70" are a "bubble of air" entrapped in powder.

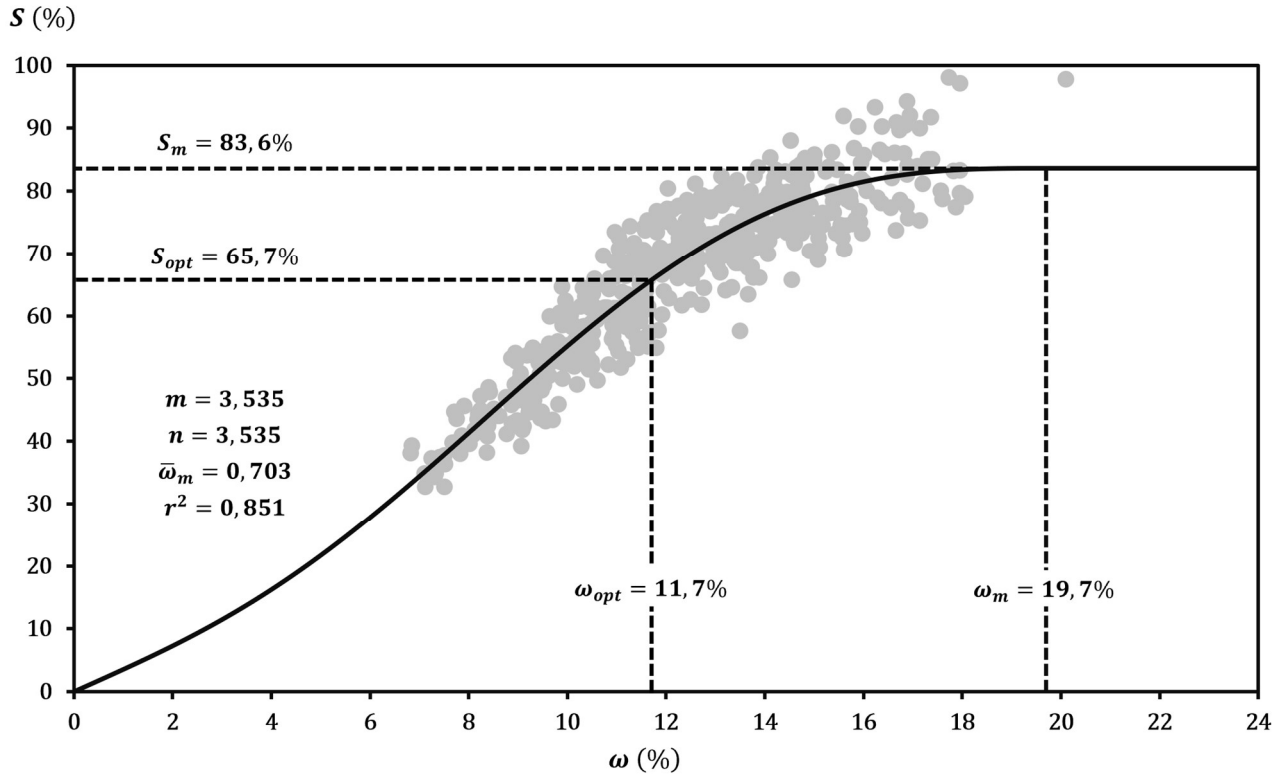

Figure 35

Ahead of any other attempt, we may see in Figure 35 what happens if a single $S(\omega)$ function is fitted simultaneously to all of 525 points from the 105 compaction tests. The mean absolute percentage error is 2,32% for the dry unit weight prediction and 6,26% for the void ratio prediction. For 95% of the determinations of dry unit weight, the absolute percentage error is less than 5,65% and for, the same quantile, the absolute percentage error is less 15,19% percent for the void ratio. The resulting model parameters are stated on the figure.

Complementary to this last figure, Figure 36, on the next page, shows the average compaction curve in terms of the ratio e/G_s ($= \omega/S$). At the optimum point of compaction, the minimum void ratio achieved with the normal

Proctor energy has a mean value of 0,559 and a standard deviation of 0,047. Note that the "55-70" filtered tailings are not the same as those used on the case introduced earlier on Chapter 2, which had a coarser grading.

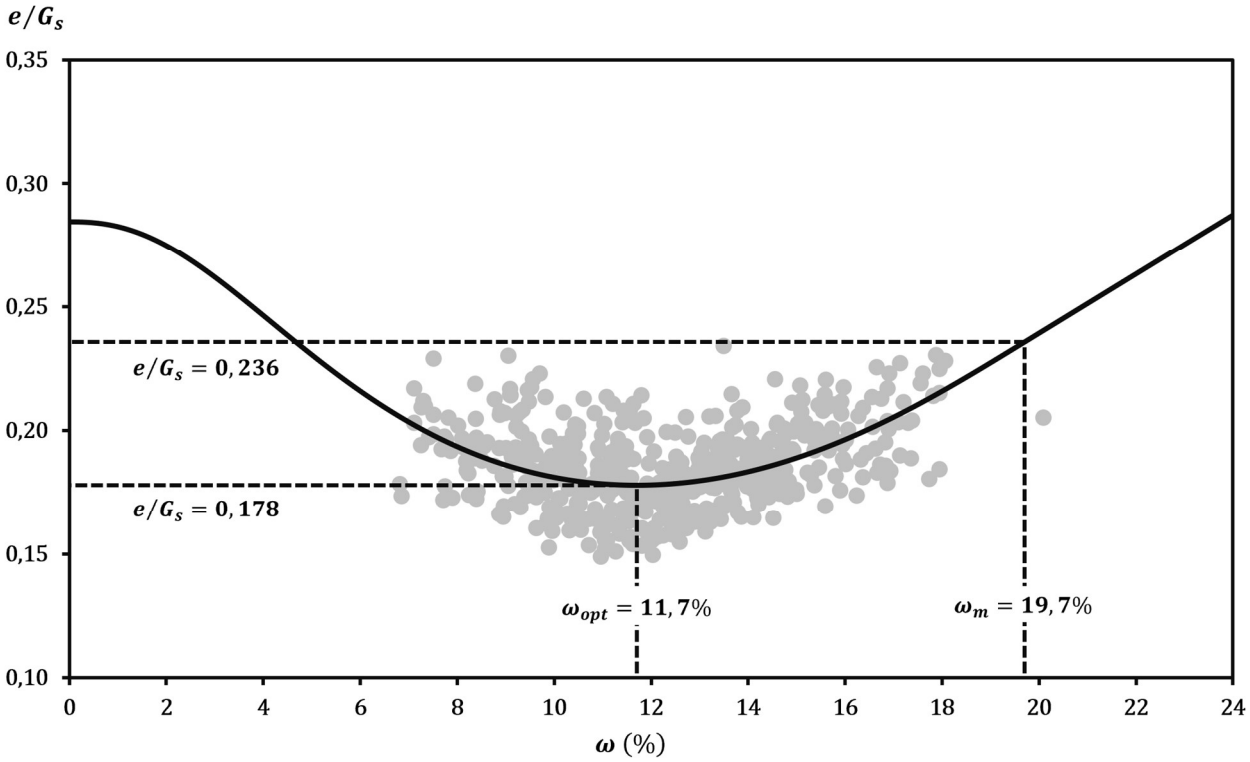

Figure 36

Once we have chosen the fines content to identify the material, it makes some sense to figure out if that granulometric characteristic helps explaining the variability of results identified around the mean tendency. For that purpose, all model parameters will be held constant and equal to the ones used on the previous attempt, except the values of ω_m and S_m. As a first guess, the simplest dependency function between the fines content and the each one of the two model parameters assumed to be dependent is a linear one. We can see in Figure 37, on next page, the results of this first and acritical correlation trial between the compaction curve model parameters and a variable which is related to the granulometry of the material.

Qualitatively, we are led to the conclusion that the material containing more fines becomes, upon compaction with the same energy, denser (lower void ratio) than that containing less fines. Looking at the particle size distributions in Figure 32, we may infer that, for the "55-70", the greater the fines content is, the better is the gradation of the mix in terms of its uniformity and curvature. It is reasonable to accept that a better gradation results on a tighter particle packing, even if besides a fine grained, non-plastic, soil. In line with the first finding, we can also conclude from Figure 37 that the material containing more fines requires less water (lower water content), in relation to the weight of solids, to reach the maximum density, whilst a greater volume of voids is occupied by water (greater saturation degree). We will explore these aspects latter on. The correlations leading to the best fit are:

$$\omega_m = 29{,}72 - 0{,}158 \times FC \quad [113]$$

And:

$$S_m = 58{,}19 + 0{,}422 \times FC \qquad [114]$$

And the values of the remaining parameter values, kept constant, are stated on Figure 37. The three curves presented on this figure correspond to an interval of 1,645 times the standard deviation of the fines content of our sampling, meaning that 90% of the values should lie within the bounding curves.

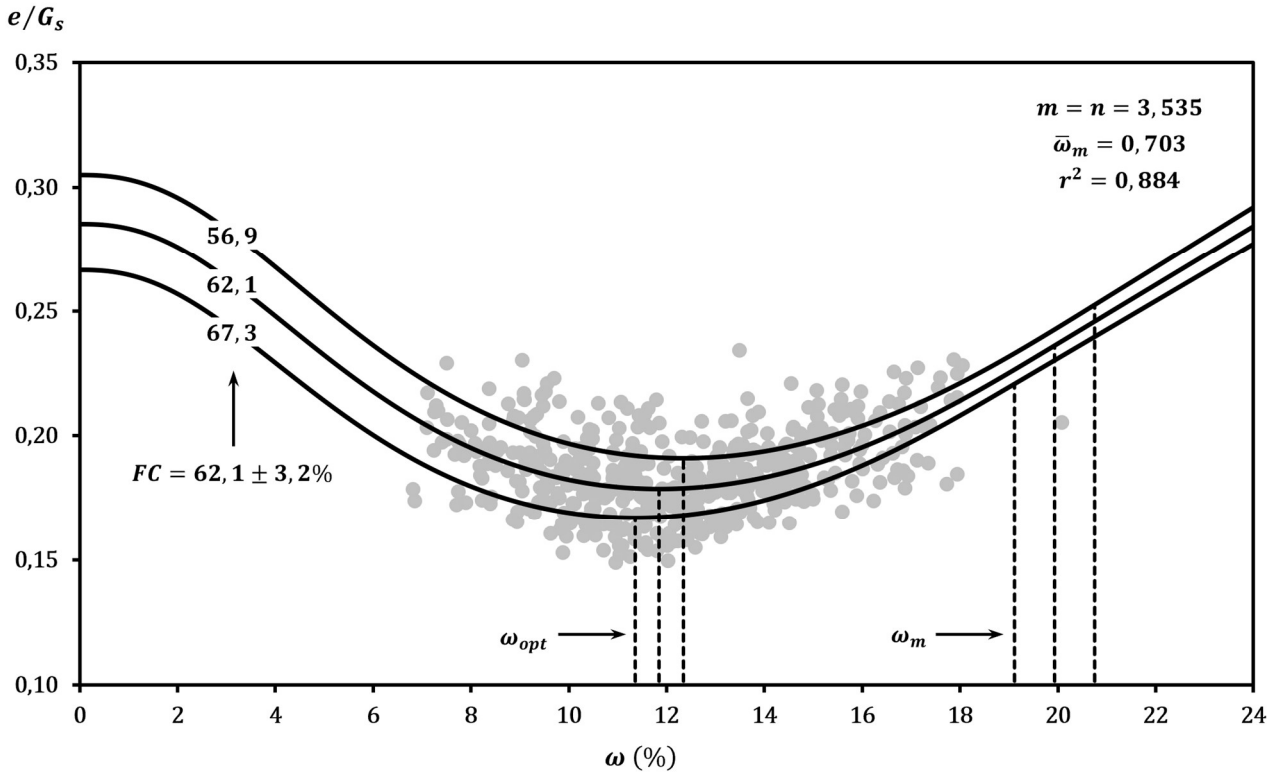

Figure 37

The mean absolute percentage error is now 2,34% for the dry unit weight prediction and 6,31% for the void ratio prediction. For 95% of the determinations of dry unit weight, the absolute percentage error is less than 5,66% and for, the same quantile, the absolute percentage error is less 14,67% percent for the void ratio. There is no improvement of the prediction in relation to the single curve case presented before. For the saturation degree, which is our response variable, the mean absolute percentage error increased from 6,30% to 6,35% because of introducing a dependency of ω_m and S_m on FC. The same way, for 95% of the determinations, the absolute percentage error barely increased from a maximum value of 15,40% to a maximum value of 15,43%.

If the material grading is effectively a factor that explains, even if partially, the variability on the compactability of our “55-70”, there are countless of combinations of particle sizes or particle size ratios that could be tried as correlation parameters. This booklet is already bad enough for us to transform it on the report of an endless quest for the perfect multiparameter correlation that probably does not exist. If there is no simple and intuitive correlation that is not dictated by statistics, then the failure is ours.

Andreasen, A. H. M. and Andersen, J., in Denmark, published their optimum particle packing theory on the thirties of last century and it applies to continuous particle size distributions, with a maximum diameter D_{max} and unlimited inferiorly. Apart from being largely used on several powder-related industries along the years, the model fulfils the simplicity that we seek for and the prerequisites seems to fit our material as a glove. Being D the diameter of a particle corresponding to a fraction P of the mix with equal or lower size, the densest packing will be attained with a composition given by:

$$\frac{P}{100} = \left(\frac{D}{D_{max}}\right)^{\nu} \qquad [115]$$

Where the exponent ν is known as the granulometric distribution modulus and that, following the authors´ experiences, should assume a value between 1/3 e 1/2. For the "55-70", we will be considering that the maximum particle size is $D_{max} = 0{,}25$mm, being the respective fraction $P \geq 98{,}5\%$ for any of the 105 samples available.

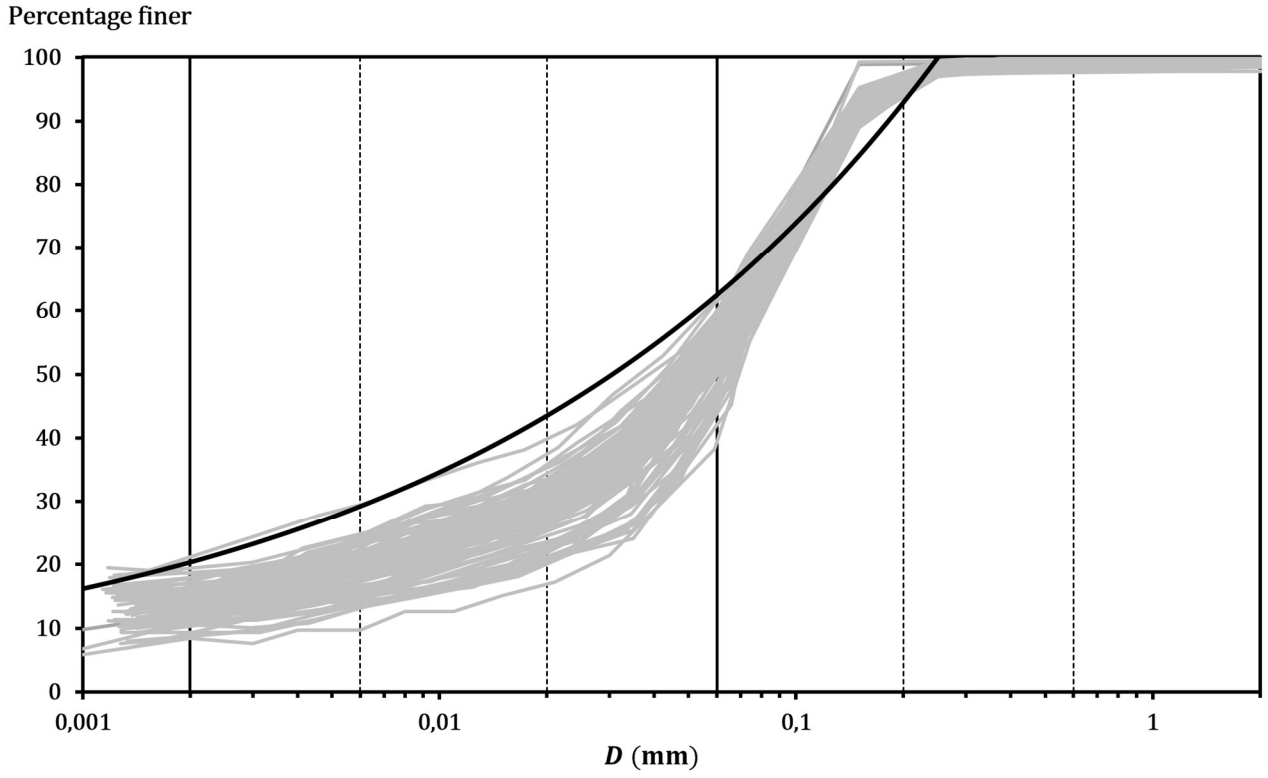

Figure 38

Figure 38 shows, in grey lines, the 105 particle size distributions of our "55-70" tailings and over them, in a black line, the theoretical particle composition leading to the densest mix for $D_{max} = 0{,}25$mm and ν =1/3. For our purpose we do necessarily need to know the value of the theoretical distribution modulus, being enough to accept that the modulus of each particle size distribution can act as the distinguishing factor of the material compactability in what depends on its grading. The modulus of the granulometric distribution of each sample can be calculated as follows:

$$\nu = \sum_{i=1}^{\infty}\left(\log\left(\frac{D_i}{D_{max}}\right)\cdot\log\left(\frac{P_i}{100}\right)\right)\Big/\sum_{i=1}^{\infty}\left(\log\left(\frac{D_i}{D_{max}}\right)^2\right) \quad [116]$$

Just below, Figure 39 presents the grading of two "55-70" samples on bilogarithmic scale, where the slope of the regression lines corresponds to the respective granulometric distribution modulus ν. The sample with lower modulus value, $\nu = 0{,}395$, has a content of fines of 67,0% and at the optimum compaction point the void ratio corresponds to $e/G_s = 0{,}164$. The sample with greater modulus value, $\nu = 0{,}724$, has a content of fines of 61,3% and at the optimum compaction point the void ratio corresponds to $e/G_s = 0{,}231$. This supports the initial expectation that Andreasen, A. H. M. and Andersen, J. particle packing theory may positively help understanding the role of the material grading on the variability exhibited by its compaction curves. We will see in continuation if that is so.

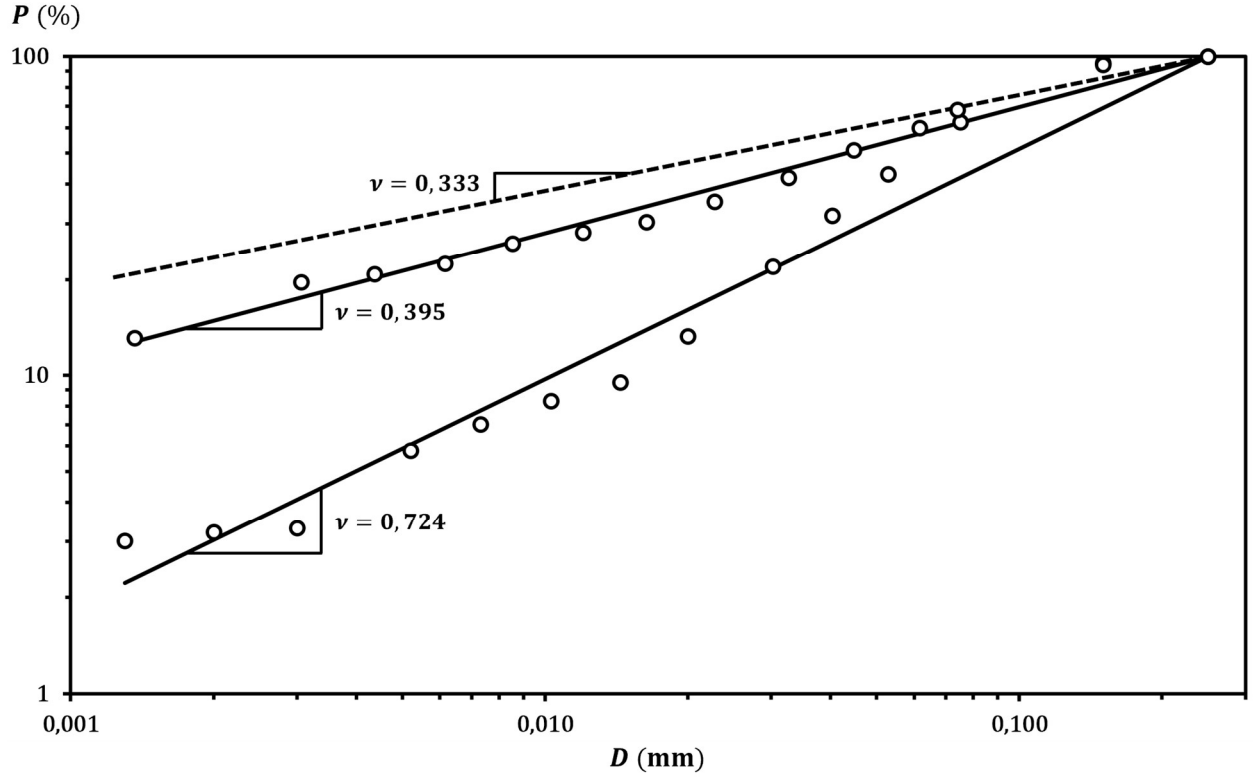

Figure 39

For our 105 samples of "55-70" tailings, the modulus value has a mean value of 0,439 and a standard deviation of 0,040. To enlarge the validity of the correlations on a wider interval, 15 additional samples of material with more or less fines content than that of the base material were also considered, but all of them having a maximum particle diameter of 0,25mm (for $P \geq 98.5\%$). The overall mean value of the granulometric distribution modulus is 0,487 and the standard deviation is 0,147. In any case, the metrics used to evaluate the model goodness of fit refers only to the 525 determinations of the base material. The correlations leading to the best fit are:

$$\omega_m/S_m = 0{,}175 + 0{,}185 \times \nu \quad [117]$$

$$S_m = 100{,}00 - 32{,}23 \times \nu \quad [118]$$

$$m/n = 0{,}047 + 0{,}493 \times \nu \quad [119]$$

And:

$$n = 19{,}72 - 11{,}88 \times \nu \quad [120]$$

Being two of them, Equation 118 and Equation 120, linear functions of the modulus and the other two, Equation 117 and Equation 119, complete quadratic functions of the same variable.

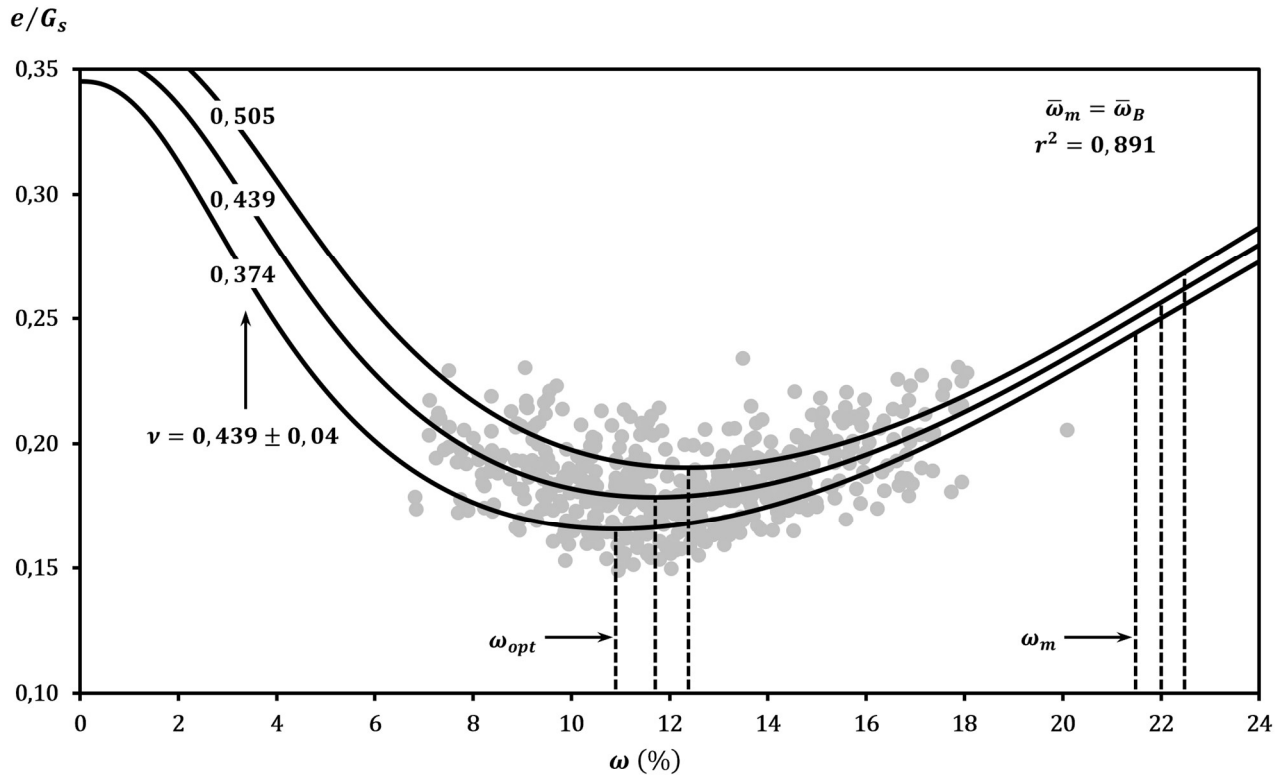

Figure 40

Analogously to Figure 36 or Figure 37, the compaction curves in terms of the ratio e/G_s are presented on Figure 40 for this latter correlation attempt with a variable describing the material grading. The bounding curves presented on this figure correspond to an interval of 1,645 times the standard deviation of the modulus value of our "55-70" samples. Regardless of the evaluation metrics, we can immediately see that inference made before regarding the fines content relation with the modulus number is valid, yielding both similar compaction curves. Also, using the coefficient of determination, r^2, for reference, we can conclude that the gains of increasing the complexity of correlations is modest. However, this last attempt seems to be the most rational one and the only one that can be extended to different gradings' families, adding another explicative variable to the correlations. The choice is easy to guess and that would be the maximum particle diameter, D_{max}, of the

mixtures. If we were on the teaching business, this would be the point where demonstrations were left as "homework" for the pupils.

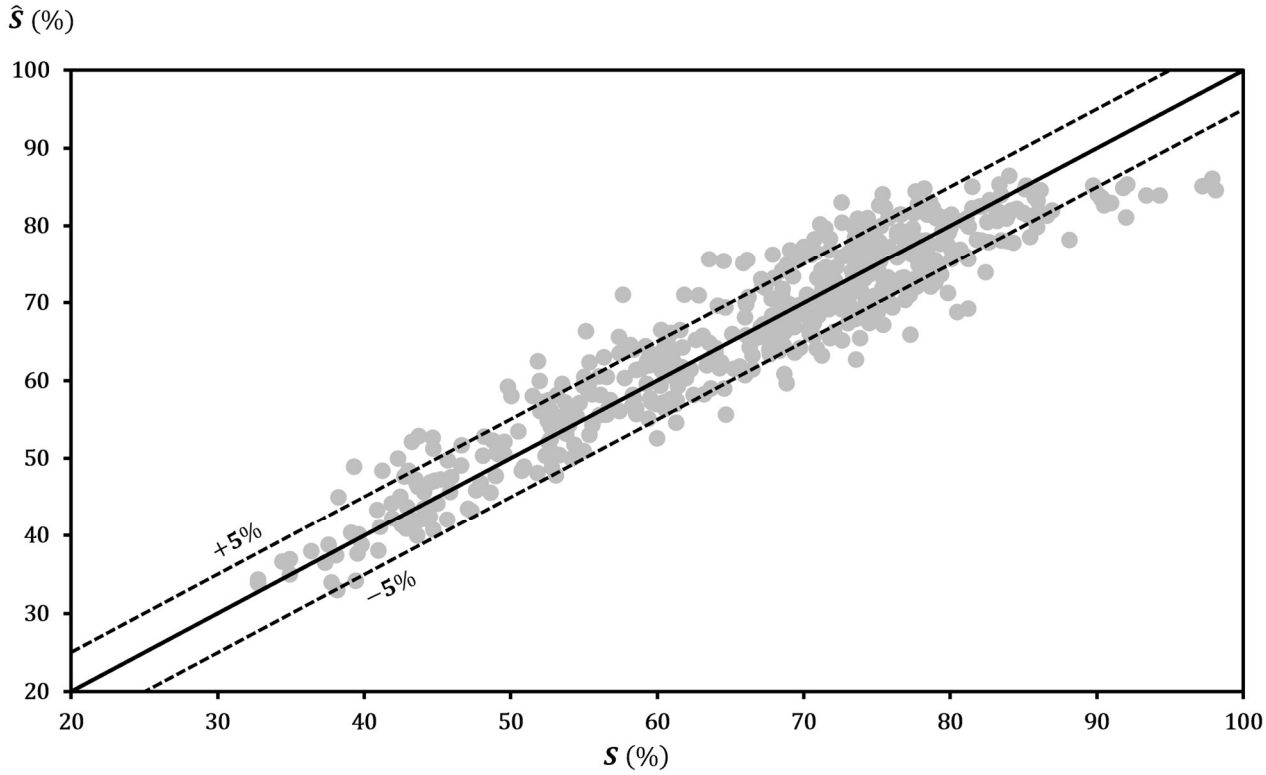

Figure 41

And now to the boring metrics. Figure 41 compares the indirectly measured values of the Proctor compaction test samples degree of saturation, S, with the values predicted by the model, $\hat{S}$, using the latter correlations with the granulometric distribution modulus. Disappointing? For the response variable of our model, the degree of saturation, the mean absolute percentage error becomes 5,40% and, for 95% of the determinations, the absolute percentage error becomes equal or lower than 13,79%.

Relatively to the previous attempt, using the fines content as correlation variable, there is a reduction of 14,9% on the mean value of the error and a reduction of 10,6% on the extreme value of the error. So much work for so little reward, one may think. The mean absolute percentage error is now 2,00% for the dry unit weight prediction and 5,38% for the void ratio prediction. For 95% of the determinations of dry unit weight, the absolute percentage error is less than 5,16% and for, the same quantile, the absolute percentage error is less than 13,43% percent for the void ratio. With respect to the previous attempt, a reduction of 8,8% and 8,4% is achieved for the mean absolute percentage error, respectively for the dry unit weight and the void ratio and, for the extreme value of the absolute percentage error, the achieved reduction is 14,6% and 14,7%, respectively for the dry unit weight and the void ratio. It is useful to go back to Subchapter 3.4 and think about the effect that measurement errors may have on such a modest achievement as ours is.

Figure 41 indicates that the residuals of the saturation degree prediction have a nearly constant variance, and a quantile-quantile (Q-Q) plot would show a symmetric distribution of residuals with thin tails. Figure 42, on next page, shows how a cumulative normal distribution function with null mean and standard deviation of 4,443 compare with the predicted degree of saturation residuals.

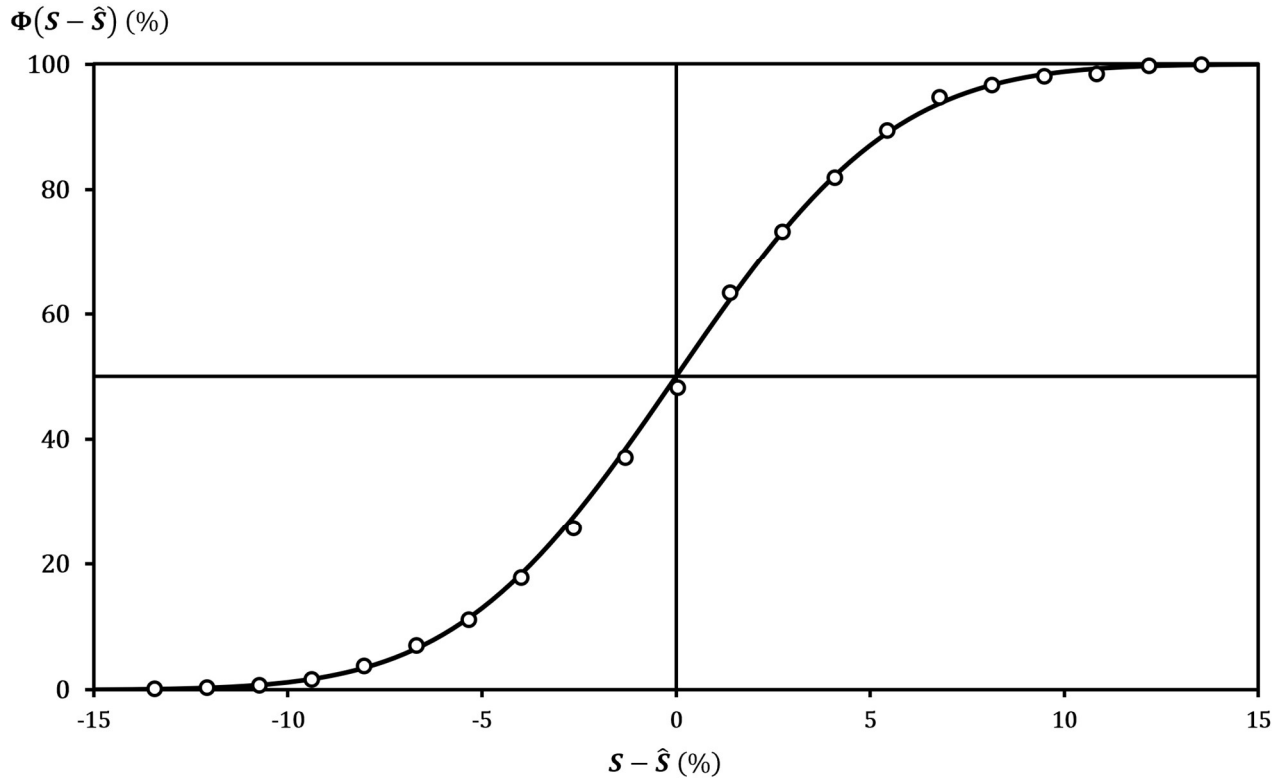

Figure 42

Rather than focusing on the statistical aspects, a simple example may be more enlightening about the reasons behind the apparently poor prediction based on the grading of the soil.

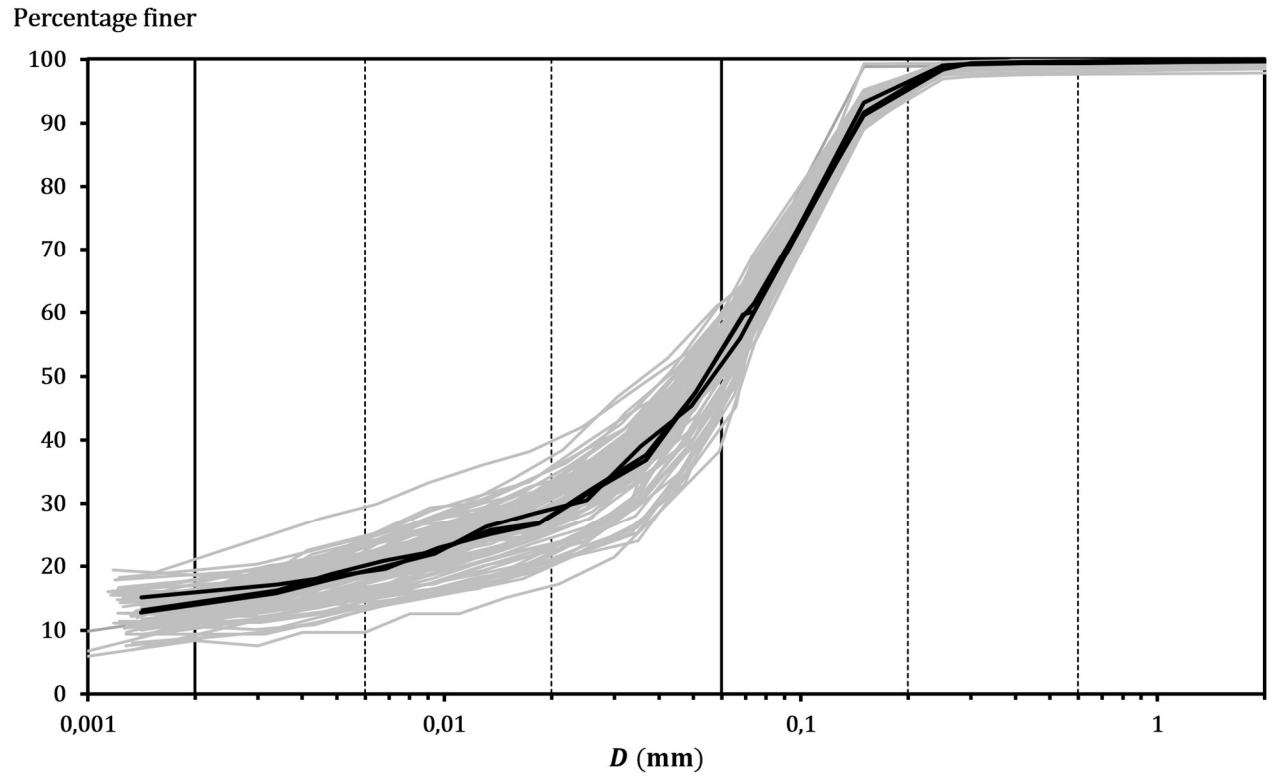

Figure 43

Three samples of "55-70" tailings with nearly coincident granulometric distributions, as shown in Figure 43 on the previous page, were taken. The fines content of these samples is 60,1%, 61,5% and 60,2% and the respective granulometric distribution modulus is 0,436, 0,430 and 0,427.

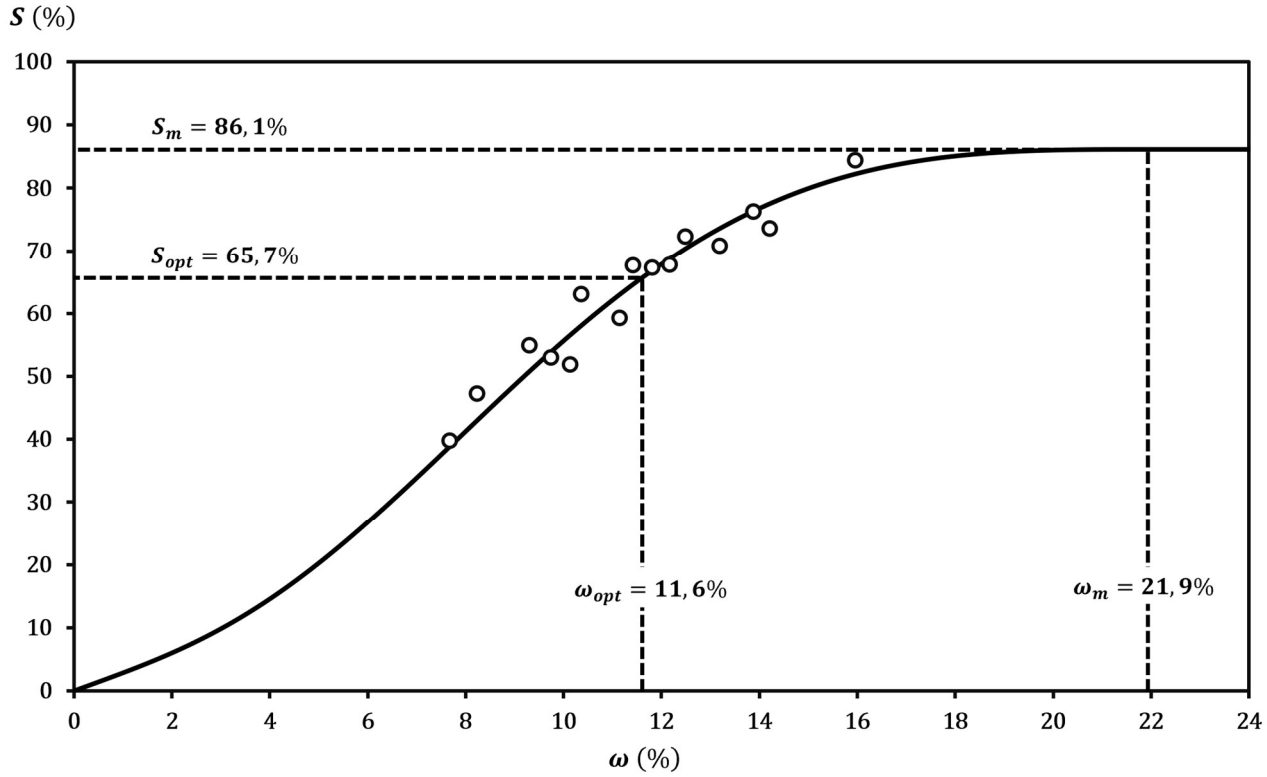

Figure 44

If the mean value of the modulus is used to derive the $S(\omega)$ function parameters and the curve obtained is plotted against the 15 test determinations from the 3 samples, the result is as presented on Figure 44. Although the three samples can be considered as "unique" as man-made soil can be, the mean absolute percentage error on the saturation degree prediction is 4,35%, with a maximum value of 8,80% for 95% of the determinations. The coefficient of determination is $r^2 = 0{,}931$. If the same three samples were analysed individually, without constraining the values of the model parameters, the coefficient of determination would be 0,995, 0,999 and 0,998. In summary, there is a randomness on the test data that survives any attempt to establish a full correlation between compactability and basic physical properties, such as the material particle size distribution. Of course, better ideas to work and rework the same test data are there to found, not speaking of data from other tests designed to increase predictability on what regards to compaction. The question is: Do we need to predict better? The answer was to great extent provided ahead, on the previous subchapter, where the word prediction was not employed, or even before, when we pretended to be paying an innocent, but surely deserved, tribute to Jack Hilf in subchapter 3.3.

To better visualise the spread of the data around the trend lines, Figure 45, on next page, shows the $S(\omega)$ curves for two subgroups of the "55-70" compaction test results. The total sample was ordered in function of the granulometric distribution modulus of each material tested and the results grouped in 7 subparts of the same size. The figure shows the $S(\omega)$ functions obtained with the parameter values given by Equations 117 to 120

using the mean value of the modulus of each subgroup and are presented for the first and seventh mean value of the modulus.

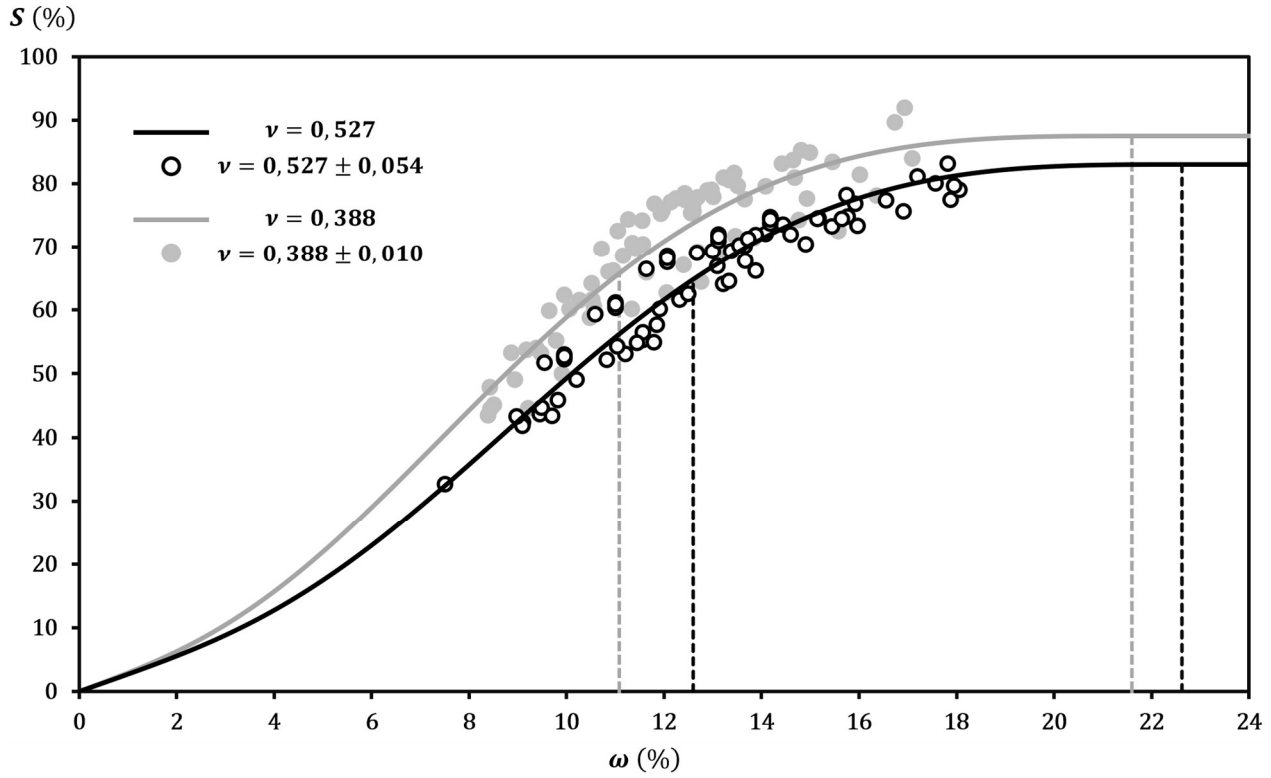

Figure 45

After some other attempts to increase predictability of the model using parameter values correlated to the material grading, one concludes that the gains do not justify the effort. Possibly a larger database could lead to better results, but, especially, an increase on the number of test points on each single compaction test and some repeated testing on the same samples would be indispensable for a more successful endeavour. And here we are complaining as everybody else about how things could have been if they had not been as they were. “When small men attempt great enterprises, they always end by reducing them to the level of their mediocrity”, said Napoleon Bonaparte.

Returning to our “0,6 maximum void ratio” quest, a flow of probability distributions was used to generate 100.000 random values of void ratio for the “55-70” filtered tailings. First, random values of the granulometric distribution modulus and specific gravity of solids, both normally distributed, were used to generate compaction curves with our model and the point of maximum dry unit weight or minimum void ratio was retained. Assuming that the field degree of compaction is also a random process, independent from any other, the probability distribution obtained for the field compaction of the tailings introduced on Chapter 2, and further discussed on Subchapter 5.2, was used to generate the desired sample of hypothetical field void ratios, allowing the compaction degree to vary without any restriction.

The resulting cumulative distribution function is presented in Figure 46, on top of next page, where it can be appreciated that, without any rejection of as-compacted material, the probability of having a void ratio greater than 0,6 is around 20%.

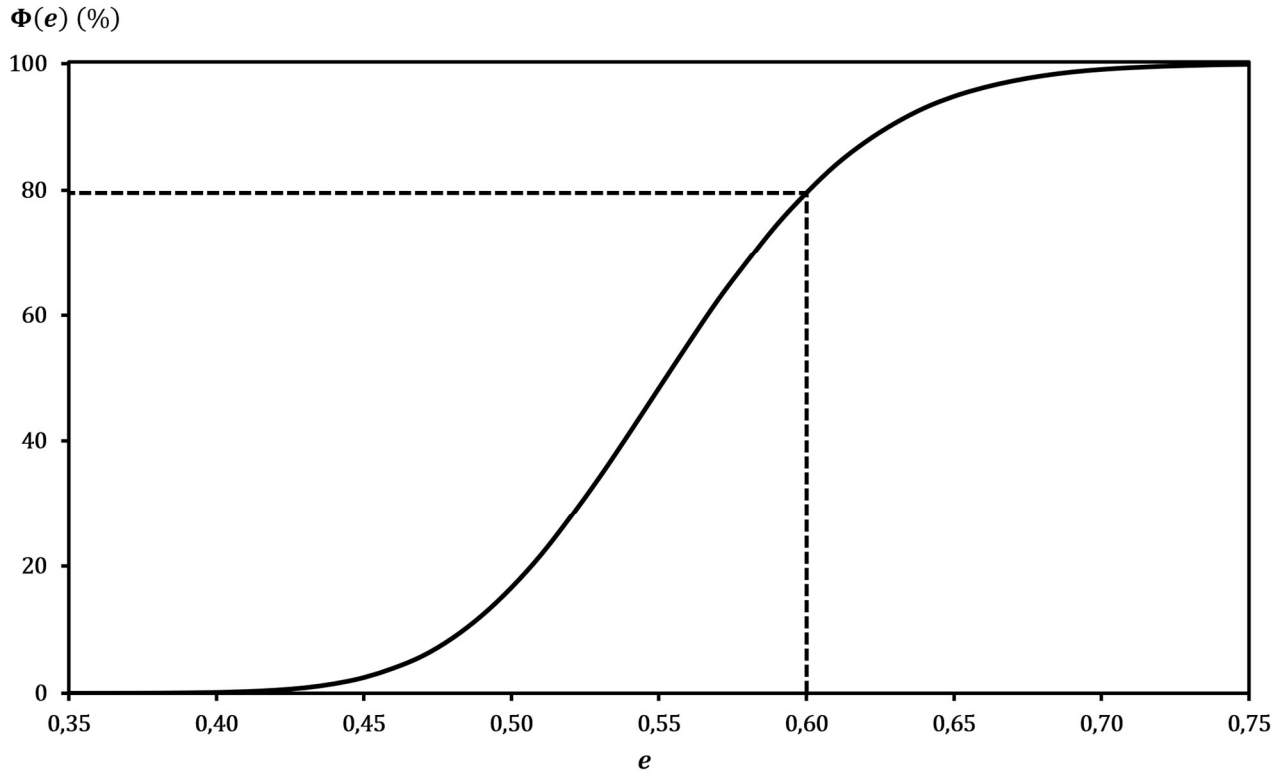

Figure 46

All this for the same field compaction effort employed on the first stage of construction of the tailings pile that motivated this booklet, where supposedly all material placed has a void ratio greater than 0,6. Admitting that upon rejection of some compaction strips for having a degree of compaction lower than 98%, the probability of accepting some material with a void ratio greater than 0,6 was satisfactory, we are led to the conclusion that, for the tailings pile where the "55-70" was going to be stored, the insufficient compaction energy used somewhere else for placing other tailings could be enough for this one. That is, we would be achieving the same objective with 4 or 5 times less energy than the one that ended up being used for the other tailings on another pile.

We can speculate the father of the "0,6 maximum void ratio" compaction control criterium to tell us for reply that the 0,6 figure is a just a site-specific value. Preventing any misunderstand, we will continue our quest, replacing the "0,6 maximum void ratio" by a more general "maximum void ratio" criterium. Why should we have to limit the void ratio of a "55-70" tailings pile to 0,557? Or 0,549? Or…

5.4. Is there a family of "55-70" curves?

If the compaction curves produced with our model using parameter values estimated from the granulometric distribution modulus were a sufficiently good approximation, it would be reasonable and especially advantageous to use them for compaction quality control. A single field point determination of water content and dry unit weight would allow locating, within a family of curves, the one to which the point belongs and easily estimate its degree of compaction and deviation of water content from optimum. For that, we would be assuming that between any two reference compaction curves of the same family, there is a single curve, equidistant from the reference ones, to which any point exclusively belongs. As a good example of this approach,

the Ohio's Typical Moisture-Density Curves, developed by the end of the fifties of last century, comes immediately to one's mind for its pioneering.

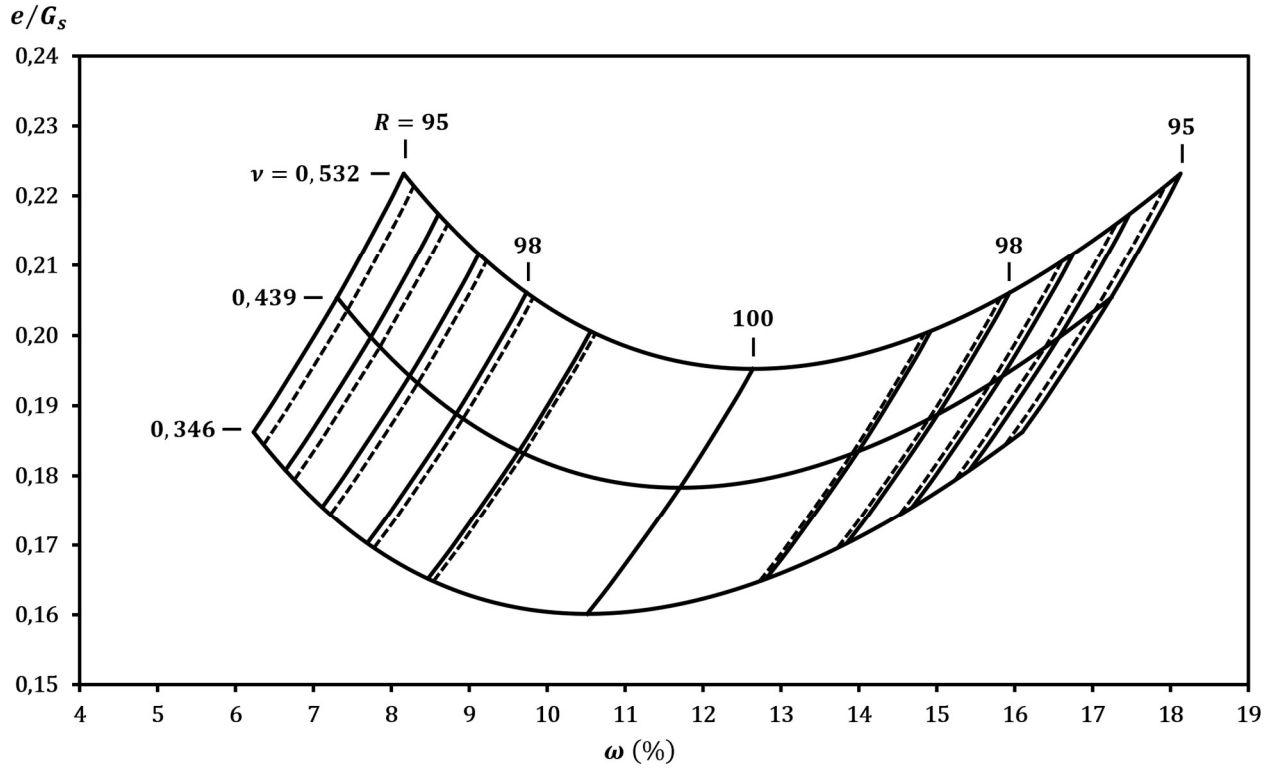

Figure 47

Following the family of curves concept, Figure 47 shows, for the "55-70" tailings, the domain where the compaction points, in terms of the ratio e/G_s, would be expected to fall according to their degree of compaction, if the normal Proctor energy was used. On the figure, a dashed line appears parallel to each line of equal degree of compaction. While the continuous lines of equal degree of compaction correspond to a lower bound of the specific gravity of solids (mean value less 2,326 standard deviations), the dashed lines correspond to the same degree of compaction for an upper bound of the specific gravity of solids (mean value plus 2,326 standard deviations).

A simple point counting exercise allows to explain that the family of curves method, although informative, difficultly could be successful for controlling the compaction of filtered tailings. Interpreting individually each of the 105 compaction tests available for the "55-70", the degree of compaction and deviation of water content from optimum of each of the 525 determinations can be derived and plotted on the diagram shown on the figure. 56,9% of the test points have a degree of compaction between 95% and 99% and 37,9% have a degree of compaction between 99% and 100%. From the total, 28,7% of the points would fall outside the compaction lines that constitute the upper and lower limits of the family of curves acceptance domain, meaning that they were, wrongly, identified as not belonging to the "55-70" family. From a merely deterministic perspective, that percentage of excluded points could be eventually reduced by improving further the correlations with the granulometric distribution modulus, what would require a larger sample of tests to be available and a more acute understanding of the factors contributing to the variability of its compactability. Engineers always complain…

Further data filtering would remove plus 2,7% of points from the total number, for having a degree of compaction below 95% according to the modelled curves. At the end, inside the domain defined for a degree of compaction equal or greater than 95%, just 68,7% of the original test points would remain. From the individual interpretation of the 105 compaction tests, one could expect 94,1% of the 525 points to have a degree of compaction greater than 95%. After filtering the data, within the family of curves acceptance domain, 2,5% of points from total remain with a degree of compaction between 93% and 95%.

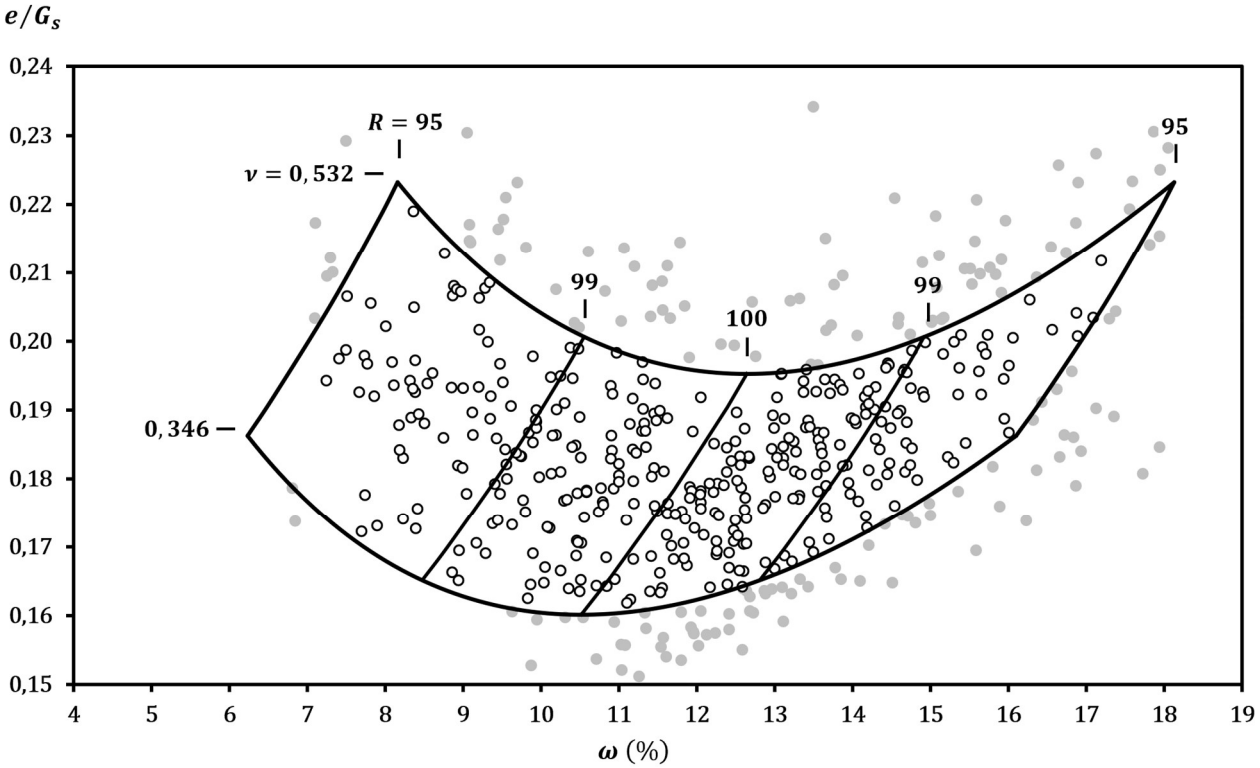

Figure 48

Figure 48 plots the 525 test data points on the diagram shown in Figure 47, being the points excluded represented by grey filled dots. Analogously, inside the 95% plus degree of compaction domain, 65,0% of the test points remaining (68,7% × 65,0% = 44,6% of total) would have been identified as having a degree of compaction equal or greater than 99%. From the individual test interpretation, just 59,9% of the latter points (59,9% × 44,6% = 26,7% of total) had effectively a degree of compaction equal or greater than 99%, although 63,4% of them having a degree of compaction greater than 98% (59,9% × 63,4% = 41,2% of total). The points identified as having a degree of compaction lower than 99% are identified on Figure 49, on next page, with grey filled dots. All the points excluded from the 99% region have effectively a lower degree of compaction, according to the individual interpretation of each 5-points compaction tests.

So far, on this discussion, we have intentionally left aside the water content. If Figure 47 is observed again, we can conclude that the range of moulding water contents within which a degree of compaction equal or greater than 95% can be reached is around 9,9%, with a deviation from optimum ($R = 100\%$) of around 4,4% to the dry side and a deviation of around 5,5% to the wet side. Moreover, the range of moulding water contents within which a degree of compaction equal or greater than 98% can be reached is around 6,2%, with a deviation from optimum of around 2,9% to the dry side and a deviation of around 3,3% to the wet side. If the water content was of no importance for the end-product required properties, our “55-70” would be an easy to compact

material. That is, with a relatively low compaction effort, a wide range of water contents could be considered acceptable for compaction. Instead of compaction control, policing of the site activity would be enough.

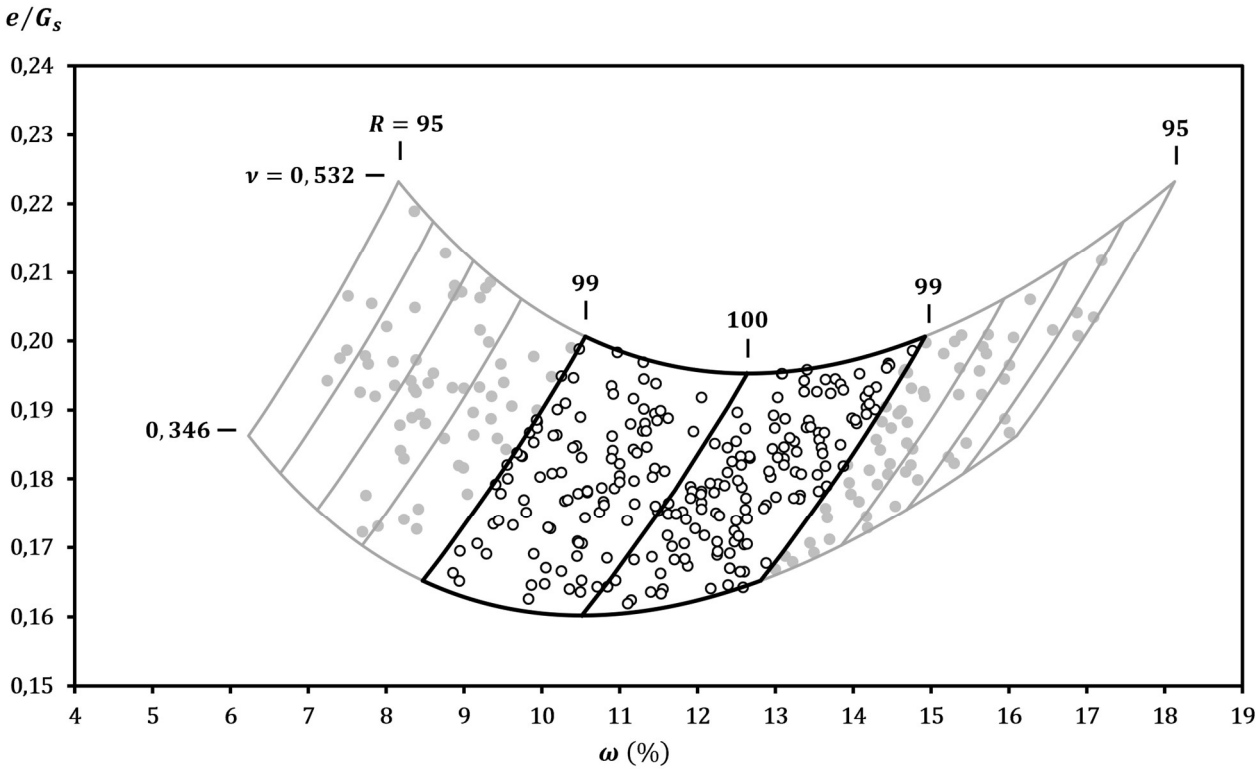

Figure 49

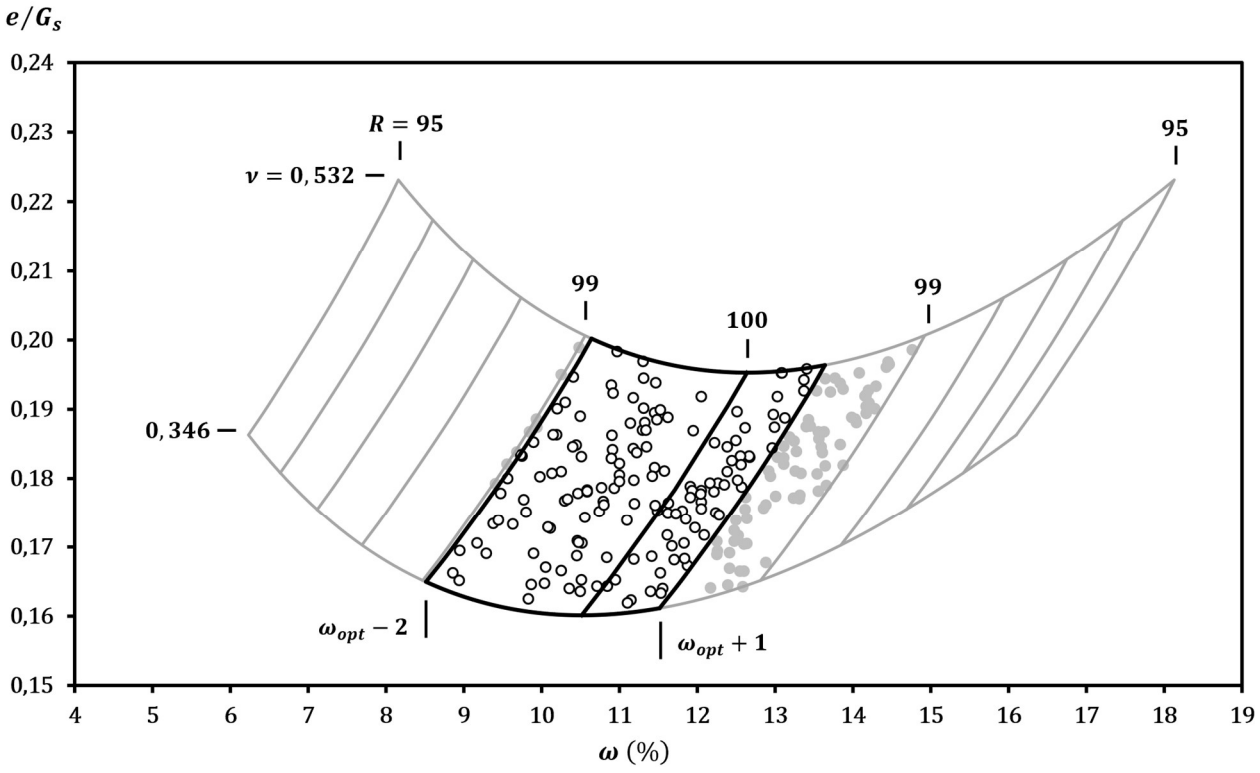

Figure 50

When the typical limits for the water content deviation from optimum, $-2\% \leq \omega - \omega_{opt} \leq +1\%$, are imposed over the minimum degree of compaction limits, the domain where we could expect the "55-70" acceptable compaction points to lie would shrink as represented in Figure 50, on the bottom of previous page.

On the dry side, the line of ω_{opt} -2% is practically coincident with the line corresponding to a degree of compaction of 99% and, on the wet side, the line of ω_{opt} $+1\%$ practically bisects the region corresponding to a degree of compaction between 99% and 100%. On Figure 50, grey filled dots correspond to the points with a degree of compaction equal or greater than 99% that would be excluded for having an excessive water content deviation. From the initial number of test points, 44,6% were identified as belonging to the "55-70" family of curves and having a degree of compaction equal or greater than 99%. The introduction of limits to the moulding water content reduces that fraction by 35,3%, mainly for having too much water.

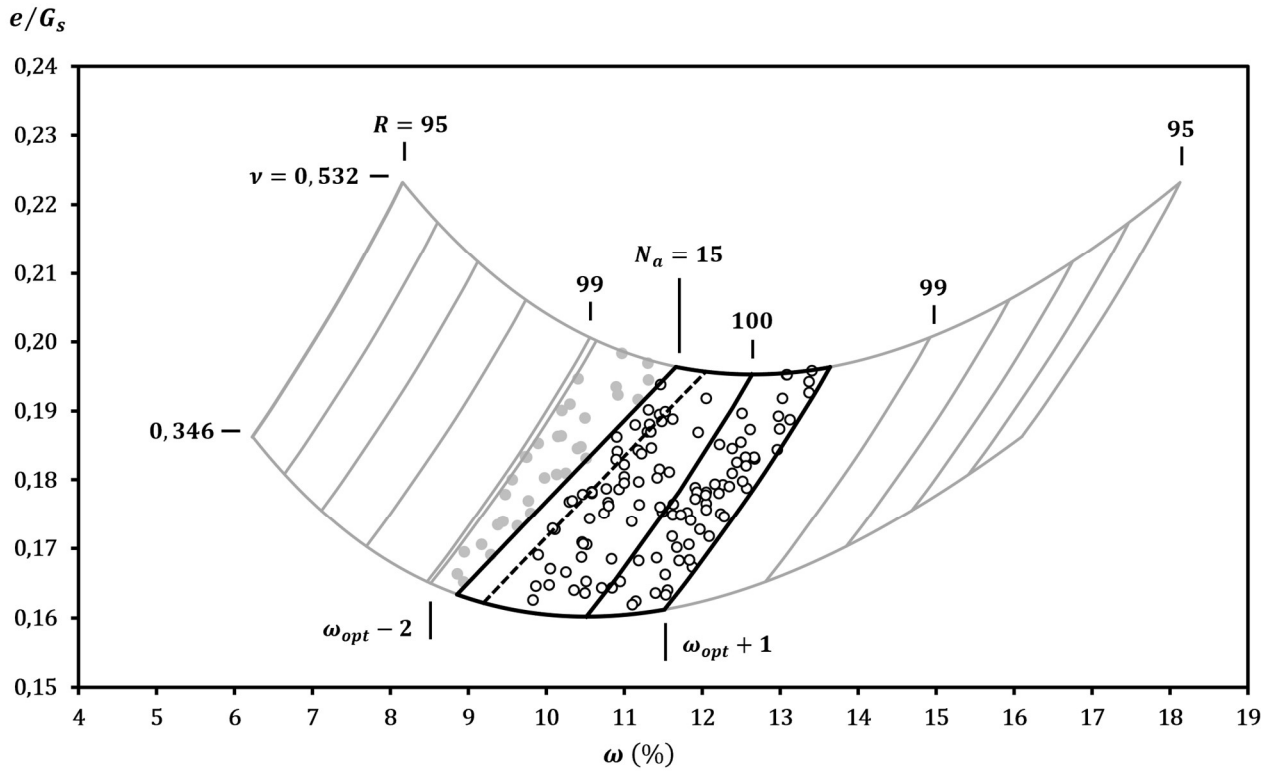

Figure 51

Additionally, if the percentage of air voids was also limited, say to 15%, the domain of acceptance defined with the "55-70" family of curves would be further reduced, as represented in Figure 51. As before, the black line representing the 15% maximum percentage of air void corresponds to a lower bound value of the specific gravity of solids and parallel to it, dashed, appears the line of 15% maximum percentage of air void corresponding to an upper bound value of the specific gravity of solids. From the points remaining inside the domain, amounting to 28,8% of the total, an additional fraction of 22% would be excluded for having an excessive percentage of air voids.

In comparison, the analysis based on the individual interpretation of the 105 5-point compaction tests, before imposing a limit on the percentage of air voids, would lead to the acceptance of 75,2% of the 525 test points, while the analysis based on the family of curves would lead to the acceptance of 28,8% of the same number of points. After introducing a limitation of 15% as the maximum percentage of air voids, the analysis based on the

individual interpretation would lead to the acceptance of 41,0% of the total number of test points, while the analysis based on the family of curves would lead to the acceptance of 22,5% of the same number of points. A much more refined definition of a family of curves for the "55-70" tailings would be required so that it could match the success rate of approvals allowed by the circumstantial analysis of each individual tests. Having said this and revisiting Figure 44 and Figure 45, the fact that the family of curves method seem to be more excluding does not necessarily make it is less rigorous, otherwise we would have to surrender to the total randomness of compaction.

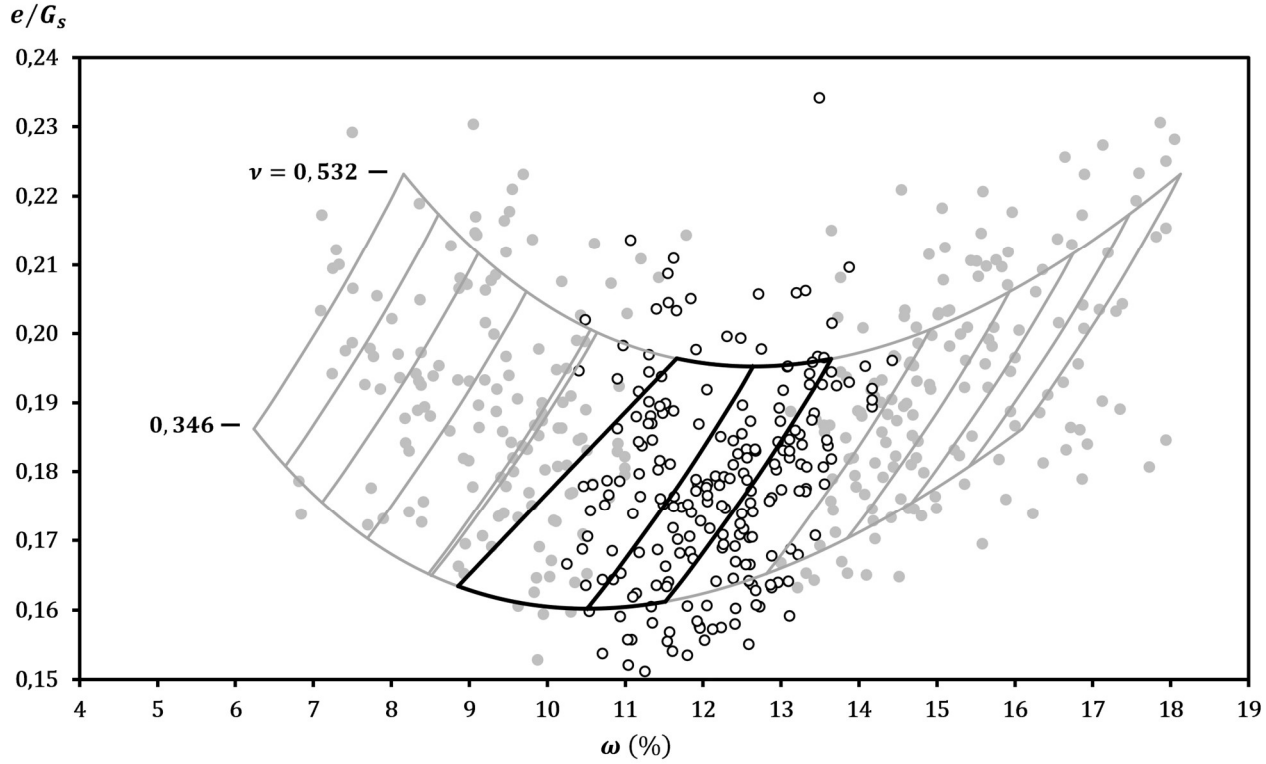

Figure 52

Figure 52 shows all the 525 test points, distinguishing with filled grey dots those that among them do not satisfy the acceptance criteria ($R \geq 95\%$, $-2\% \leq \omega - \omega_{opt} \leq +1\%$ and $N_a \geq 15\%$) when applied to each compaction test interpreted individually. We can see that the acceptance domain defined with the family of curves is somehow shifted to the dry side and distorted in relation to the vertical, leading to the exclusion of a significant number of points on the wet side. In part, this bias can be corrected by changing the values of the $S(\omega)$ function parameters that resulted from the earlier attempt to correlate them with the granulometry of the material. Such change would not be a sleight of hand to convince an assembly of mountain builders about the merits of the family of curves method, once there are many combinations of parameter values that provide almost the same level of determination on the model curve fitting to test data. It should be noted that the chosen model parameters, developed in turn of a point (ω_m, S_m) that is not targeted on testing, do not preclude using the point of maximum dry unit weight (ω_{opt}, S_{opt}) as the control parameter on curve fitting to test data, once both points are easily interchangeable on the model formulation.

Finally, on next page, Figure 53 shows how the line of optimums of the "55-70" family of curves compares with the points derived from the interpretation of individual tests, either in terms of the maximum dry density, on part (a), or in terms of the optimum water content, on part (b), both expressed as a function of the granulometric

distribution modulus. Apart from the 105 points of "55-70" tailings, the figure includes 13 other points from materials of from different families, with fines content outside de 55% to 70% interval, but having in common a maximum particle size D_{max} of 0,25mm.

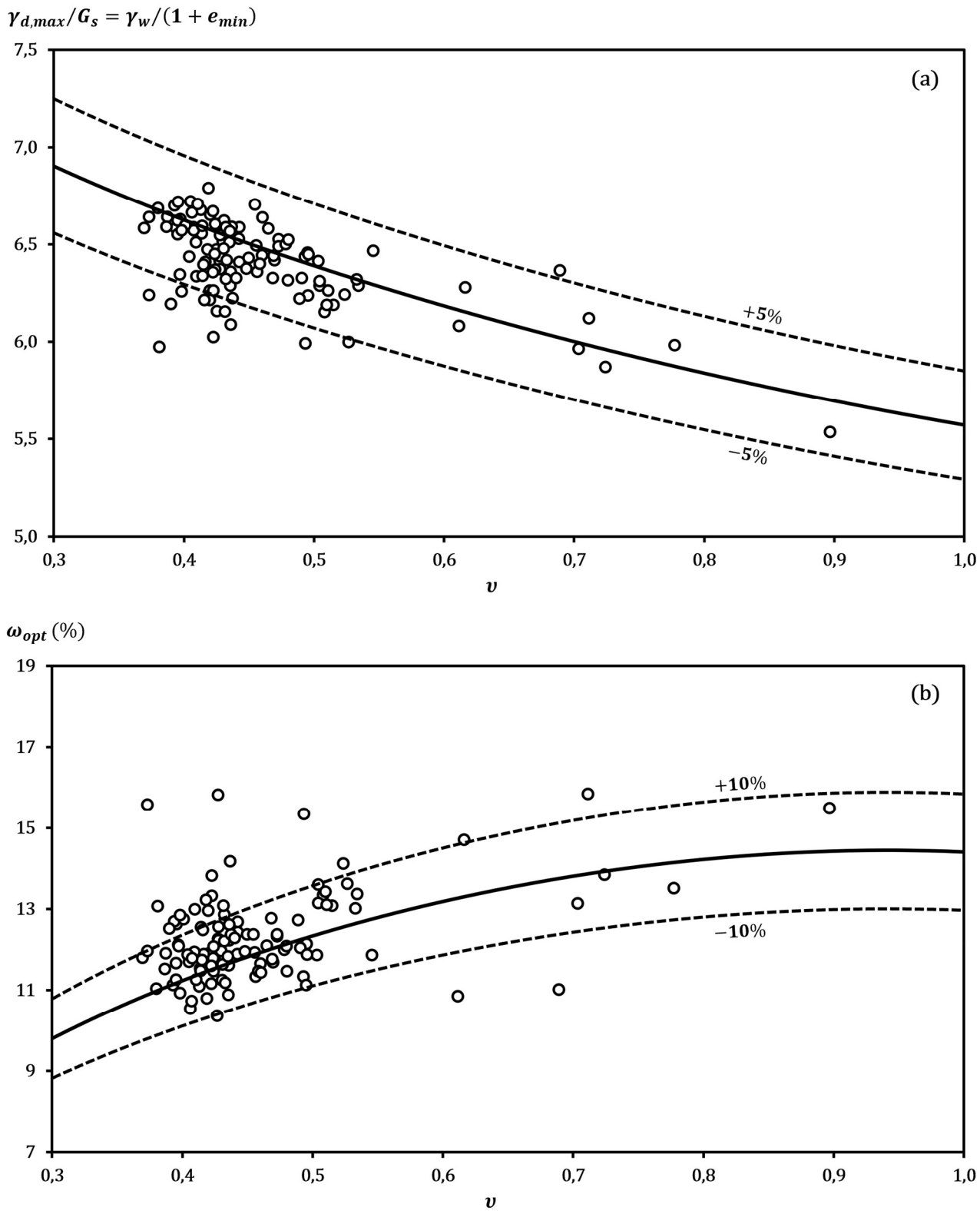

Figure 53

In any case, the interest of Subchapter 5.2 and its apparently premature presentation on this same chapter should now be better understood. We are not trying to reinvent the wheel, just saying that sometimes it is better to keep it round. Or perhaps not… as the high energy impact compactor in Figure 54 suggests on contrary.

Figure 54

Taking some credit for our own work, it is of some importance to explain why we have been intentionally studying a narrow-banded material, like the "55-70", knowing that who does it may miss the forest for the trees. It is not the case.

Indeed, studying mine waste is not our first "compactive" experience, just one that circumstantially sparked our curiosity. Yet, fate decided that, among so many good things, we ended up talking about poetry with the taxman. Remember, right from the start, that one thing is a void and another one, completely unrelated to it, is the solid matter that enrobes the void. Said the taxman. The original study covered a wider range of dewatered tailings gradings, all from iron-ore mines, from which just 194 samples subjected to complete basic testing could be gathered. There are literally thousands of thousands of samples with complete basic testing waiting on servers to play with, let them be available. And someone that wants to play with data and return with news from the playground.

For each of the 194 samples, Figure 55, on the next page, shows the relationship between the minimum void ratio obtained with the standard Proctor energy and the fines content of the material. This chapter of the booklet is precisely about zooming-in and trying to find a practicable non-statistical explanation for the dispersion that becomes disguised when zooming-out. There is also something on this last figure that highlights a conclusion evinced on these two last subchapters. Possibly because of the proliferation of articles about the role of silt on the density of binary mixtures with uniform sands, many would be tempted to think that the greater the content of fines is beyond a threshold, typically around 30%, the greater is the minimum void ratio of the mixture. For continuous gradings, evidence proves the opposite. Zoom-in. Zoom-out.

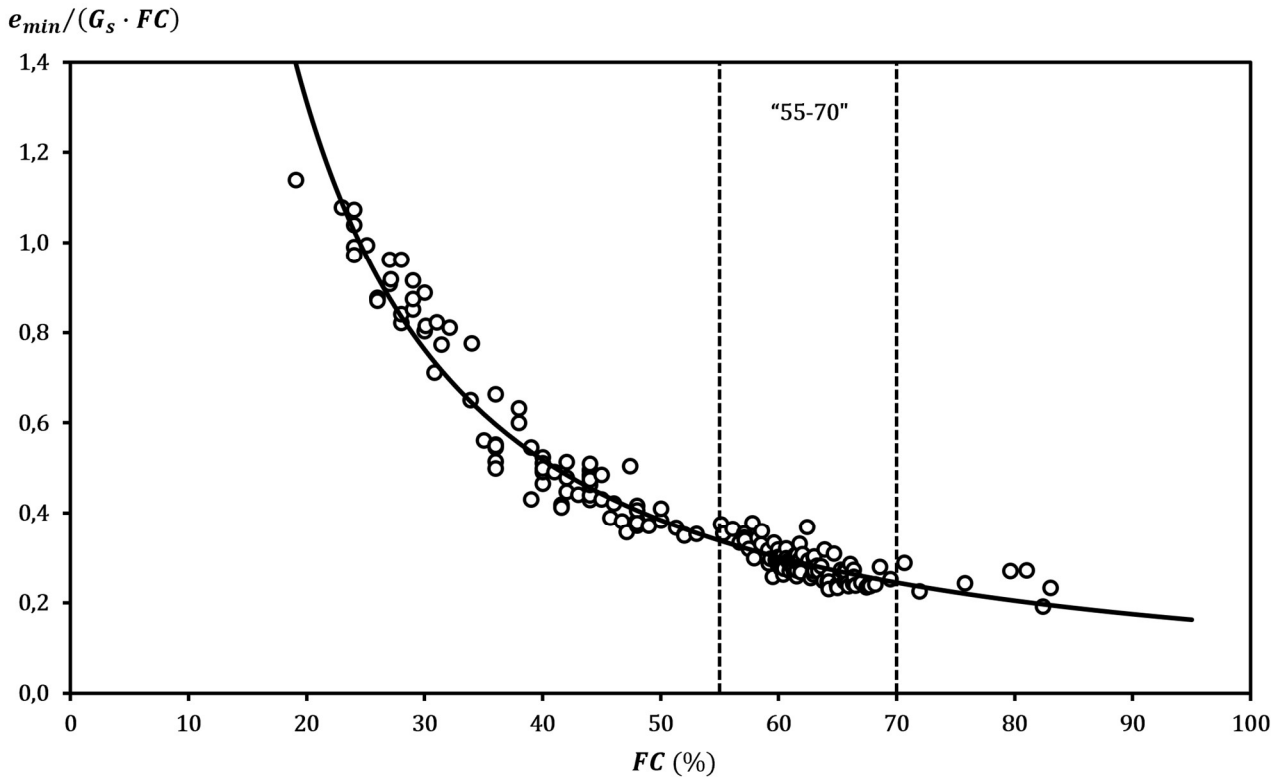

Figure 55

If it serves for anything, this chapter serves to remember, those who might have forgotten it, about the practical impossibility of resuming real-world clouds of points to trend lines and this applies to our compaction model as well, if not better, as it does to lines of critical states and critical state lines. With a couple of tests points all we can shine with exquisite line drawings. And here is our own model joyful burial.

6. THE SHEAR STRENGTH OF COMPACTED DRY TAILINGS

6.1. Dilatancy, finally

On the absence of any other information regarding the birth of the "maximum void ratio" criterium for compaction specification and control, we have insinuated along this text that we suspect it may be linked to the builder's desire of obtaining a material compacted to such a dense state that it would be forced to dilate before shearing completely no matter its location on a pile, a type of structure that we have been addressing as mountains of powder due to the gigantic size these earthworks can reach and to the power sized material that is meant to form them. On other powder industries, like potato starch, a non-dilatant behavior is surely preferable, to avoid vibrations inside a silo, for example. We will be writing on this presuppose.

The work of the Emeritus Malcom Bolton, in the 80's of last century, obtaining pragmatic empirical correlations to describe the dilatancy potential of sands, according to their density and depending on state of stress acting on them, will be tentatively followed here, obviously not with the same eloquence and elegance. In fact, this last sentence says almost everything. It is not just about the material state of density; it is also about the state of stress to which the material is subjected. We have also referred to liquefaction a couple of times on the way, because there is an unwritten clause on the laws of modern geotechnical engineering that says that everything that does not dilate can spontaneously liquefy, even if unsaturated. We will get back to liquefaction.

In simple terms, the secant peak angle of shearing resistance, φ'_p, of a dilative soil contains an additional strength component, described by the angle of dilatancy, ψ, over the strength that will end up being mobilised at large strains, while the failing material is deforming at constant volume. The latter component is represented here by the critical state angle of shearing resistance, φ'_{cv}. A relationship of the following type will be pursued:

$$\varphi'_p = \varphi'_{cv} + a \cdot \psi \qquad [121]$$

Where a is a coefficient with a value ranging between 0 and 1. We will be working with a database of triaxial compression tests, from where the above-referred angles will be extracted. Although other definitions are possible, here, the angle of dilatancy is defined as:

$$\sin\psi = -\frac{\delta\varepsilon_v/\delta\varepsilon_1}{2 - \delta\varepsilon_v/\delta\varepsilon_1} \qquad [122]$$

Being $\delta\varepsilon_v$ and $\delta\varepsilon_1$ increments of volumetric strain and maximum principal strain (the axial strain on the triaxial apparatus), respectively. At failure, the elastic component of strain is negligible, so the strain increments on the equation refer to the plastic strain component. As the volumetric strain on a triaxial compression test is given, on the hypothesis of small strains, by:

$$\delta\varepsilon_v = \delta\varepsilon_1 + 2 \cdot \delta\varepsilon_3 \qquad [123]$$

Equation 121 can also be written as:

$$\sin\psi = -\frac{\delta\varepsilon_1/\delta\varepsilon_3 + 2}{\delta\varepsilon_1/\delta\varepsilon_3 - 2} \quad [124]$$

Being $\delta\varepsilon_3$ the minimum principal strain increment (the radial strain on the triaxial apparatus).

Following Peter Rowe's stress-dilatancy theory:

$$\left(\frac{\sigma'_1}{\sigma'_3}\right)_p = \left(1 - \frac{\delta\varepsilon_v}{\delta\varepsilon_1}\right) \cdot \left(\frac{\sigma'_1}{\sigma'_3}\right)_{cs} \quad [125]$$

And knowing that:

$$\left(\frac{\sigma'_1}{\sigma'_3}\right)_p = \frac{1 + \sin\varphi'_p}{1 - \sin\varphi'_p} \quad [126]$$

And:

$$\left(\frac{\sigma'_1}{\sigma'_3}\right)_{cs} = \frac{1 + \sin\varphi'_{cs}}{1 - \sin\varphi'_{cs}} \quad [127]$$

Where σ'_1 and σ'_3 are the maximum and minimum principal stresses at the peak or at the critical state, the following definition of angle of dilatancy may be obtained:

$$\sin\psi = \frac{\sin\varphi'_p - \sin\varphi'_{cs}}{1 - \sin\varphi'_p \cdot \sin\varphi'_{cs}} \quad [128]$$

Equivalently:

$$\sin\varphi'_{cs} = \frac{\sin\varphi'_p - \sin\psi}{1 - \sin\varphi'_p \cdot \sin\psi} \quad [129]$$

Or even:

$$\sin\varphi'_p = \frac{\sin\varphi'_{cs} + \sin\psi}{1 + \sin\varphi'_{cs} \cdot \sin\psi} \quad [130]$$

Manipulating this last equation with some trigonometric relationships, the secant value of the peak angle of shearing resistance arises:

$$\tan \varphi'_p = \frac{\sin \varphi'_{cs} + \sin \psi}{\cos \varphi'_{cs} \cdot \cos \psi} = \frac{\tau_p}{\sigma'_n} \quad [131]$$

Being τ_p the peak value of the shearing resistance for a normal stress σ'_n acting on the plane of failure.

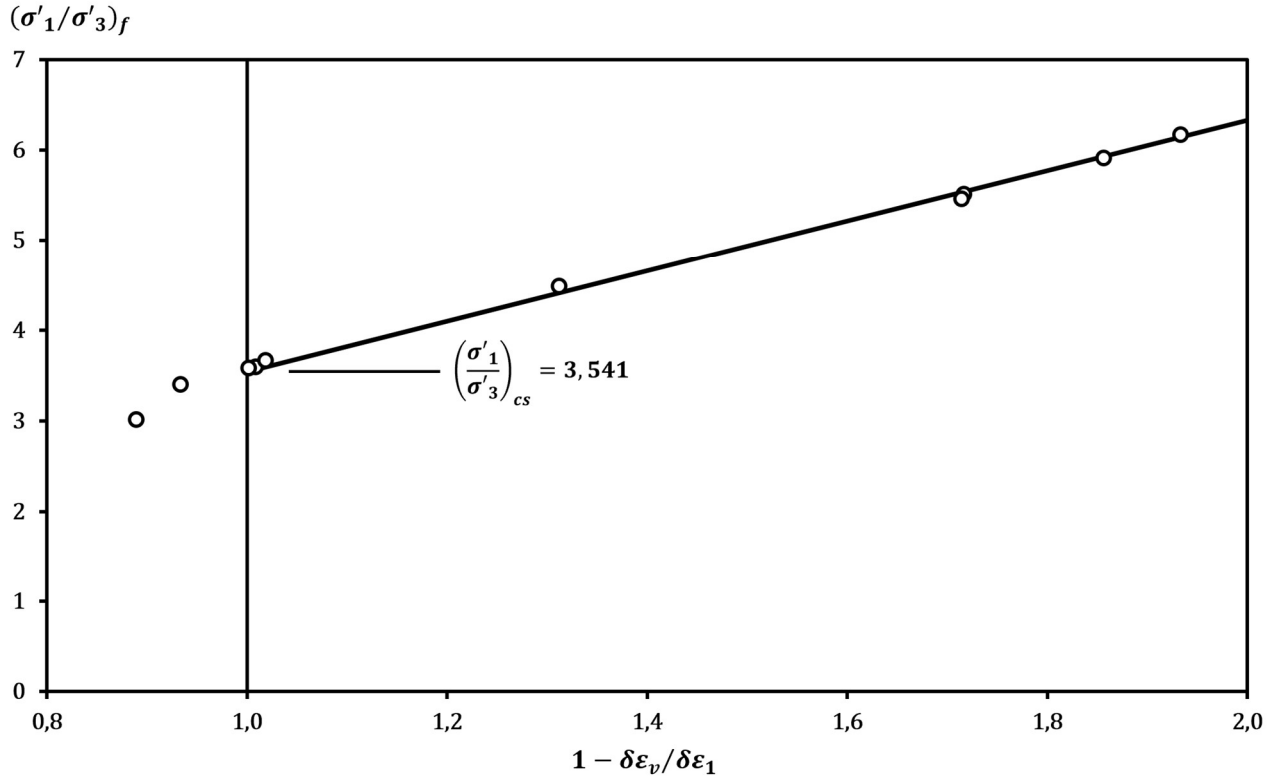

Figure 56

While the critical state angle of shearing resistance, φ'_{cs}, is conceptually independent of σ'_n, the angle of dilation, ψ, is not, from where the peak value is not constant, rather a non-linear function of the normal stress at failure. Figure 56 illustrates, for a sample of tailings, how the value of the critical state angle of shearing resistance was derived from the results of CIDC triaxial tests. Points represent the maximum principal stress ratio and the respective dilatancy parameter for each of the specimens tested, 10 on this case, having each one being prepared with a different compaction effort and subjected to different consolidation pressures. The point of maximum obliquity is assumed to represent the instant of failure of a specimen, from where, according to equation 126, the peak value of the angle of shearing resistance is:

$$\text{sen}\, \varphi'_p = \frac{(\sigma'_1/\sigma'_3)_f - 1}{(\sigma'_1/\sigma'_3)_f + 1} \quad [132]$$

When the dilatancy rate, $\delta\varepsilon_v/\delta\varepsilon_1$, is null, the peak value coincides with the critical state value and the excess angle of shearing resistance is null. This simple way we can move on to equation 121 pursuit. For the less mindful, it might be this shearing resistance excess, instantaneously available on the shearing process, that the mountain builders may be looking for. One can believe that for this fine grained non-plastic artificial soil, called dewatered

tailings, there is nothing beyond the critical state, being $\tan \varphi'_p = \tan \varphi'_{cv}$ the lowest, but always available, coefficient of friction on a sliding soil mass.

On the Emeritus Professor Bolton own written words and as proved by facts, equation 125 is "operationally indistinguishable" from equation 121 and, by using the friction angle excess $\varphi'_p - \varphi'_{cv}$ as the dilatancy variable in lieu of the angle of dilatancy, the latter equation can be transformed into a linear function of some convenient measure of the soil initial density and, simultaneously, of some measure of the confining stress at failure. Defining first the so-called relative dilatancy index, I_R, such that:

$$\varphi'_p - \varphi'_{cv} = a \cdot \psi = b \cdot I_R \quad [133]$$

And introducing on I_R of the explicative variables:

$$I_R = D_r \cdot \left(o - \ln p'_f\right) - r \quad [134]$$

Where p'_f is the mean effective stress at failure and D_r is the relative density given by equation 11 on Chapter 1. Unfortunately, we do not know the relative density of the specimens, for what the values of the maximum and minimum void ratio were required to be known. Using the degree of compaction, we will replace D_r by a scaled compaction index R^*:

$$R^* = \frac{R_{PM} - R_{min}}{R_{max} - R_{min}} \quad [134]$$

Being R_{min} the degree of compaction corresponding to a dilatancy rate of 1 (null dilatancy) and R_{max} the degree of compaction corresponding to a dilatancy rate of 2. R_{PM} is the degree of compaction referred to the maximum unit dry weight obtained with the Proctor modified energy, so that R^* just exceeds a unit value due to an eventual measurement error or to an excessive abnormal compaction. For the same tailings sample used to produce Figure 56, Figure 57 on next page shows the location of the triaxial tests specimens (two points are coincident) on the space ω-R^* and, as well, the compaction curves for the normal and modified Proctor energy.

If each specimen tested on the triaxial apparatus is prepared with a certain target dry weight but an arbitrary water content, that point (ω, γ_d) can belong to any compaction curve, not necessarily one obtained with the normal or the modified Proctor energy. The degree of compaction alone is insufficient to describe the effect of compaction on the shearing resistance. For the same compaction energy, on both sides of the optimum point of compaction there are always two points with the same degree of compaction, each with a different moulding water content and a different shearing behaviour. However, poor is the author, this is the example of the best testing programme that we have at our disposition and there is little that can be done with it to consistently inquire the influence of the moulding water content.

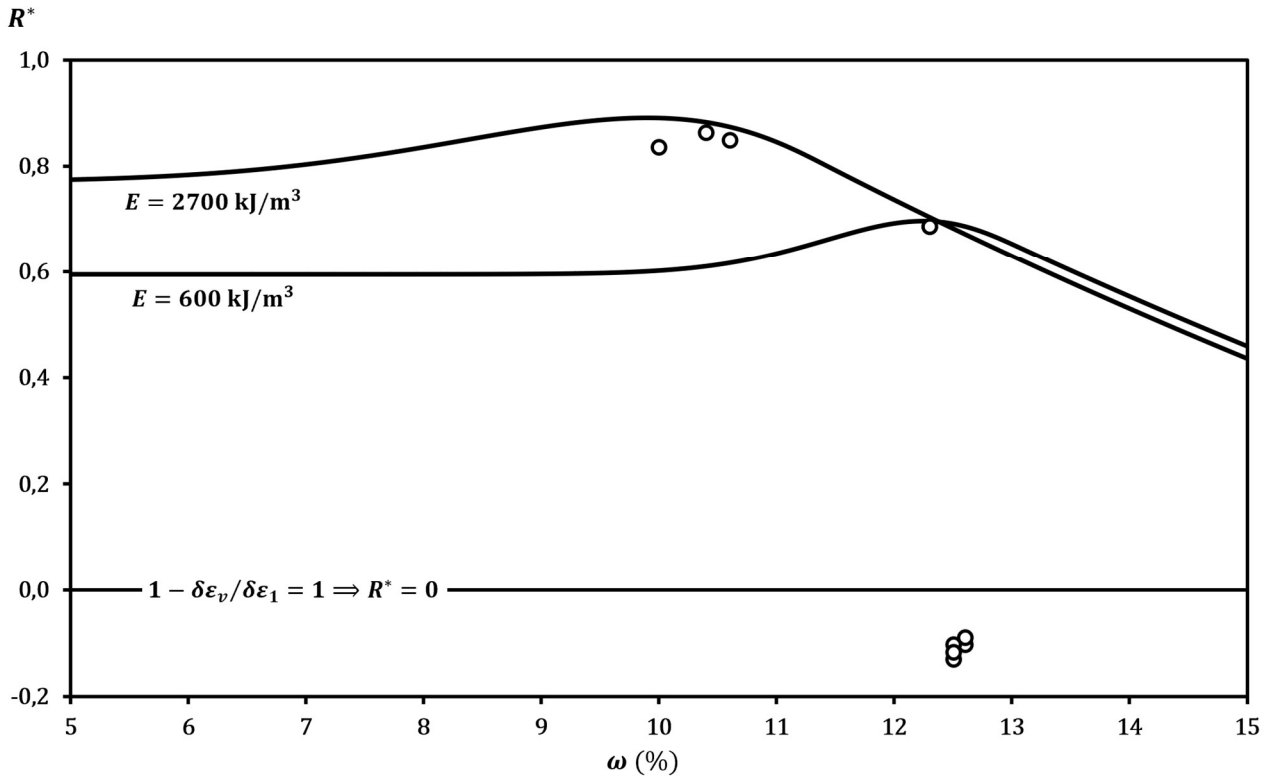

Figure 57

A simple linear regression:

$$\frac{\varphi'_p - \varphi'_{cv}}{b} + R^* \cdot \ln p'_f = o \cdot R^* - r \qquad [135]$$

Will allow determining the values of the two coefficients o and r that provide the best fit to test data, being known the value of the compaction index, R^*, and the value of the mean effective stress at failure of each specimen tested.

Figure 58, on next page, shows, for the same sample used to produce the previous figures, the predicted variation of the excess angle of shearing resistance with the mean effective stress at failure, for three different levels of compaction. $R_{PM} = 1{,}00$ corresponds to 100% degree of compaction with the modified Proctor energy and $R_{PM} = 0{,}946$ and $R_{PM} = 0{,}899$ correspond to 100% and to 95% degree of compaction with the normal Proctor energy. A second example is given further down, for a sample of a different tailings sample subjected to the same testing programme.

As Equation 132 and Equation 133 were shouting at us, dilatancy does not exist as an intrinsic material property. So, dilatant soils do not exist in abstract. What exists are soils in a state of density such that under certain confining stresses can mobilise a certain excess of shearing resistance, over the one we called the critical state shearing resistance, leaving other theoretical complexities apart. This is the same to say that in a tailings pile, even if the material had been compacted to the same exact state, each point, if forced to shear by some loading, would dilatate differently and in some points would not dilatate at all, because a critical value of the confining stress was eventually exceeded. We will try to quantify how many points would not dilatate in a mountain of

powder if compacted to a specified minimum value of the void ratio. It depends on the size and shape of the mountain… one may replay.

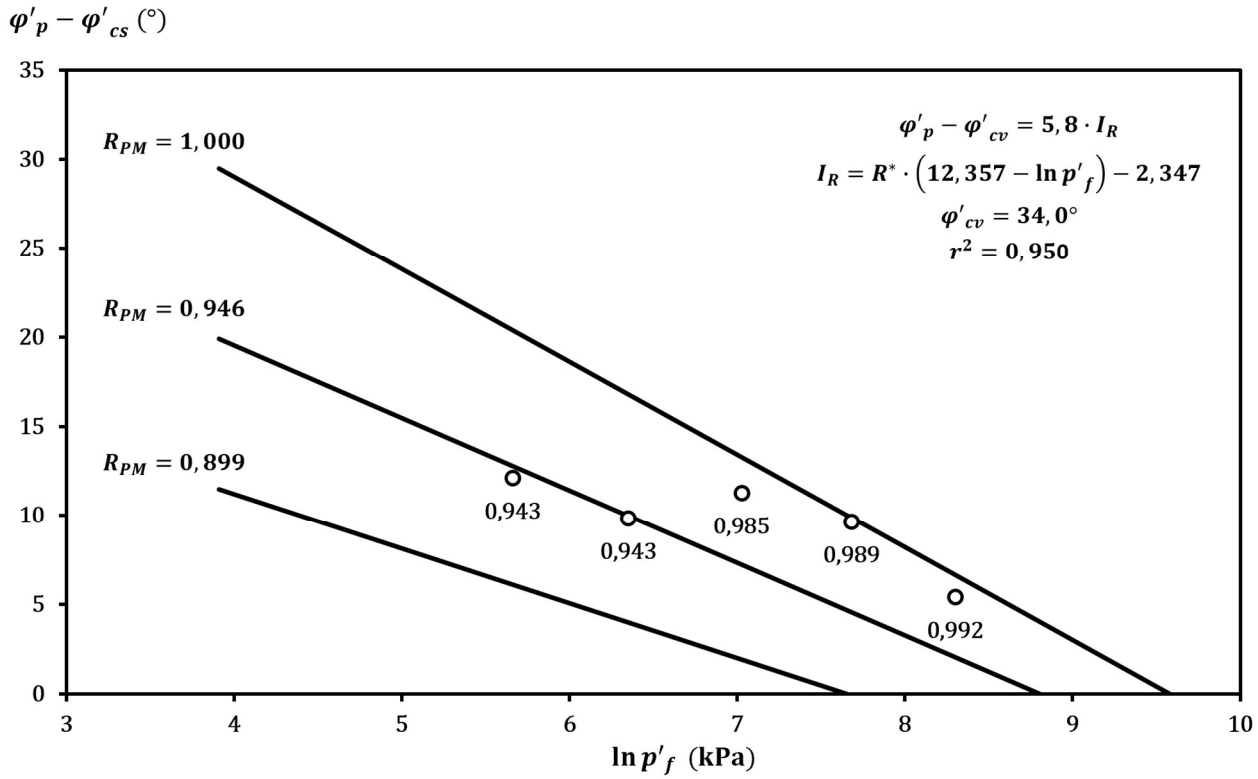

Figure 58

As each point is a point and we can difficulty say what point is the point we are pointing to, we can imagine that the father of the "maximum void ratio" criterium choose some strategically located points on the pile he was constructing, not all the points and one more for reserve. This fair thought makes our quest too cumbersome.

What Figure 58 helps doing is putting some numbers over the concepts. Let us consider a dry stacking tailings pile where the stored material was uniform and its shear strength was deterministically as given in the figure. If questioned about the maximum mean effective stress at failure that could act on any point of the structure without making dilatancy to evanish, one could reply that such stress would be of 2,11MPa ($\ln p'_f = 7,652$) if the degree of compaction was equal or greater than 95% of the Proctor normal energy. For 100% of the Proctor normal energy, the allowable mean effective stress at failure could be of 6,66MPa ($\ln p'_f = 8,805$). If the predicted confining stress at failure in any point was lower than the first allowable value, then we could establish a "0,72 maximum void ratio" compaction criterium and if the allowable value was the second one, than a "0,63 maximum void ratio" criterium would have to be established instead. We could interchangeably change the criteria names from "maximum void ratio" to "minimum dilatancy". It happens that compaction control criteria based on the degree of compaction exists for ages and there is no reason at all to re-baptise it and invite all the mountain builders to the baptism celebration just to receive the invitees' gifts.

Perhaps the use of the mean effective stress at failure does not allow an immediate perception of the size of a pile. So, let us assume a conical pile and take the centre point of the base as the one governing the choice of the compaction effort to be applied. Admitting that there are no arching effects, the maximum vertical effective stress at that point corresponds to the weight of a soil column with the maximum pile height and can be

considered the maximum effective principal stress. Using Jacky's coefficient of earth pressure at rest, the following relation between the mean effective stress at failure (under CK_0DC triaxial conditions) and the mean effective stress at-rest, p'_c, can be derived:

$$\frac{p'_f}{p'_c} = \frac{3 - \sin\varphi'}{3 - 2 \cdot \sin\varphi'} \qquad [136]$$

For a dilatancy supressed material, $\varphi' = \varphi'_{cs}$, the above stress ratio acquires the value of 1,3. If the material was compacted to 100% of the Proctor energy, the maximum height of this hypothetical conical pile could be of 297m.

Alternatively, a "$\varphi'_p - \varphi'_{cs}$ minimum excess of shearing resistance" criterium could be defined. Say we were not available to have anything but $\varphi'_p - \varphi'_{cs} = 5°$ on any point of our conical pile, which was going to have a maximum height of 86,8m. In such hypothetical case, the allowable mean effective stress at failure at the centre of the base would be 1,95MPa ($\ln p'_f = 7{,}575$). Trusting on the results provided on Figure 58, the required compaction effort would correspond 100% degree of compaction using the normal Proctor energy for reference. We have seen before that the $R \geq 100\%$ compaction control criterium was equivalent to a "0,63 maximum void ratio" criterium. Now, we have the "$\varphi'_p - \varphi'_{cs} = 5°$ minimum excess of shearing resistance" compaction criterium as another synonym. The marguerite becomes a daisy. Everyone looks for fast construction rhythms and pauses for control testing and approval of compaction strips are unwelcomed. One can imagine what would happen if compaction control was done based on dilatancy criteria.

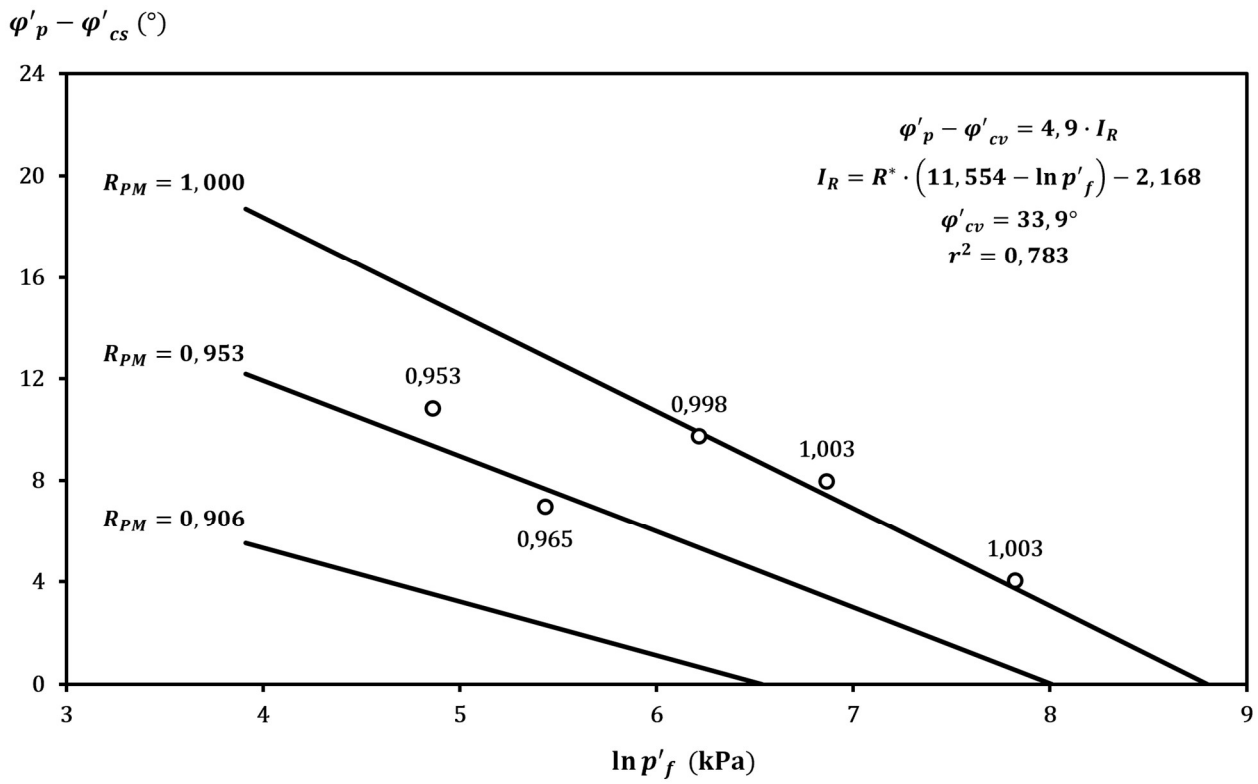

Figure 59

We would not fall into the tentation of considering the findings shown on Figure 58 anything else than a relatively successful attempt to describe the role of the as-compacted material state and the role of the confining stress on the mobilisation of shear strength of a sample of our powdered size material.

Much more tests would have to be analysed to try some sort of generalisation of the figures and trends presented herein. And to analyse tests results, data from tests is required and we run unfunded. Nevertheless, Figure 59, on the previous page, provides a second example of attempting to explain the contribution of dilatancy to shear strength as a function of the as-compacted density state and of the confining stress. This second example is also from an iron-ore dry tailings sample and, looking at the difference on the results relatively to the ones presented on Figure 58, it is easy to perceive how extensive and careful an investigation programme would have to be in order to obtain a reliable estimation of the available peak shearing resistance of an enormous mass of compacted tailings, even if their grading was narrow banded like our “55-70” material .

One may think that the results presented for the two former tailings samples were not obtained for a predominantly silty soil, such is the dilatancy exhibited by them.

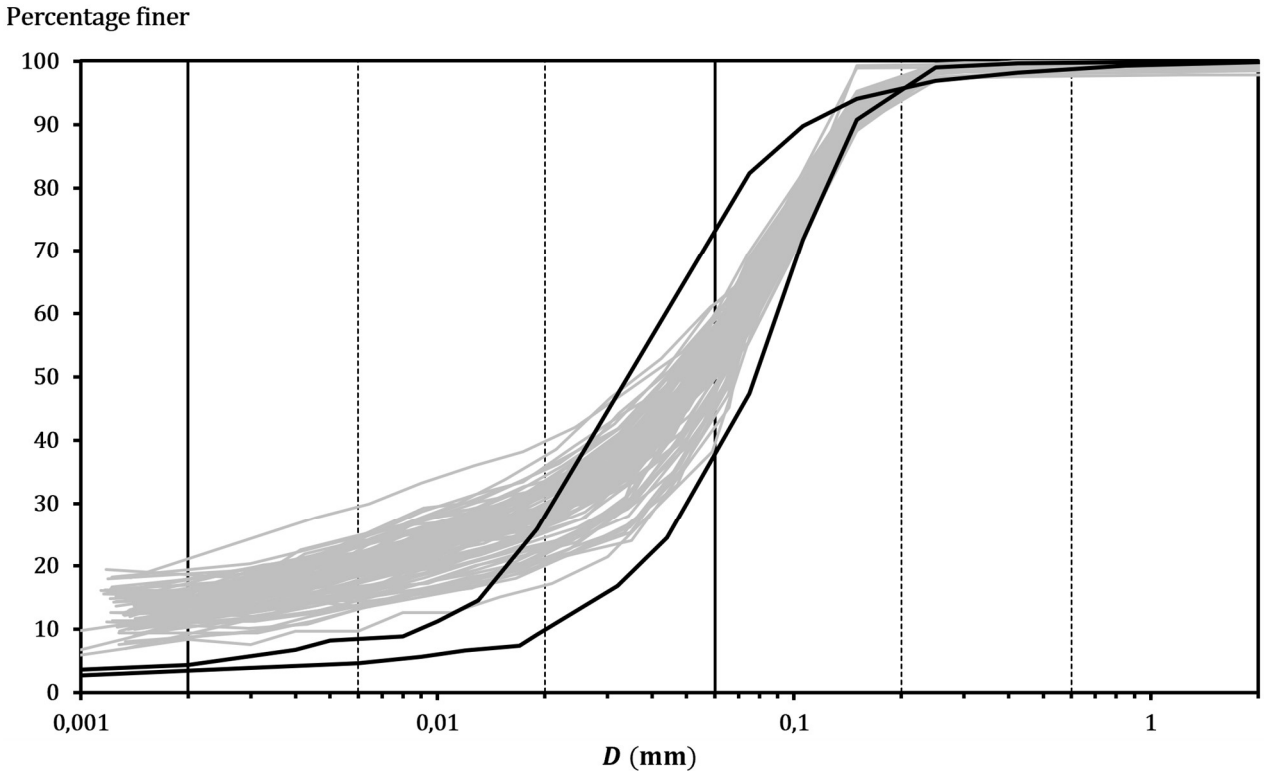

Figure 60

As shown in Figure 60, the two samples used to produce Figure 58 and Figure 59 are not from the “57-70” tailings family, as one of them has a fines content of 82,4% and the other one a fines content of 47,4%, following the same order of presentation. The granulometric distribution modulus of the sample with a lower fine sand content is 0,611 and, for the one with greater fine sand content, the modulus value is 0,777. The minimum void ratios obtained with the modified Proctor energy are 0,546 and 0,600, respectively.

Placing the same question as before about the size of a hypothetical dry stacking tailings pile, let us alternatively consider a facility where the stored material was uniform and its shear strength was deterministically as given

in Figure 59. In that case, to keep dilatancy alive, the value of the allowable mean effective stress would be of 0,69MPa ($\ln p'_f = 6{,}537$) or 3,01MPa ($\ln p'_f = 8{,}010$), respectively for degrees of compaction of 95% and 100% with the Proctor normal energy. For the lower value of the allowable confining stresses at failure, a "0,77 maximum void ratio" would be appropriate and for the greater one, a "0,68 maximum void ratio" would be sufficient. So, the "minimum void ratio" compaction criterium can be speculatively related to a dilatancy need, as we postulated initially. As said before, the complication comes from the variability of soil properties, including here their dilatancy. It is worth noticing that the estimated value of the critical state angle of shearing resistance is the same, $\varphi'_{cs} = 34°$, for the two different material samples.

At the best of your ability, or closer to it, we have just concluded that the "0,6 maximum void ratio" criterium was born, with an elevated binomial probability, from the desire of building mountains of dilatant powder. We cherish the idea. We have also demonstrated that, compaction-wise, a "minimum void ratio" criterium is a hand full of nothing. For this humble engineer, the very first reason to compact a soil to a fixed minimum and mean value of dry density, within controlled water contents, does not come from any pilgrim theory about the existence of a (one) critical state, but from earthworks construction practice. Theatrical engineering acts may have helped us filling our belly but ended up emptying our soul, or quiet.

6.2. Contractibility, in the end

Even if we put all our money on a bet for the father and motherhood thinking behind the "0,6 maximum void ratio", we have still not tried to explain what for one needs a powder mountain to be dilatant. Everyone would agree that it is better to have more than less, if the price is no problem. Perhaps the best way to reach an explanation is to approach the question from the opposite side. If someone seeks for a minimally dilatant material, that is likely to be because a contractile material is a source of geotechnical safety problems.

To discuss the inverse problem, it is necessary to have straight ideas about opening or closing the tap, referring to the tap that precludes or allows the generation of excess pore pressures on a triaxial apparatus. If the boundary conditions of a boundary value problem are changed, the solution of the problem will be different, but the material inside the domain may well be the same. On the previous subchapter, testing was done with the tap open. For this subchapter nothing else changes, except that the tap is closed. The tap is closed or open by someone´s decision, not by the will of the specimens. On the nature, there are no taps waiting for men to decide whether to close or to open them.

Figure 61, on next page, puts the problem in the correct perspective, using the results of two CAUC triaxial tests on two samples of the same tailings material, the finer one of the two presented on the previous subchapter. Both specimens were consolidated anisotropically to the same stress level and the difference on the response to the same loading, under the same boundary conditions (tap closed), results from the different initial degree of compaction of the two specimens. The effective stress path C1-F1-P1 was followed by a specimen with a degree of compaction corresponding to $R_{PM} = 0{,}815$ or $R^* = 0{,}224$ and the effective stress path C2-F2-P2 was followed by a specimen with a degree of compaction corresponding to $R_{PM} = 0{,}902$ or $R^* = 0{,}537$. Note that for 100% degree of compaction with the Proctor normal energy $R_{PM} = 0{,}946$ or $R^* = 0{,}696$. Points P1 and P2 represent the point of maximum obliquity (σ'_1/σ'_3 maximum), which theoretically is the instant of failure of a material obeying to Coulomb´s friction law. Points F1 and F2 represent the instant where the maximum deviatoric stress is reached and is commonly used to define a soil undrained shear strength in terms of total stress ($s_u = q_{max}/2$).

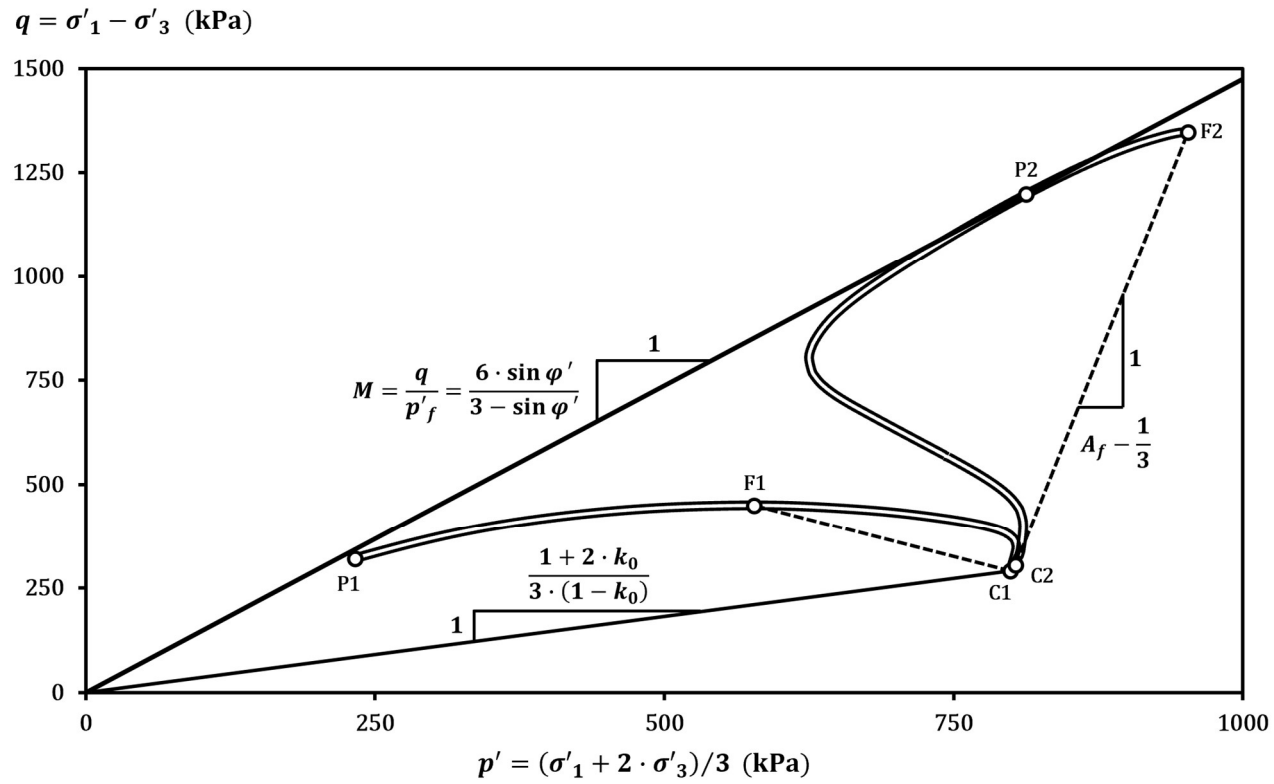

Figure 61

Going back to the previous subchapter and namely to Figure 58, one may conclude that the loosest sample would not dilatate beyond a critical mean effective stress at failure $p'_f = 3{,}7$kPa and the densest would not dilatate beyond a critical mean effective stress at failure of $p'_f = 2{,}32$MPa. If the volumetric deformation of the densest specimen was not artificially impeded by blocking its drainage, an excess angle of shearing resistance of $\varphi'_p - \varphi'_{cs} = 3{,}3°$ would be mobilised at failure. On Figure 61 the failure line corresponding to the denser specimen is shown and its slope value is $M = 1{,}474$, corresponding to a peak value of the angle of shearing resistance equal to $\varphi'_p = 36{,}3°$. For the loosest specimen, the slope of the failure line is $M = 1{,}379$, corresponding to a value of the angle of shearing resistance very close to the critical state one, $\varphi'_p = 34{,}1° \cong \varphi'_{cs}$. All this apart from the meaningless precisionism of stating values rounded to the third decimal case.

The difference on the response of the two specimens is well described by Sir Alec Skempton´s pore pressure coefficient, A, which, in terms of the Cambridge stress invariants, writes:

$$\Delta u = \Delta p + \frac{1}{3} \cdot (3 \cdot A - 1) \cdot \Delta q \qquad [136]$$

Being Δu the pore pressure excess increment due to increments of the mean total stress Δp and the deviatoric stress Δq resulting from the applied triaxial loading, under conditions of blocked drainage. As illustrated on Figure 61 with dashed lines, the secant effective stress path to failure is completely defined by the value of the coefficient A at failure, A_f. If the maximum deviatoric stress is assumed as the failure criterium (Tresca's criterium), the value of the pore pressure coefficient at failure is $A_f = +1{,}792$ (path C1-F1) for the loosest of the two specimens and $A_f = +0{,}191$ for the densest (path C2-F2). If the Mohr-Coulomb failure criteria is

adopted for compatibility with the effective stress shearing resistance, the value of the pore pressure coefficient at failure is $A_f = +19{,}437$ (path C1-P1) for the loosest of the two specimens and $A_f = +0{,}323$ for the densest (path C2-P2).

The loosest specimen is more contractile and generates more positive excesses of pore pressure when its volumetric deformation is impeded by the men that close taps. Moreover, the denser specimen would tend to dilatate if sheared with the tap open but still generates a substantial amount of excess pore pressures if sheared with the tap closed. Non-contractability does not imply generation of null or negative excesses of pore pressure under undrained loading conditions. This fact suggests us that the "minimum void ratio" compaction criterium may not have been created with the desire of having compacted dry tailings with some arbitrary target of excess of shearing resistance but rather having dry tailings dilatant to the extent of generating null or negative excess pore pressures when forced to shear under conditions of blocked drainage, even under very high confining stresses.

For the material being used as an example, we may conclude that a degree of compaction equal or lower than 95% degree of compaction with the Proctor energy ($R_{PM} = 0{,}899$ or $R^* = 0{,}696$ for 100% degree of compaction) would not be satisfying the father of the "minimum void ratio" compaction criterium, even if the effective mean stress at failure had a modest value of $p'_f = 0{,}80$MPa. If the value of the pore pressure coefficient at failure can be null or negative for dry tailings compacted under 100% of the modified Proctor energy under high confining stresses (say 5MPa or 6MPa) is what remains to be determined. Nothing of this changes a letter on the words that closed the previous subchapter.

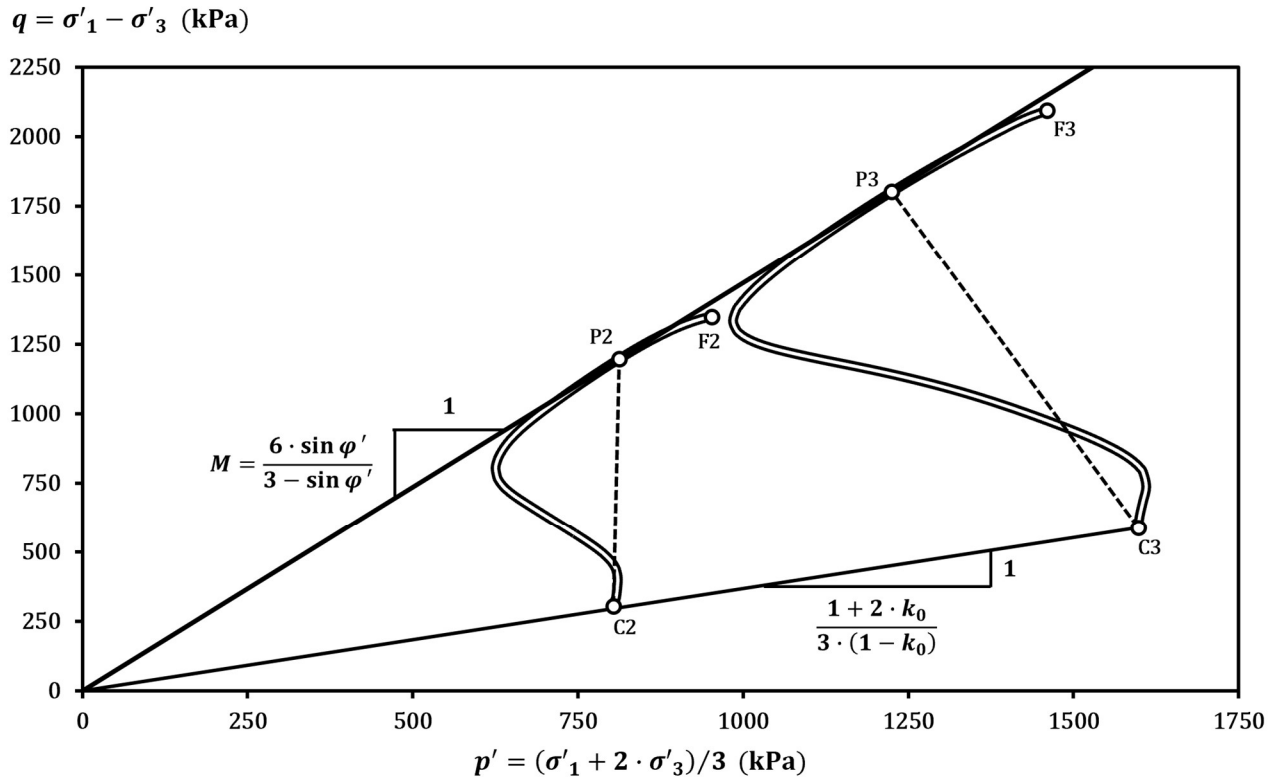

Figure 62

Exactly for the same reasons, associated to the dilatancy tendencies, that make the excess of shearing resistance decreasing with the increase of the mean effective stress at failure, the pore pressure coefficient at failure

increases with the increase of the mean effective stress at failure. Figure 62, on the previous page, shows two specimens compacted equally but anisotropically consolidated to different stress levels, being one of them the densest of the two previously referred samples. For the specimen subjected to the lower confining stress, we have seen that the pore pressure coefficient at failure is $A_f = +0{,}323$ (path C2-P2), following the Mohr-Coulomb failure criteria. The new specimen was consolidated to a mean effective stress which is twice than the one used for the first one. At the instant of maximum obliquity, the pore pressure coefficient at failure is $A_f = +0{,}641$ (path C3-P3), curiously about the double of the value manifested on the other specimen.

For this new specimen, the mean effective stress at failure was $p'_f = 1{,}22$MPa and, just remembering, both were compacted slightly above the 95% degree of compaction with the normal Proctor energy, slightly on the wet side of optimum. There are at least two conditions for these findings to apply to a real mountain of powder. Firstly, the material must be completely saturated as much a soil can be completely saturated on a mountain of material placed too far away from full saturation. Secondly, someone needs to close the tap that does not exist in nature. Perhaps a poorly conceived basal drainage system and a diluvium will help the mountain builders having something like a monstruous conical heap fully saturated. The second condition, having the tap closed in nature, requires discussing dogmas and dogmas are not discussable.

At this point, it should be completely clear that there is always a reason or two to compact soils, and that reason or two, is not the same for all earthworks. Changing the name of the compaction control criterium is not necessary, nor it is sufficient. But it is also clear that, unless the cost matters, it is better to have a denser mountain of powder than a looser one. Call it sustainability.

A word on liquefaction. Suppose a new specimen of the fine-grained tailings we have been using so far on this chapter was carefully prepared on the laboratory to such a loose state that point P1 on Figure 61 had hit the origin of the graph. At that instant, the effective stresses would be zero and the material on the specimen would be said to have liquified or to have the same properties of a liquid as the word suggests. Transposing the phenomenon to a pile of tailings, that would be the moment when the mountain swallowed the hiker. Based on the example, if the compaction of dry stacking tailings had the pure objective of preventing liquefaction, instead of controlling the level of excess pore pressures that the material could generated if the tap had been closed, then, looking at point P1, we could say that the 86% degree of compaction with the Proctor normal energy was enough to prevent the phenomenon, strict sense. The pamphlets that the mining industry emanates making promises of mountains of dilatant powder and announcing their tireless fight against liquefaction are just what they are. If dilatancy had a required quantity, instead of propaganda, the promises would be engineering facts and nowadays engineering facts worth less than cheap pamphleteering.

6.3. Dilatating “55-70” on the triaxial apparatus

On Chapter 5, using a relatively narrow banded filtered tailings, we have seen how difficult it is, at least for us, to explain mathematically the compaction curves at cost of material properties, such is the dispersion of data that runs away from the mean logical trends. It is not expectable from the start that better results can be reached when addressing state dependent variables as dilatancy or the lack of it. Nevertheless, having the results of triaxial CIUC tests on a total of 60 specimens of our “55-70” tailings it may be worth to give it a try.

The three “55-70” gradings shown in Figure 63, on next page, were submitted to a series of 5 triaxial tests with 4 specimens each, compacted to the same degree and consolidated isotopically under different stress levels (3 gradings × 5 densities × 4 consolidation stress).

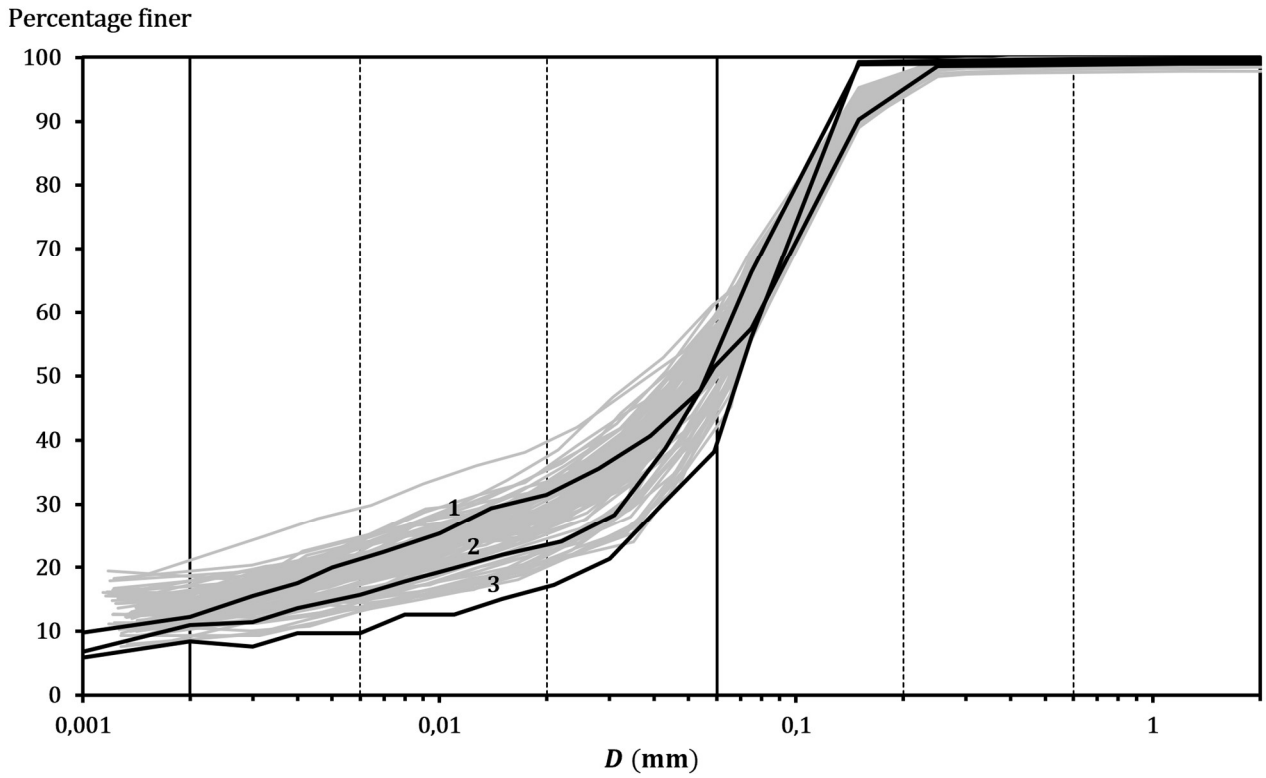

Figure 63

As explained on the previous subchapter, our attention as turned to excessive contractibility, once there is the belief that soils choose their stress path to failure regardless of the loading and, if so, excessively contractile soils may well choose to fail as if the tap was closed, generating dangerous positive excess pore pressures. Sir Alec Skempton's pore pressure coefficient at failure, A_f, is therefore the variable selected to establish associations with the as-compacted state of the tailings and the level of confining stress, which we have seen in Subchapter 6.1 being good predictors of dilatancy.

Before presenting some results, it may be worth distinguishing the pore pressure coefficient in relation to the instant chosen to represent the soil failure (points P against points F in Figure 61 and Figure 62). If shearing resistance is defined by the Mohr-Coulomb failure criteria in terms of effective stresses, the coefficient A_f (points P in Figure 61 and Figure 61) will allow a unique relationship between the shear stress at failure, τ_f, in conditions of blocked drainage and the angle of shearing resistance. For the case of a CIUC triaxial test:

$$\tau_f = (\sigma_n - \Delta u) \cdot \tan \varphi' = \frac{\sigma'_c \cdot \sin \varphi'}{1 + (2 \cdot A_f - 1) \cdot \sin \varphi'} \cdot \cos \varphi' = s_u \cdot \cos \varphi' = \tau_{max} \cdot \cos \varphi' \qquad [137]$$

Being σ'_c the effective consolidation stress and s_u the undrained shear strength in terms of total stress. τ_f is the shear stress acting on failure planes, making an angle of $\pi/4 - \varphi'/2$ with the direction of the maximum principal stress and τ_{max} is the maximum shear stress acting on planes making an angle of $\pi/4$ with the direction of the maximum principal stress.

Starting with the values of the pore pressure coefficient at the instant of maximum obliquity, the results obtained on the 60 specimens are plotted altogether in Figure 64 as a function of their compaction index, R^* introduced earlier in this chapter.

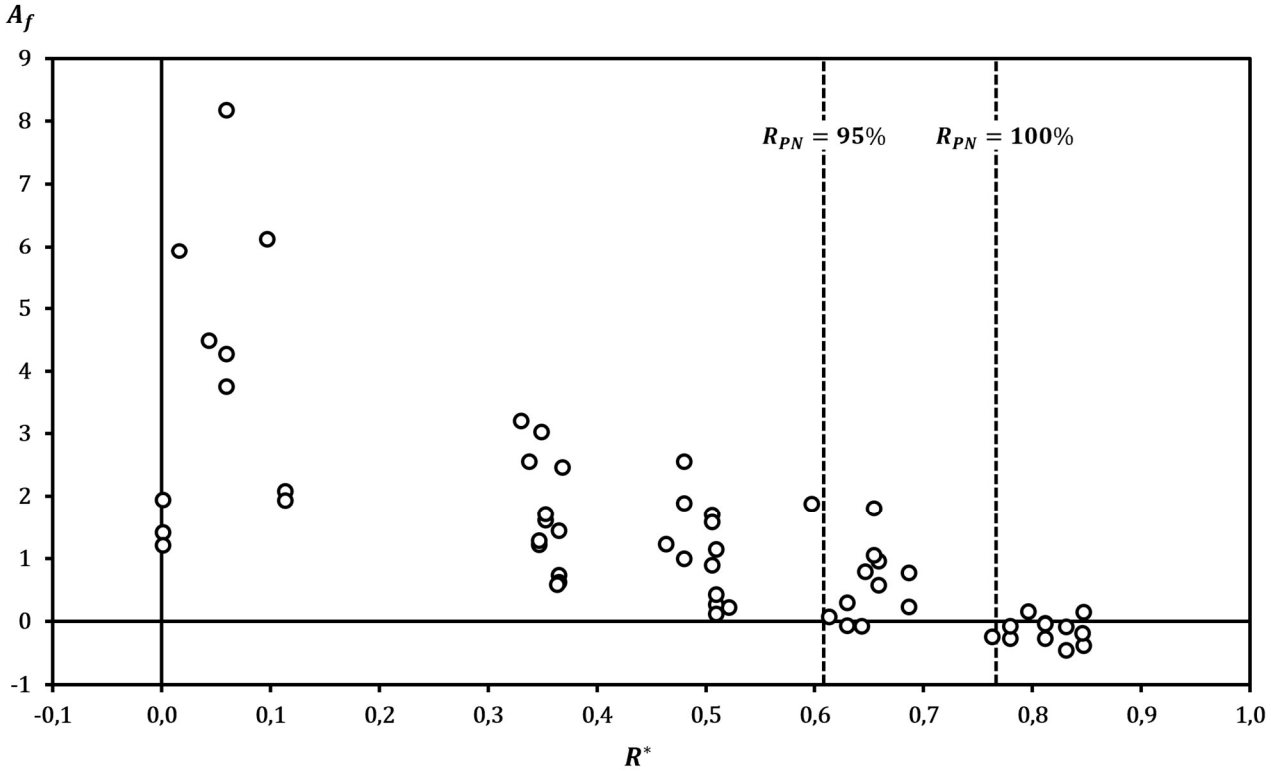

Figure 64

On this figure, dashed lines indicate the compaction index corresponding to 100% and 95% degree of compaction using the Proctor normal energy, R_{PN}. As a reference for limit equilibrium analysis by the method of slices, conducted in terms of effective stress, the explicit consideration of excess pore pressures may be omitted when:

$$A_f \leq \frac{1}{2} \cdot (1 - \sin \varphi') \qquad [137]$$

For the samples considered here, omission of excess pore pressures would be safe as long as a marginal fraction of soil with $A_f \leq +0{,}25$ was left within the earthwork. According to Figure 64, we could say that, unless the field degree of compaction did not exceed 98% with the Proctor normal energy except for a residual fraction of compacted material, undrained failures would be conditioning the safety of the structure. Yet, this conclusion is precipitated, because the required degree of compaction depends on the size of the structure, that is, on the level of confining stress that is expected on the structure or on the zones of the structure where its stability is governed.

Isotropic consolidation stresses used on the triaxial testing programme we are using ranged between 100KPa and 800KPa (100KPa, 200kPa, 400kPa and 800kPa). This is the triaxial testing program that a mountain builder adopted to support the post-mortem design of “55-70” tailings pile already in construction and that is expected to reach a height of over 230m. So, the maximum consolidation effective mean stress on the real structure will

surpass the maximum test value 3 or 4 times and, therefore, the previous conclusion was misleading. Assuming that no one on the mountain building business specifies degrees of compaction under 95% with the Proctor energy, even for small earthworks, testing specimens in completely loose state just serves the purpose of demonstrating what everyone on the business should know and that is why no one specifies degrees of compaction under 95% with the Proctor energy. Furthermore, on the previous chapter it was shown that, using a field compaction curve corresponding to the normal Proctor energy one, it would be nearly impossible, within a wide range of practical moulding water contents, to have material with a degree of compaction below 98%.

If data on Figure 64 is separated in function of the isotropic consolidation stress of the specimens, it would be eventually concluded that, using the modified Proctor energy ($R^* = 1$), the maximum stress under which the generation of pore water pressure excesses could be neglected ($A_f \approx +0{,}25$) is in the order of 1,8MPa. Holding this true or not, there is a limit on the height of a compacted tailings pile beyond which the material buried inside it will generate non-negligible excess of pore pressures if taken to failure under conditions of blocked drainage. At least for the case of our "55-70" tailings, the size of the mountains being built with it are overly in excess of that presumable limit. It will not be based on a testing programme destined to show that uncompacted materials can come close to liquefaction, that one may determine beyond which level of stress well compacted materials may still generate unwanted excesses of pore pressure. The focus of the studies would have to be recentred, before making promises of dilatant behaviour. Naturally, we do not know what studies have been made, but we know that decisions were made based on the data presented here and it is very unlikely, as seen on Chapter 2, that what has already been done will be one day redone. Sooner than that, the fallacy of undrained failures will fall.

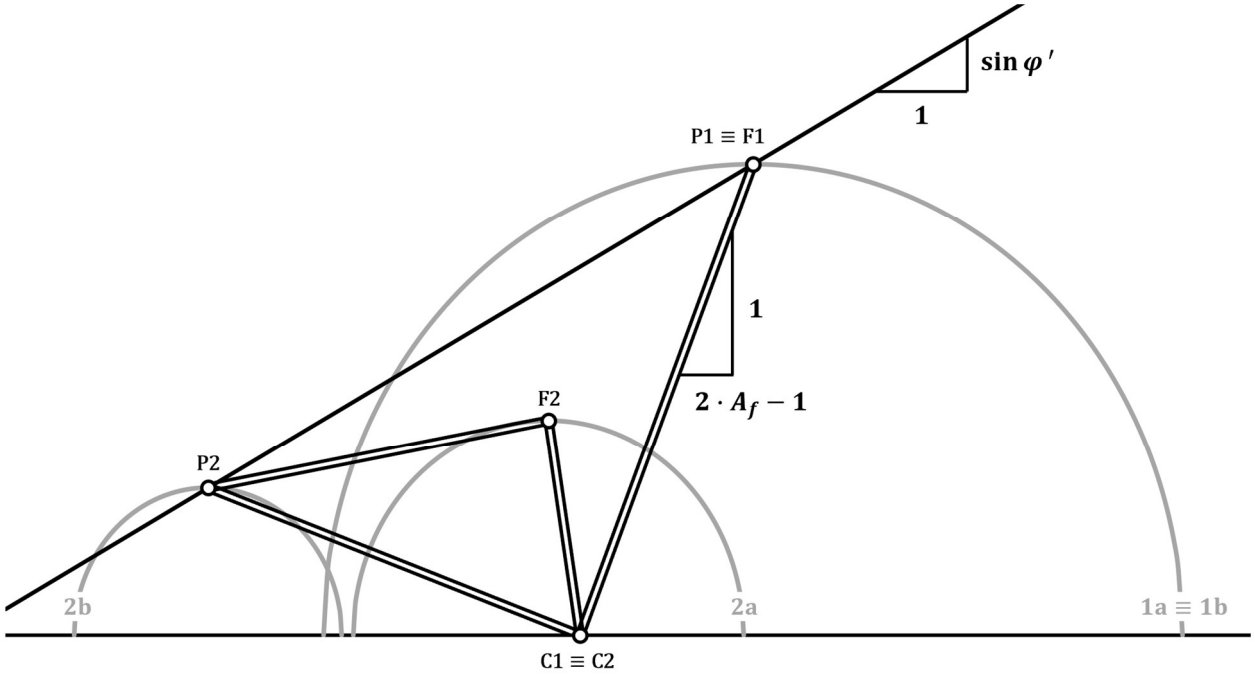

Figure 65

As seen in equation 137, the secant value of the pore pressure coefficient at failure is useful if one is convinced that the Mohr-Coulomb failure criterium is the one that better describes the shear strength of a soil, regardless the failure conditions being drained or undrained, or partially drained on a broad sense. Knowing the value of the coefficient is quite useless if one admits that the failure criteria is the Tresca one, which assumes that failure

occurs when the maximum shear stress (half the maximum deviatoric stress) is reached on any plane. The latter criterium is represented on Figure 61 and on Figure 62 by the generic points F.

There is however a maximum value of the pore pressure coefficient bellow which using any of the two failure criterium leads to differences that are of no substantive practical importance. Figure 65, on the previous page, illustrates the ditto, showing the Mohr circles of stress of two specimens of our "55-70" tailings, prepared with different compaction energies, consolidated to the same isotropic consolidation stress and sheared under triaxial compression.

The two coincident circles, $1\mathrm{a}$ and $1\mathrm{b}$, correspond to the instant of maximum obliquity (Point $\mathrm{P1}$) of a specimen prepared with a compaction index $R^* = 0{,}630$, which occurs simultaneously with the instant of maximum shear stress (Point $\mathrm{F1}$). The value of pore pressure coefficient at failure, defining a unique secant effective stress path to failure ($\mathrm{C1\text{-}F1} \equiv \mathrm{C1\text{-}P1}$) is $A_f = 0{,}299$. For a specimen on a looser state, prepared with a compaction index $R^* = 0{,}480$, we have two circles wide apart from each other. The point of maximum obliquity (Point $\mathrm{P2}$) lies on the same failure line that passes through the point of maximum obliquity of the denser specimen (Point $\mathrm{P1}$), which is the failure line according to the Morh-Coulomb failure criteria. The value of pore pressure coefficient at failure, defining a secant effective stress path to failure ($\mathrm{C2\text{-}P2}$), is $A_f = 1{,}891$ and the shear stress on the failure plane is $\tau_f = 139{,}7\mathrm{kPa} \times \cos\varphi'$.

On his way to failure, the stress path of the second specimen passes first through the point of maximum shear stress, something that can be imagined as bi-linear stress path $\mathrm{C2\text{-}F2\text{-}P2}$. The value of the pore pressure coefficient defining the first segment of the effective stress path is $A_f = 0{,}763$ and the maximum shear stress acting on planes forming an angle of $\pi/4$ with the direction of the principal maximum stress is $\tau_{max} = 204{,}0\mathrm{kPa}$. As long as the pore pressure coefficient associated to the instant of maximum obliquity is in the order if 1,5 at the maximum, there is no practical reason to renounce the Morh-Coulomb failure criterium in favour of the Tresca one, once both will yield approximately the same shear strength, either in terms of effective stress (using φ' and A_f) or in terms of total stress (using s_u).

Looking back to Figure 64, we can see that, for the range of consolidation stresses used on the testing program, all values, except one, of the pore pressure coefficient are lower than 1,5 as long as the degree of compaction exceeds 95% with the normal Proctor energy ($R^* \cong 0{,}608$). Extrapolating from the consolidation stresses used on the test program, one could expect the upper limit of the pore pressure coefficient to hold up to consolidation stresses of 3,2MPa, using the lowest level of compaction energy. In other words, we do not need to summon the phantom of liquefaction so that attention is paid to the possibility of undrained failures to occur on compacted tailings. At least while someone keeps the tap closed on the laboratory with one hand and on the nature with the other one.

The ulterior relevance of what happens under high confining stress levels needs to be emphasized and, for that purpose, a sample of a "55-70" alike tailings will be used. Its grading is shown on Figure 66, on next page, alongside with the 105 "55-70" tailings granulometric curves. The fines content of the sample is $FC = 57\%$ and the granulometric distribution modulus is $\nu = 0{,}626$, on the lower bound of the "55-70" sampling value. If the packing theory introduced on subchapter 5.3 held some significance, this sample would be an example of the poorest grading, that is, one that would end up having the greatest void ratio for the same compaction energy, within the same family of tailings. We will try to reach any conclusion with the reluctancy that the subject treatment requires. Allow us to complain again, even if falsely, about the absence of a testing program that

consistently allowed to explore all the meanders of the compaction problem. We say falsely, because the consequences of building powder mountains based on wrong premises do not affect us at all, except for a hike that we survived to.

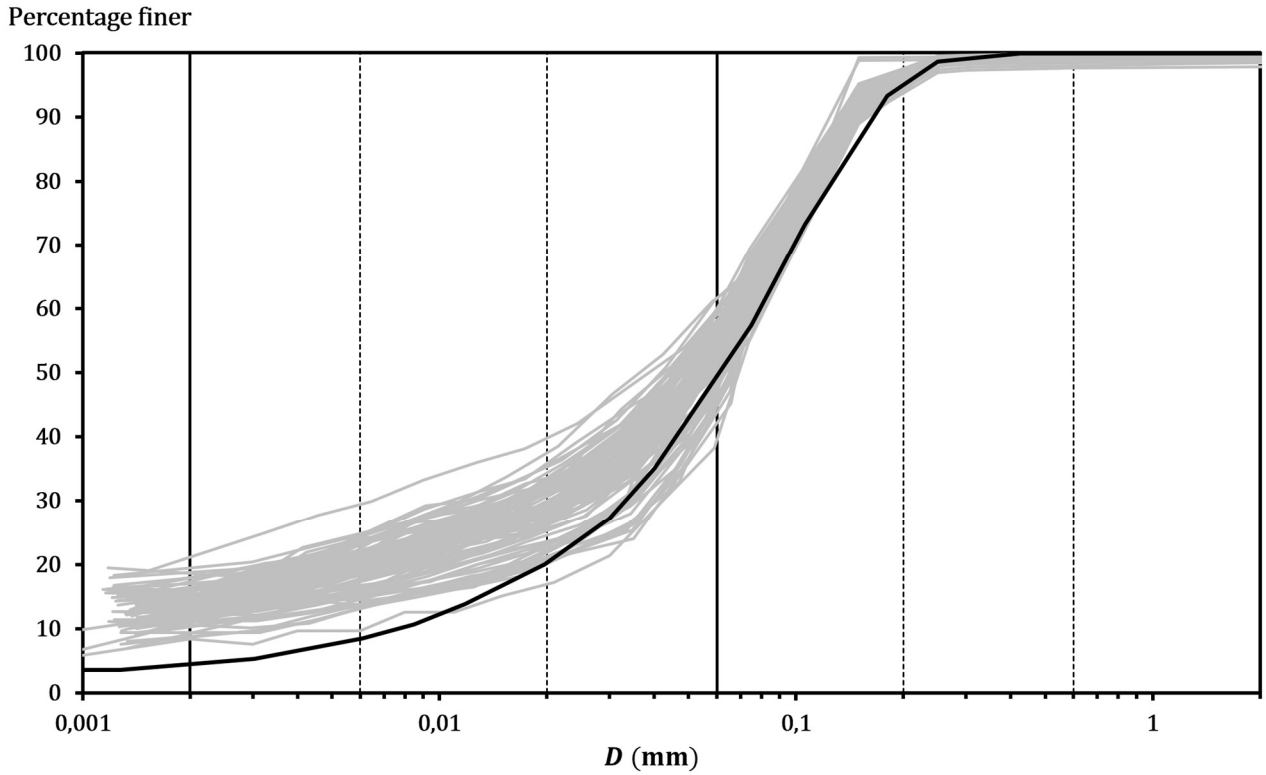

Figure 66

We will start with CIUC triaxial tests on two specimens of this "55-70" alike tailings, both prepared to a degree of compaction of 97% with the Proctor normal energy ($R^* = 0{,}672$) and subjected to different isotropic consolidation stresses, more in line with those that the material will experience on a mountain of powder like those we know about. Figure 67, on next page, shows the effective stress paths of two specimens. The value of the pore pressure coefficient at failure is $A_f = 0{,}703$ for the specimen consolidated to the lowest stress and $A_f = 0{,}995$ for the one consolidated to the highest stress. If data from Figure 64 was used for extrapolation to higher consolidation stresses, an overestimation of the value of the pore pressure coefficient of about 3 times would have resulted, what simple shows how dangerous extrapolations are. Even so, the magnitude of the excess pore pressures generated at failure on these two last specimens is everything but neglectable.

On Chapter 4, we have discussed the values that the compaction induced prestress may attain, depending on the compaction energy and the moulding water content. Difficultly, under the high consolidation stresses to which they were submitted, any of the two specimens on Figure 67 hold any memory of the compaction effort used to prepare them and even so the amount of excess pore pressures generated during shearing increase with the level of the consolidation stress. Contrary to natural clayey natural, that would be expected to generate the same amount of excess pore-pressures as soon as their eventual over-consolidation ratio is subdued, tailings, it seems, do not suffer of a limitation on the amount of excess pore pressure that they can generate with growing levels of confining stress.

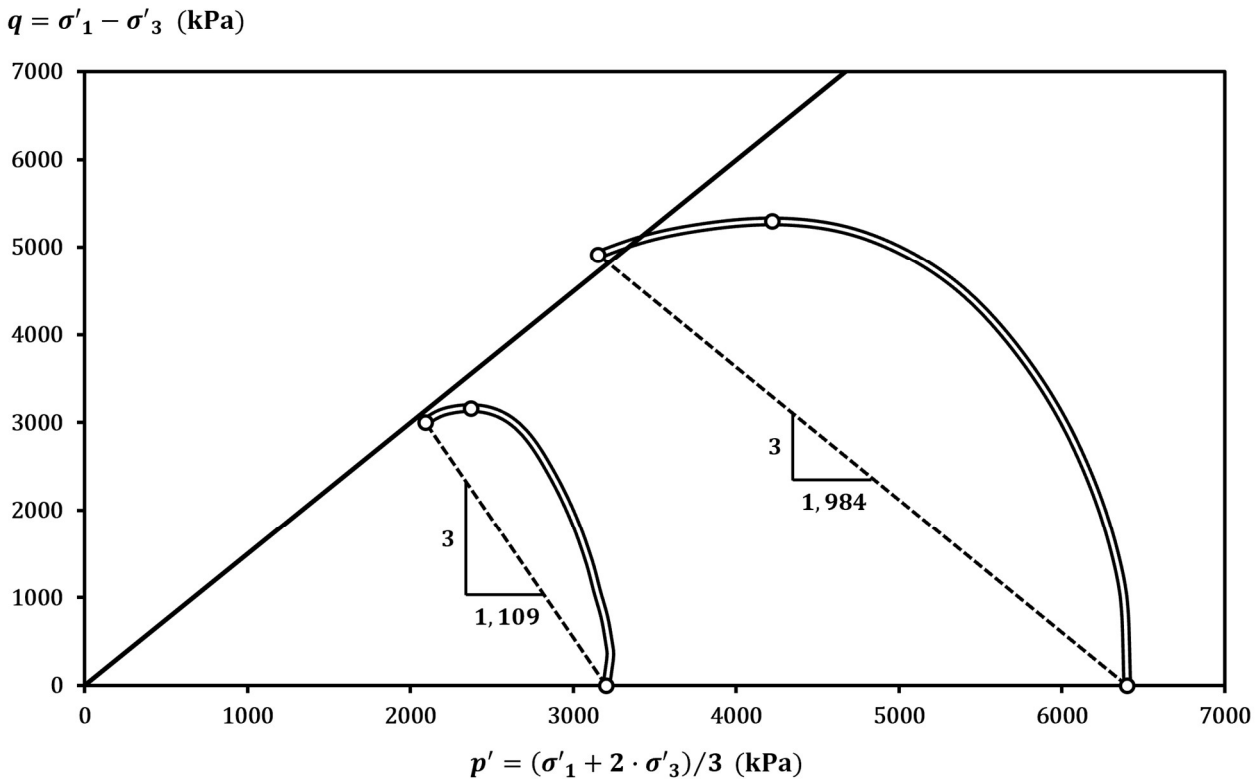

Figure 67

At light of the critical state theory, such difference becomes clear when the isotropic consolidation line and the critical state line are plotted together on the $\ln p'$-v space, being v the specific volume ($v = 1 + e$). These virtual lines are probably not parallel and the greater the consolidation stress is, the greater may be the distance between both. As so elegantly derived by Peter Wroth, for instance on the 24th Rankine Lecture that he delivered over forty years ago, if the critical state line (CSL) is parallel to the isotopic consolidation line (ISL), the pore pressure coefficient at failure is given by:

$$A_f = \frac{1}{M_{cs}} \cdot \left(\left(\frac{R_o}{r} \right)^{-\Lambda} + \frac{M_{cs}}{3} - 1 \right) \quad [138]$$

Where M_{cs} is the slope of the failure line at the critical state on the p'-q stress space, R_o is the over-consolidation ratio, r is the spacing ratio and Λ is the plastic volumetric strain ratio. Expressed in terms of mean effective stress, the compaction prestress of an isotropically consolidated specimen is:

$$p'_y = R_o \cdot p'_c \geq p'_c \quad [139]$$

Being p'_c the actual consolidation stress.

On the original Cam Clay model, the constant spacing between the critical state and the isotropic consolidation lines was translated by a fixed value of the spacing ratio. Equation 138 still applies if the lines are not parallel as schematically represented in Figure 68, on next page, but the spacing ratio will be variable, depending on the consolidation stress:

$$r = \frac{p'_A}{p'_B} = \frac{(\Gamma_{ic} - \Gamma_{cs}) - (\lambda_{ic} - \lambda_{cs}) \cdot \ln p'}{\lambda_{cs} - \kappa} \quad [140]$$

Where Γ_{ic} and λ_{ic} are the ordinate at the origin and the slope of the isotropic consolidation line, Γ_{cs} and λ_{cs} are the ordinate at the origin and the slope of the critical state line and κ is the slope of the swelling line.

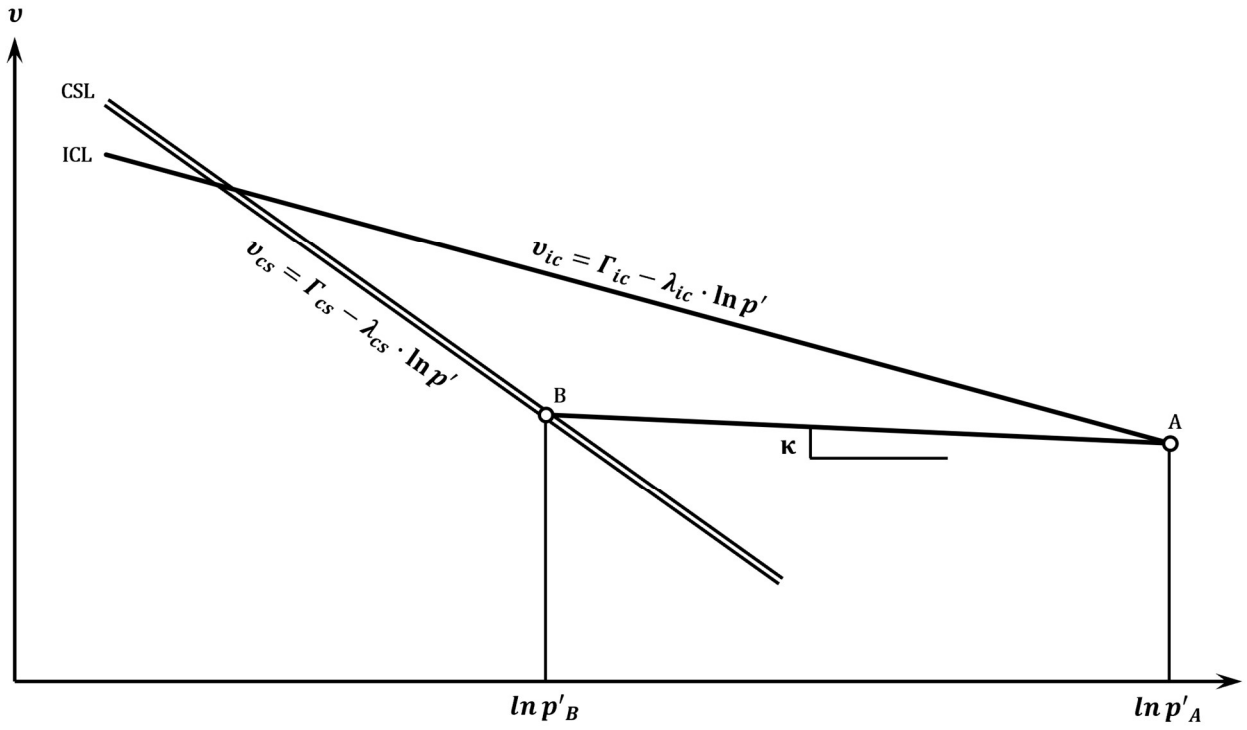

Figure 68

The plastic volumetric strain ratio, Λ, to be used with equation 139 is given by:

$$\Lambda = \frac{\lambda_{cs} - \kappa}{\lambda_{cs}} \quad [141]$$

Let us accept that the critical sate line for the two specimens used on Figure 67 was given by $v_{cs} = 1{,}970 - 0{,}054 \times \ln p'$. As said before, at stress levels used for consolidation, the specimens no longer remember the compaction prestress and, therefore, one can consider $R_0 = 1$.

Using Equation 138, it may be concluded that the isotropic consolidation line should be given by $v_{ic} = 1{,}780 - 0{,}021 \times \ln p'$ so that the exact values of the pore pressure coefficients at failure were exactly those presented earlier on ($A_f = 0{,}703$ for $\sigma'_c = 0{,}32$MPa and $A_f = 0{,}995$ for $\sigma'_c = 0{,}64$MPa). Following the same order, the respective spacing ratios are $r = 1{,}576$ and $r = 2{,}034$. Using data from the consolidation stage of the two specimens, the isotropic consolidation line would result in $v_{ic} = 1{,}783 - 0{,}029 \times \ln p'$, what somehow proofs the non-parallelism of the two state lines. This ends up being a mere curiosity, as on a mass of "unique" tailings there are many more consolidation lines than are critical state lines, and these are already close to infinite. Do not forget this when gaming with your supercomputer and someone´s 48 plus 9 parameters, or more, constitutive relationship.

Talking about curiosities, equation 138 is not specific for clays and may be used in conjunction with the so-called state parameter, ξ, often used for sands and silts. Assuming that the critical sate line and the reference consolidation line are parallel, a reference state parameter can be defined instead of the spacing ratio as a measure on the distance between both:

$$\xi_R = \upsilon_{ic} - \upsilon_{cs} = (\lambda_{cs} - \kappa) \cdot \ln r \quad [142]$$

The state parameter is the difference of the specific void at the actual state, υ, and that at the critical state, υ_{cs}:

$$\xi = \upsilon - \upsilon_{cs} = \upsilon - \Gamma_{cs} - \lambda_{cs} \cdot \ln p' \quad [143]$$

The overconsolidation ratio, R_o, can now be expressed as a function of the state parameters:

$$\ln R_0 = \frac{\xi_R - \xi}{\lambda_{cs} - \kappa} \quad [144]$$

And the ratio R_o/r in equation 138 is obtained from:

$$\ln \frac{R_o}{r} = \frac{-\xi}{\lambda_{cs} - \kappa} \quad [145]$$

Then, from here to CASM (*Clay And Sand Model*) and from CASM to eternal mountains of powder.

What we really want to stress in this subchapter is the possibility of the occurrence of an undrained response of compacted tailings under high confinement stresses and not to deny anything else, including the susceptibility of undrained instability. Using again one of the specimens on Figure 67, we can see on Figure 68, at the top of next page) that, after reaching point F′, the specimen could not sustain the stress that was being applied to it ($q - q_P < 0$ from point F′ onwards). The external loading is represented by the total stress path (TSP) on the figure. A line connecting the points of maximum deviatoric stress is said to represent the locus of instability (line with slope M_i on the figure), but that does not mean necessarily that the line of failure at the critical state (line with slope M_{cs} on the figure) cannot be reached and reached (point P) without a significative loss of shear strength on the case of minimally well compacted tailings. This is the case.

For the two specimens used on Figure 67, the ratio between the slope of the instability line, M_i, and the slope of the critical state line, M_{cs}, is equal to 0,939 for the specimen consolidated to 3,2MPa and is equal to 0,805 for the specimen consolidated to 6,4MPa. For the specimens used in Figure 64, subjected to consolidation stresses under 0,8MPa, the ratio between the slopes of the two lines is greater than one for all specimens compacted at least to a density corresponding to a compaction index $R^* = 0{,}45$ and greater than 1,3 for all specimens compacted, at least, to a density corresponding to a compaction index $R^* = 0{,}60$. Altogether, this set of triaxial tests on our “55-70” tailings, tell us that instability per-se is not a major concern on the safety of compacted powder mountains or, at least, is not a greater concern than undrained failures are, strictly speaking, as long as material is minimally well compacted.

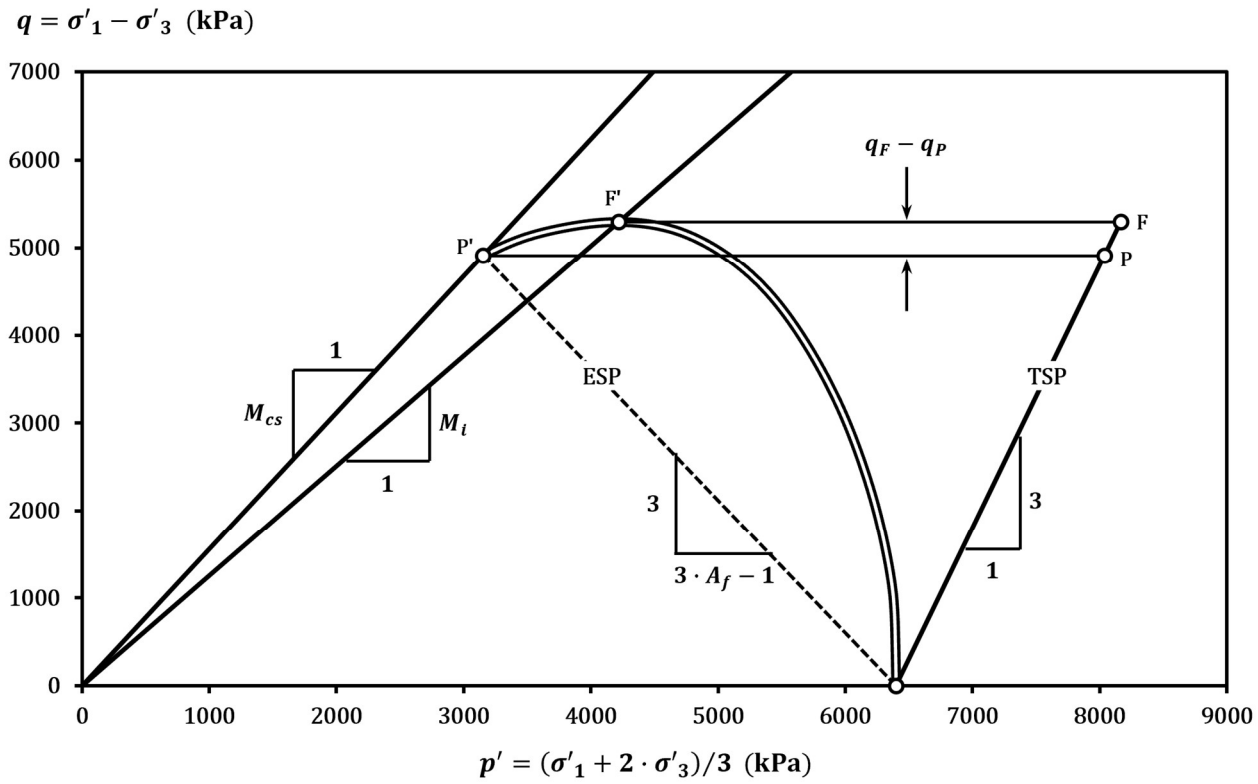

Figure 69

Most specially, none of the previous observations intends anything else than pointing out that a limit equilibrium slope stability analysis under undrained conditions, weather conducted in terms of total stress (s_u) or not (φ'_p, φ'_{cs} and A_f) should be mandatory under two conditions: (1) The material generates sufficient positive excesses of pore pressure when sheared under conditions of blocked drainage and (2) The analyst believes that the material, if allowed to choose, will always choose to follow the effective stress path associated with the generation of the maximum pore pressure excesses and defines the factor of safety in accordance with his beliefs. The latter condition means that the analyst or either is convinced that there are taps waiting to be closed on nature or pragmatically prefers not knowing and simply chooses the worst experimental case. The former condition means that before building mountains of compacted powder, a mountain builder, instead of bombastic statements about void ratios or pamphlets about dilatancy, should investigate the material he wants to store on conditions representative of how the material will be stored. The big mountains of powder that we know, and they are quite a few, may have been conceived as little backyard mounds. Or may not, who knows? The powder mountain crew of inspectors doing ultra-confidential internal audits may know.

All this seems, whatsoever, to be bad news for the mountain building business. There is a limit for everything, even to the doses of dilatancy that are been promised. Anyway, blessed are the mountain hikers for having men like the father of the “0,6 minimum void ratio” compaction criterium caring for them not to be swallowed by mountains of powder. We are truly convinced that our detective investigative work has proofed the intention of the man behind the new mountain building rule of good practice. As engineers supposedly do not judge fellow engineer´s intentions, it may well happen that the birth of the criterium is just casually related to soil mechanics, accidentally related or unrelated at all. In any case, it requires courage to say: “all this is completely wrong, here is how to do it right” and we heard that with our own hears. And the applauses that followed also.

6.4. Bells and whistles

All started with a request followed by a hike or maybe with a hike followed by a request. As we cannot precise, let's say the hike was the just the pretext for requesting. When one is exhausted by the hike, requests are easy to accept. Accepted the request, a clear and concise answer was given. Throughout this piece of writing we have been digging into the fundamentals, not the fundamentals of the answer but the request ones.

Chapter 3 creates an illusion about lines that fit to pints, Chapter 4 magnifies the illusion about surfaces that fit to lines that already fitted to points and Chapter 5 brings the disillusion with points that run away from lines and lines that run away from surfaces. And the sequence takes as back to ancestral practices of dealing with rogue points, weather they fit or not to lines and surfaces.

Hopefully, the message on compaction points, lines and surfaces is comprehended on a broader sense, because on Chapter 6 an important question is the absence of points to fit lines and surfaces too. Suppose that we had a supercomputer and installed it a software with an advanced constitutive relationship implemented on it. Let us see where curve fitting would take us using the points obtained from the two CAUC triaxial tests used before to prepare Figure 62, on subchapter 6.2. The values of the model parameter values were obtained following the best protocols using 10 complementary CIDC triaxial by an unsuspected international specialist, we might admit.

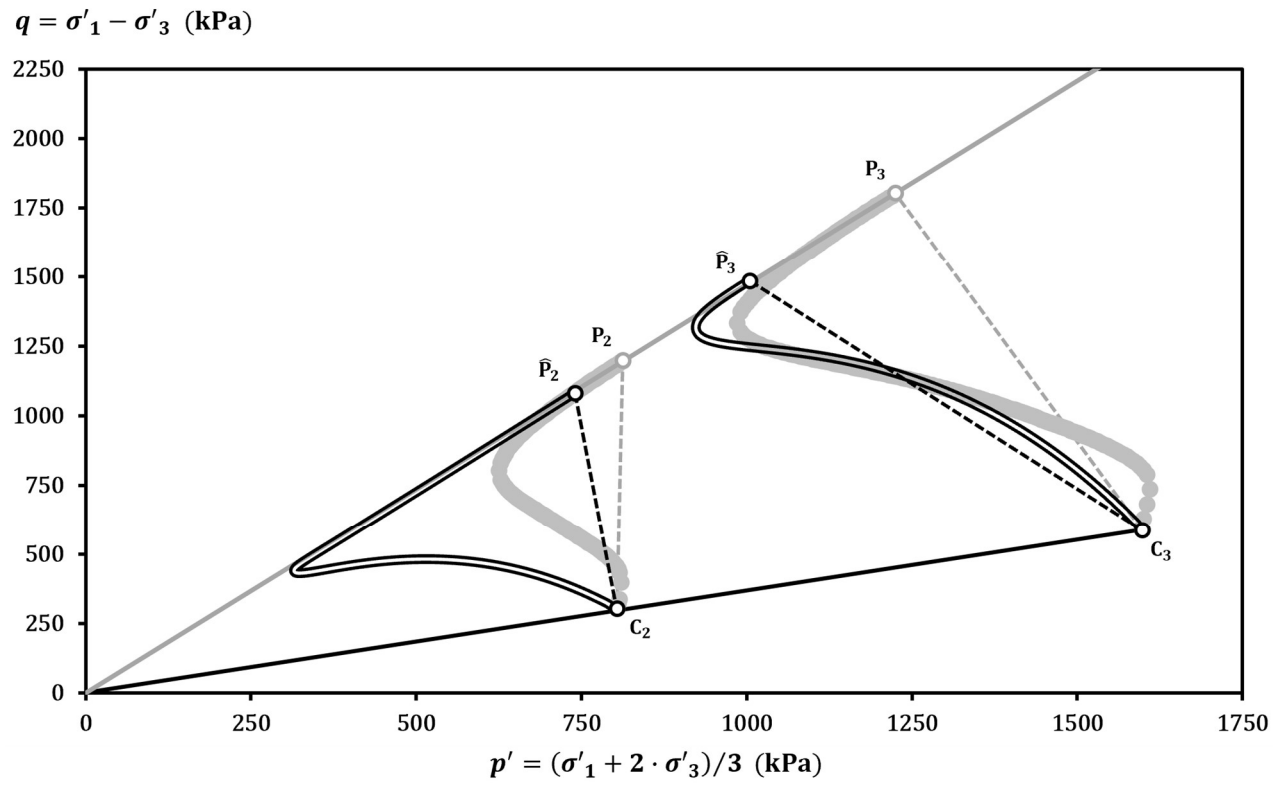

Figure 70

Figure 70 shows the result of the predictions made with the advanced constitutive relationship, being the test results shown in grey colour and the simulations in black colour. Obviously, the reader may be convinced, looking at the disparity, that he would do much better than the international specialist, twiddling here and twisting there. That is not the point. The fact of interest is that the prediction of the points representing the instant of failure is as bad as our attempt to simulate compaction curves, with the major difference that on our attempt

we used 525 points from 105 different samples of an "unique" material, and for this latter attempt we just needed to fit two lines to two pairs of points (C2-P2 and C3-P3) of the same sample and failed. We may imagine what would happen if 525 test points were available from 105 different samples. A mean value and a standard deviation are what would happen, with skewness, kurtosis and what else. The man engineer should suspect when the man scientist tells him that complex analyses are the only way out, even if it happens that the engineer and the scientist inhabit the same man's body.

It goes without saying how muddy are the fields were powder mountains grow. There are testing programs to share and there are testing programs that accidentally fall from the broken beak of magpies. No need to say which is which on the two previous subchapters. What an enlightened vision the father of the "0,6 maximum void ratio" criterium had one day that allowed him to see beyond appearances. We have just seen, with testing programs falling accidentally from the broken beak of magpies, that he really had a point. There are mountains taller than what they should be. And the problem does not get better by applying more energy on what comes above the base.

So, Chapter 6, ending with the current postlude, goes far beyond points, lines or surfaces, it brings us to mankind. It is men that chooses the points onto which lines and surfaces may or may not be fitted. The points that are shared and the points that are concealed do more than showing how lines and surfaces relate with them, they show the essence of point owners and traders. Of those who care with something and those who care about something else. Some men may try to hide points from those around them, and other men simply hide points from themselves. Among these men, many may be reputed geotechnical specialists, but perhaps few are engineers. Meanwhile, millions of dry points have been stacked and many more will be stacked. Until one day…

7. SEE YOU ON A HIKE… OR MAYBE NOT

There is nothing coincidental about the protagonists and figurants of this story and, we hope, they were all treated decently here. The author may have fictionalised on the equations and figures but could never lie about the liquifiable base of a powder mountain where inadvertently he was taken to hike. The pivotal character, the father of the "0,6 maximum void ratio" criterium, who argues that voids and solids cannot share the same volume, is not necessarily the real man responsible for the fatherhood act, but any of those that nourish the children would fit well the role. The father of the "0,6 maximum void ratio" criterium is nevertheless a controversial character. If the author had moral dilemmas, the father of the "0,6 maximum void ratio" could even be the main reason for this story to have a moral. In turn, the figurant chief inspector is nothing but an allegory about inhuman guilds of point owners and traders, who deserve all the lines and surfaces they are given, but not more credit than that they were already given here. The father of the "0,6 maximum void ratio" criterium, on the contrary, is a bad hero and a good villain at the same time. One of us. Of those, like us, that at the end of the story just have blurred victories called defeats. Puppets of the puppeteering guilds, although some are waiting for guild membership and others running away from it.

So, is there a moral of this story? Yes, of course, there is one at least. But it is not findable on the equations, nor it is on figures like it happens on cold and distant techno-scientific works. If you were asked to keep building your house after having been told to disregard the universally accepted fact that the ground beneath it was going to swallow the building soon after, would you close your eyes and keep building it? And if it was not your house, but someone´s else house, would you keep going or go even faster? What if you were the one that produced the universally accepted fact and had been disclosing it to everyone? This is where the moral resides,

buried deep on the “liquifiable” base of a powder mountain. Just like it does on the other one next to that one, perhaps too close to your door.

About the poetry talks with the taxman; we leave you with a short passage from Richard Llewellyn’s novel “How Green Was My Valley”:

> *But the slag heap moves, pressing on, down and down… Soon, perhaps in an hour, the house will be buried, and the slag heap will stretch from the top of the mountain right down to the river in the Valley. Poor river, how beautiful you were, how gay your song, how clear your green waters, how you enjoyed your play among the sleepy rocks.*

And, with a tragic picture of a man-made mountain that could not be as the last figure of the booklet, the seventy-first and more important:

Figure 71

Mind the mountains you hike.

black ribbon free publications